67 Rochelle salt ($NaKC_4H_4O_6 \cdot 4H_2O$) family

67A Pure compounds

No. 67A-1 $NaKC_4H_4O_6 \cdot 4H_2O$, Sodium potassium tartrate tetrahydrate (Seignette salt, Rochelle salt, RS)

(M = 282. 22; [D: 294. 30])

1a Ferroelectricity of Rochelle salt was first reported by Valasek in 1920. — 20Val
See also — 21Val

b — 24Val, 37Jaf

phase	III		II		I
state	P		F		P
crystal system	orthorhombic		monoclinic		orthorhombic
space group	$P2_12_12 - D_2^3$		$P2_1 - C_2^2$		$P2_12_12 - D_2^3$
Θ [°C]		–18		24	

For $NaKC_4H_2D_2O_6 \cdot 4D_2O$, $\Theta_{III–II}$ = –22 °C and $\Theta_{II–I}$ = 35 °C; see also Fig. 67A-1-042 in subsection 5a. — 40Hol
P_s || [100]. — 21Val
T_{melt} = 55 °C; see also Fig. 67A-1-001.
$\rho = 1.775 \cdot 10^3$ kg m^{-3}. — 39Mas1
For $NaKC_4H_2D_2O_6 \cdot 4D_2O$, $\rho = 1.830(3) \cdot 10^3$ kg m^{-3}. — 40Hol
Transparent, colorless. — 62Jon
Deliquescence and efflorescence: Fig. 67A-1-001.

2a Crystal growth: cooling or evaporation method from aqueous solution. — 49Miy
Solubility in H_2O: Fig. 67A-1-002.

b Crystal form: Fig. 67A-1-003, Fig. 67A-1-004.
In the ferroelectric phase (monoclinic), crystallographic axes *a*, *b*, *c*, usually accepted, are parallel or nearly parallel to those of the paraelectric phase (orthorhombic), namely the diad axis is *a* instead of *b*.

3a Unit cell parameters: Table 67A-1-001.

b Z = 4. — 41Bee
Crystal structure: Fig. 67A-1-005, Fig. 67A-1-006, Fig. 67A-1-007, Fig. 67A-1-008, Fig. 67A-1-009, Fig. 67A-1-010, Fig. 67A-1-011.
Fractional coordinates and temperature parameters: Table 67A-1-002, Table 67A-1-003, Table 67A-1-004, Table 67A-1-005, Table 67A-1-006, Table 67A-1-007.
Atomic displacements due to spontaneous polarization: Table 67A-1-008.
Structure of tartrate ion: Fig. 67A-1-012, Fig. 67A-1-013, Fig. 67A-1-014, Fig. 67A-1-015.
Interatomic distances: Table 67A-1-009; Fig. 67A-1-016, Fig. 67A-1-017, Fig. 67A-1-018, Fig. 67A-1-019, Fig. 67A-1-020.
For the structure of phase II under E_{bias}, see — 74Mit

---

4 Lattice distortion: Fig. 67A-1-021.
Thermal expansion: Fig. 67A-1-022; see also — 35Vig, 35Hab
Thermal expansion coefficients: Fig. 67A-1-023, Fig. 67A-1-024; see also Table 67A-1-001 in subsection 3a.
Density change: Fig. 67A-1-025.

5a Dielectric constant below 1 kHz: Fig. 67A-1-026, Fig. 67A-1-027, Fig. 67A-1-028, Fig. 67A-1-029, Fig. 67A-1-030, Fig. 67A-1-031.
Dielectric dispersion in microwave region: Fig. 67A-1-032, Fig. 67A-1-033, Fig. 67A-1-034, Fig. 67A-1-035; see also Fig. 67B-1-021, Fig. 67B-1-022, Fig. 67B-1-024 in No. 67B-1.
Dielectric dispersion in millimeter and submillimeter wave region: Fig. 67A-1-036, Fig. 67A-1-037, Fig. 67A-1-038, Fig. 67A-1-039, Fig. 67A-1-040.
Dielectric constant at constant strain: see Fig. 67A-1-058, Fig. 67A-1-059 in subsection 7a.
Curie-Weiss law: Table 67A-1-010.
Effects of hydrostatic pressure on Θ: Fig. 67A-1-041, Fig. 67A-1-042.
Pressure dependence of the Curie temperatures: 38Ban

Compound	$(d\Theta_{II-I}/dp)_{p=0}$	$(d\Theta_{III-II}/dp)_{p=0}$	
$NaKC_4H_4O_6 \cdot 4H_2O$	$10.93 \cdot 10^{-8}$	$3.84 \cdot 10^{-8}$	[K Pa^{-1}]
$NaKC_4H_2D_2O_6 \cdot 4D_2O$	$10.2 \cdot 10^{-8}$	$3.3 \cdot 10^{-8}$	[K Pa^{-1}]

See also 65Sam, 68Sam

Two phase transitions of the first kind exist at 3.7 GPa and 5.9 GPa at 20 °C. 72Myl
Effects of two dimensional pressure T perpendicular to [100]:
$d\Theta_{II-I}/dT = 22(1) \cdot 10^{-8}$ K m^2 N^{-1}, $d\Theta_{III-II}/dT = 30(2) \cdot 10^{-8}$ K m^2 N^{-1}. 72Mor
Effects of uniaxial pressure: see 67Unr

b Nonlinear dielectric properties:
$E = [(T - \Theta_p)/\varepsilon_0 C]\, P + \xi P^3$, $\xi = 4.7(6) \cdot 10^{13}$ V m^5 C^{-3}. 40Mue
$E_a = (\beta_{11} + \xi_{11} D_a^2 + \xi_{12} D_b^2 + \xi_{13} D_c^2) D_a$, 68For
$\xi_{11} = 5.9 \cdot 10^{13}$ V m^{5}C^{-3}, $\xi_{12} = 3.3 \cdot 10^{13}$ V m^5 C^{-3}, $\xi_{13} = -3.5 \cdot 10^{12}$ V m^5 C^{-3}.

c Spontaneous polarization: Fig. 67A-1-043.
Coercive field: Fig. 67A-1-044.
For frequency and applied field dependence of E_c: see 58Wie, 64Abe

d Electrocaloric effect: Fig. 67A-1-045.

6a Heat capacity: Fig. 67A-1-046, Fig. 67A-1-047, Fig. 67A-1-048.
Transition heat ΔQ_m and transition entropy ΔS_m: 78Tat

	Θ_{III-II}	Θ_{II-I}
ΔQ_m [J mol^{-1}]	7.51	9.86
ΔS_m [J K^{-1}mol^{-1}]	0.029	0.021

b Thermal conductivity: Fig. 67A-1-049.

7a Piezoelectric constants: Table 67A-1-011; Fig. 67A-1-050, Fig. 67A-1-051, Fig. 67A-1-052, Fig. 67A-1-053, Fig. 67A-1-054, Fig. 67A-1-055, Fig. 67A-1-056, Fig. 67A-1-057.
Electromechanical coupling factor: Fig. 67A-1-058, Fig. 67A-1-059, Fig. 67A-1-060.

b Electrostriction: Fig. 67A-1-061, Fig. 67A-1-062.
Electrostriction around Θ_{II-I}: see 84Bei1

c Nonlinear electromechanical properties: Fig. 67A-1-063.

8a Elastic properties:
Resonance method: Table 67A-1-012; Fig. 67A-1-064, Fig. 67A-1-065, Fig. 67A-1-066, Fig. 67A-1-067, Fig. 67A-1-068; see also Fig. 67A-1-059 in subsection 7a.
Pulse method: Fig. 67A-1-069, Fig. 67A-1-070.
Brillouin scattering: Fig. 67A-1-071.

	Piezoelectric line in NQR: Fig. 67A-1-072.	
	Elastic compliance around Θ_{II-I}: see	84Bei1
b	Nonlinear elastic constants: see	83Bei, 84Bei2
9a	Refractive indices: Fig. 67A-1-073, Fig. 67A-1-074.	
	Indicatrix parameters: Table 67A-1-013.	
	Change in rotation angle of optical indicatrix during domain switching: see Fig. 67A-1-106 in subsection 15b.	
	Optical axial angle: Fig. 67A-1-075.	
	Birefringence: Fig. 67A-1-076.	
	Optical absorption: Fig. 67A-1-077.	
	Optical absorption due to VO^{2+}: see	85Aga
	Far-infrared spectra: see subsection 5a.	
b	Electrooptic constants: Table 67A-1-014; Fig. 67A-1-078, Fig. 67A-1-079, Fig. 67A-1-080.	
	Change in birefringence by applied electric field: Fig. 67A-1-081, Fig. 67A-1-082, Fig. 67A-1-083, Fig. 67A-1-084.	
c	Piezooptic effect: Table 67A-1-015.	
d	Optical rotatory power: Fig. 67A-1-085.	
	Gyration tensor: $g_{11} = -8.6(5) \cdot 10^{-6}$, $g_{22} = -6.7(15) \cdot 10^{-6}$, $g_{33} = 7.2(16) \cdot 10^{-6}$ at 21 °C for $\lambda = 632.8$ nm.	75Vlo
10a	Raman scattering: Table 67A-1-016; Fig. 67A-1-086, Fig. 67A-1-087.	
b	Brillouin scattering: Fig. 67A-1-088.	
	Elastic stiffness obtained from Brillouin scattering: see Fig. 67A-1-071 in subsection 8a.	
11	Electrical conductivity: Fig. 67A-1-089, Fig. 67A-1-090.	
	Breakdown field: $2 \cdot 10^4$ kV m^{-1}.	69Gur
12	Effect of magnetic field on the phase transition: see	81Ism
13a	NMR of proton and deuteron: Table 67A-1-017; Fig. 67A-1-091, Fig. 67A-1-092, Fig. 67A-1-093.	
	NMR of ^{23}Na: Table 67A-1-018, Table 67A-1-019; Fig. 67A-1-094, Fig. 67A-1-095, Fig. 67A-1-096, Fig. 67A-1-097.	
b	ESR: Table 67A-1-020, Table 67A-1-021; Fig. 67A-1-098.	
14a	Integrated intensity of Bragg reflection: Fig. 67A-1-099, Fig. 67A-1-100, Fig. 67A-1-101.	
15a	Domain structure: Fig. 67A-1-102, Fig. 67A-1-103.	
	Domain structure observation by polarized light: see	50Fur, 53Mit
	Domain structure observation by X-ray topography: see	83Kla, 85Ume
	Domain structure observation by powder pattern method: see	59Pea, 73Hat
b	Direct observation of domain wall motion by polarized light: see	53Mit, 60Wie
	Switching current, switching time: Fig. 67A-1-104, Fig. 67A-1-105.	
	Change in rotation angle of optical indicatrix during domain switching: Fig. 67A-1-106.	
	Polarization reversal investigated by means of electro-optic Kerr effect [a]) and by optical gyration and rotation of indicatrixes [b]).	[a]) 60Wie, [b])91Kob1, 91Kob2

16	Surface layer: see	76Man
	Radiation damage: see	67Oka, 67Suz
	Dislocation and macroscopic defects: see	61Nak, 83Kla
	Etchant: H_2O.	61Nak
	Effects of humidity: see	49Kaw

Table 67A-1-001. $NaKC_4H_4O_6 \cdot 4H_2O$. Unit cell parameters *a*, *b*, *c*.

Ref.	[34Sta]	[41Bee]	[46Ubb]		
			T = –50 °C	T = +20 °C	T = +35 °C
a [Å]	11.91(4)	11.93	11.815	11.867(7)	11.878
b [Å]	14.32(5)	14.30	14.203	14.236(8)	14.246
c [Å]	6.20(2)	6.17	6.195	6.213(4)	6.218

Table 67A-1-002. $NaKC_4H_4O_6 \cdot 4H_2O$. Structure of phase I (RT) [41Bee]. Fractional coordinates. See the caption of Fig. 67A-1-006.

	$X = a$	$Y = b$	$Z = c$		$X = a$	$Y = b$	$Z = c$
K (1)	0.00	0.00	0.05	H_2O (7)	0.40	0.08	0.50
K (2)	0.00	0.50	0.15	H_2O (8)	0.25	0.05	0.87
Na	0.23	0.99	0.52	H_2O (9)	0.44	0.30	0.05
O (1)	0.12	0.10	0.37	H_2O (10)	0.42	0.40	0.45
O (2)	0.22	0.20	0.12	C (1)	0.15	0.18	0.28
O (3)	0.23	0.40	0.82	C (2)	0.12	0.28	0.42
O (4)	0.06	0.37	0.85	C (3)	0.17	0.27	0.65
OH (5)	0.16	0.36	0.32	C (4)	0.15	0.35	0.80
OH (6)	0.29	0.24	0.63				

Table 67A-1-003. $NaKC_4H_4O_6 \cdot 4H_2O$. Structures of phase I (35 °C) and phase III (–64 °C) [57Maz]. Fractional coordinates and temperature parameters. B_M, B_m: along the direction of the maximum, minimum thermal vibration. δ: angle between the direction of the maximum thermal vibration and a^* axis. Temperature factor = exp $(-B_\varphi \sin^2\theta/\lambda^2)$. $B_\varphi = B_M\cos^2(\varphi - \delta) + B_m\sin^2(\varphi - \delta)$. φ: angle between radius vector (h k 0) and a^*axis in reciprocal space.

Atoms	Structure at –64 °C			Structure at +35 °C		
	Coordinates		Temperature factors [Å^2]	Coordinates		Temperature factors [Å^2]
	x	*y*		*x*	*y*	
K(1)	0	0	$B_M = 5.45$, $B_m = 1.19$, $\delta = -30°$	0	0	$B_M = 7.78$, $B_m = 1.49$, $\delta = -35°$
K(2)	1/2	0	$B_M = 1.78$, $B_m = 1.19$, $\delta = -35°$	1/2	0	$B_M = 2.25$, $B_m = 1.49$, $\delta = -35°$
Na	0.232	0.992	$B_M = 1.14$, $B_m = 0.47$, $\delta = 0°$	0.232	0.992	$B_M = 1.14$, $B_m = 0.47$, $\delta = 0°$
C(1)	0.153	0.188	$B = 1.11$	0.153	0.188	$B = 1.11$
C(2)	0.127	0.271	$B = 1.11$	0.127	0.271	$B = 1.11$
C(3)	0.175	0.267	$B = 1.11$	0.175	0.267	$B = 1.11$
C(4)	0.170	0.356	$B = 1.11$	0.170	0.356	$B = 1.11$
O(1)	0.121	0.109	$B = 1.11$	0.121	0.109	$B = 1.11$
O(2)	0.211	0.202	$B = 1.11$	0.209	0.202	$B = 1.11$
O(3)	0.232	0.407	$B_M = 2.59$, $B_m = 1.11$, $\delta = 0°$	0.235	0.406	$B_M = 2.59$, $B_m = 1.11$, $\delta = 0°$
O(4)	0.050	0.359	$B = 1.11$	0.054	0.361	$B = 1.11$
O(5)	0.154	0.356	$B = 1.11$	0.154	0.356	$B = 1.11$
O(6)	0.298	0.249	$B = 1.11$	0.297	0.249	$B = 1.11$
O(7)	0.397	0.084	$B = 1.11$	0.397	0.084	$B = 1.11$
O(8)	0.244	0.040	$B_M = 4.79$, $B_m = 1.85$, $\delta = 0°$	0.248	0.040	$B_M = 5.53$, $B_m = 3.84$, $\delta = 0°$
O(9)	0.440	0.305	$B = 2.56$	0.440	0.301	$B_M = 5.53$, $B_m = 3.84$, $\delta = 90°$
O(10)	0.426	0.395	$B = 2.56$	0.427	0.396	$B = 2.59$

Table 67A-1-004. $NaKC_4H_4O_6 \cdot 4H_2O$. Structure of phase I [89Iwa]. Fractional coordinates and anisotropic temperature parameters at 24 °C. b_{ij} is defined by Eq. (b) in Introduction. Values multiplied by 10^4 are shown.

Atom	x	y	z	b_{11}	b_{22}	b_{33}	b_{12}	b_{13}	b_{23}
Na	2313(1)	9929(1)	5226(3)	36(1)	23(1)	144(4)	–1(1)	–6(2)	7(2)
K1	0	0	472(3)	105(2)	53(1)	193(5)	–39(1)	0	0
K2	0	5000	1591(2)	41(1)	33(1)	128(3)	4(1)	0	0
O1	1193(3)	1091(2)	3511(5)	39(2)	20(1)	131(8)	–4(1)	–5(4)	–5(3)
O2	2096(3)	2026(2)	1193(5)	61(3)	26(2)	117(8)	1(2)	17(4)	–4(3)
O3	2339(3)	4060(2)	8125(6)	68(3)	28(2)	168(9)	–9(2)	–6(5)	–20(4)
O4	537(3)	3626(3)	8439(6)	51(3)	41(2)	144(9)	14(2)	5(4)	–20(4)
O5	1634(3)	3573(2)	3248(5)	54(2)	17(1)	105(8)	1(2)	0(4)	1(3)
O6	2950(3)	2481(2)	6275(6)	40(2)	25(2)	171(9)	6(2)	–14(4)	2(3)
O7	3956(3)	821(2)	4837(6)	42(2)	30(2)	210(10)	1(2)	22(5)	6(4)
O8	2444(4)	412(2)	8852(5)	141(5)	27(2)	99(9)	9(2)	22(6)	3(3)
O9	4378(3)	3016(3)	347(8)	53(3)	80(3)	263(13)	9(3)	–20(6)	–16(6)
O10	4251(3)	3984(3)	4188(8)	49(3)	67(3)	397(17)	23(2)	–49(6)	–80(6)
C1	1543(4)	1876(3)	2850(7)	27(3)	19(2)	98(10)	2(2)	–16(5)	–3(4)
C2	1249(3)	2734(3)	4235(7)	28(3)	18(2)	102(10)	0(2)	6(5)	–4(4)
C3	1784(4)	2642(3)	6449(7)	34(3)	21(2)	99(10)	1(2)	3(5)	0(4)
C4	1525(4)	3515(3)	7805(7)	51(3)	22(2)	76(10)	6(2)	–17(5)	3(4)

Table 67A-1-005. $NaKC_4H_4O_6 \cdot 4H_2O$. Structure of phase II [94Suz]. Fractional coordinates and anisotropic temperature parameters at 273 K. b_{ij} is defined by Eq. (b) in Introduction. Atoms with suffix A are related to atoms with suffix B through 2_1 axis parallel to *b* axis in phase I.

	x	*y*	*z*	b_{11}	b_{22}	b_{33}	b_{12}	b_{13}	b_{23}
Na(A)	0.2674(2)	0.4933(1)	0.4760(4)	0.0037(2)	0.0016(1)	0.0135(6)	0.0000(1)	–0.0004(2)	–0.0002(2)
Na(B)	0.2308(2)	0.9931(1)	0.5198(4)	0.0034(1)	0.0014(1)	0.0165(6)	–0.0001(1)	–0.0007(2)	0.0011(2)
K(1)	–0.0033(3)	1.0013(1)	0.0461(3)	0.0098(1)	0.0044(1)	0.0202(4)	–0.0034(1)	–0.0015(3)	0.0009(1)
K(2)	–0.0011(2)	0.5011(1)	0.1595(2)	0.0044(1)	0.0027(1)	0.0135(3)	0.0003(1)	0.0000(1)	0.0002(1)
C(1A)	0.1537(5)	0.1883(4)	0.2821(9)	0.0030(4)	0.0010(2)	0.0097(2)	0.0000(2)	–0.0012(5)	–0.0000(4)
C(1B)	0.3437(5)	0.6884(4)	0.7174(9)	0.0033(4)	0.0015(2)	0.0084(2)	–0.0002(2)	–0.0015(5)	0.0012(4)
C(2A)	0.1242(5)	0.2740(4)	0.4217(9)	0.0031(4)	0.0012(2)	0.0084(2)	0.0000(2)	–0.0005(5)	0.0001(4)
C(2B)	0.3742(6)	0.7735(4)	0.5765(9)	0.0034(4)	0.0013(2)	0.0085(2)	0.0000(2)	–0.0004(5)	0.0014(4)
C(3A)	0.1777(5)	0.2641(4)	0.6429(9)	0.0031(4)	0.0013(2)	0.0085(2)	0.0001(2)	–0.0008(5)	–0.0003(4)
C(3B)	0.3209(5)	0.7637(4)	0.3525(9)	0.0030(4)	0.0015(2)	0.0096(2)	–0.0003(2)	–0.0016(5)	0.0005(4)
C(4A)	0.1525(6)	0.3517(4)	0.7766(8)	0.0053(5)	0.0015(2)	0.0036(1)	0.0005(2)	–0.0016(6)	–0.0004(3)
C(4B)	0.3484(7)	0.8507(4)	0.2207(10)	0.0055(5)	0.0016(2)	0.0089(3)	–0.0007(3)	–0.0020(6)	0.0008(4)
O(1A)	0.1188(4)	0.1087(3)	0.3494(8)	0.0036(3)	0.0011(1)	0.0178(3)	–0.0001(2)	–0.0001(5)	0.0011(3)
O(1B)	0.3790(4)	0.6093(3)	0.6510(7)	0.0038(3)	0.0011(1)	0.0128(1)	0.0001(2)	–0.0003(5)	–0.0006(3)
O(2A)	0.2086(5)	0.2032(3)	0.1171(7)	0.0060(4)	0.0018(2)	0.0094(1)	0.0003(2)	0.0022(5)	–0.0005(3)
O(2B)	0.2881(5)	0.7029(3)	0.8801(7)	0.0051(4)	0.0019(2)	0.0111(1)	0.0003(2)	0.0028(5)	0.0014(3)
O(3A)	0.2334(5)	0.4057(3)	0.8124(9)	0.0066(4)	0.0018(2)	0.0193(5)	–0.0010(2)	–0.0022(7)	–0.0012(4)
O(3B)	0.2683(6)	0.9070(3)	0.1889(9)	0.0067(4)	0.0022(2)	0.0202(5)	0.0006(2)	–0.0006(7)	0.0029(4)
O(4A)	0.0539(5)	0.3633(3)	0.8446(9)	0.0049(4)	0.0028(2)	0.0151(3)	0.0011(2)	0.0009(6)	–0.0017(4)
O(4B)	0.4481(5)	0.8598(3)	0.1524(8)	0.0056(4)	0.0030(2)	0.0106(1)	–0.0015(2)	–0.0003(5)	0.0010(4)
O(5A)	0.1626(5)	0.3569(3)	0.3200(8)	0.0055(4)	0.0010(1)	0.0114(1)	–0.0005(2)	–0.0011(5)	0.0008(3)
O(5B)	0.3347(4)	0.8569(3)	0.6739(7)	0.0049(3)	0.0010(1)	0.0100(0)	0.0000(2)	–0.0002(5)	0.0002(3)
O(6A)	0.2951(4)	0.2482(3)	0.6231(8)	0.0037(3)	0.0018(2)	0.0156(2)	0.0006(2)	–0.0015(5)	–0.0002(4)
O(6B)	0.2037(4)	0.7484(3)	0.3692(8)	0.0031(3)	0.0016(2)	0.0171(3)	–0.0004(2)	–0.0006(5)	0.0009(4)
O(7A)	0.3944(5)	0.0827(3)	0.4845(10)	0.0039(3)	0.0018(2)	0.0218(5)	–0.0001(2)	0.0019(6)	–0.0004(4)
O(7B)	0.1041(5)	0.5829(3)	0.5173(11)	0.0033(3)	0.0020(2)	0.0279(8)	0.0002(2)	0.0019(6)	0.0000(5)
O(8A)	0.2392(7)	0.0397(4)	0.8833(8)	0.0136(8)	0.0020(2)	0.0084(1)	0.0014(3)	0.0029(8)	–0.0003(4)
O(8B)	0.2546(7)	0.5417(4)	0.1121(9)	0.0108(7)	0.0022(2)	0.0165(4)	–0.0012(3)	0.0018(8)	0.0025(5)
O(9A)	0.4373(6)	0.3001(6)	0.0379(13)	0.0048(5)	0.0071(5)	0.0260(1)	0.0013(4)	–0.0039(8)	0.0000(8)
O(9B)	0.0608(6)	0.8038(6)	0.9622(11)	0.0054(5)	0.0056(4)	0.0229(8)	–0.0010(3)	–0.0030(8)	0.0018(7)
O(10A)	0.4244(6)	0.3992(5)	0.4192(14)	0.0048(5)	0.0051(4)	0.0368(6)	0.0024(3)	–0.0040(9)	–0.0068(8)
O(10B)	0.0768(6)	0.8933(5)	0.5697(11)	0.0046(4)	0.0041(3)	0.0265(1)	–0.0011(3)	–0.0038(7)	0.0024(6)

Table 67A-1-006. $NaKC_4H_4O_6 \cdot 4H_2O$. Fractional coordinates of atoms in phase III [96Shi]. T = 253 K and 153 K.

	253 K	153 K		253 K	153 K
Na			O(3)		
x	0.2316(2)	0.2322(2)	*x*	0.2319(5)	0.2288(4)
y	0.9934(2)	0.9932(2)	*y*	0.4051(3)	0.4061(3)
z	0.5214(4)	0.5159(3)	*z*	0.8146(9)	0.8196(7)
K(1)			O(4)		
x	0.0000	0.0000	*x*	0.0518(5)	0.0479(3)
y	0.0000	0.0000	*y*	0.3602(4)	0.3586(3)
z	0.0444(5)	0.0428(3)	*z*	0.8462(10)	0.8488(7)
K(2)			O(5)		
x	0.0000	0.0000	*x*	0.1660(4)	0.1667(3)
y	0.5000	0.5000	*y*	0.3564(3)	0.3572(3)
z	0.1595(4)	0.1605(3)	*z*	0.3226(9)	0.3233(7)
C(1)			O(6)		
x	0.1547(6)	0.1548(4)	*x*	0.2969(4)	0.2969(3)
y	0.1900(5)	0.1894(4)	*y*	0.2491(4)	0.2495(3)
z	0.2855(13)	0.2832(9)	z	0.6278(9)	0.6323(7)
C(2)			O(7)		
x	0.1240(6)	0.1242(5)	*x*	0.3961(4)	0.3964(3)
y	0.2739(5)	0.2737(4)	*y*	0.0850(4)	0.0852(3)
z	0.4237(12)	0.4230(9)	*z*	0.4828(9)	0.4859(7)
C(3)			O(8)		
x	0.1766(6)	0.1768(4)	*x*	0.2422(6)	0.2369(4)
y	0.2622(5)	0.2630(4)	*y*	0.0417(3)	0.0421(3)
z	0.6463(13)	0.6484(9)	*z*	0.8878(8)	0.8806(6)
C(4)			O(9)		
x	0.1500(7)	0.1480(5)	*x*	0.4380(5)	0.4404(3)
y	0.3502(6)	0.3499(4)	*y*	0.3012(4)	0.3062(3)
z	0.7790(13)	0.7831(9)	*z*	0.0370(10)	0.0323(7)
O(1)			O(10)		
x	0.1199(4)	0.1202(3)	*x*	0.4263(5)	0.4232(3)
y	0.1097(3)	0.1093(3)	*y*	0.3943(4)	0.3911(3)
z	0.3503(9)	0.3489(7)	*z*	0.4223(11)	0.4295(8)
O(2)					
x	0.2102(5)	0.2126(3)			
y	0.2039(4)	0.2045(3)			
z	0.1184(9)	0.1182(6)			

Table 67A-1-007. $NaKC_4H_4O_6 \cdot 4H_2O$. Fractional coordinates and equivalent temperature parameters U_{eq} in phase II [96Suz]. T = 273 K. $U_{eq} = (1/3)\Sigma_i\Sigma_j U_{ij}\, a_i^* a_j^*\, a_i\, a_j$. U_{ij} is defined by Eq. (d) in Introduction.

	x	y	z	U_{eq} [10^4 Å^2]
Na(A)	0.2684(4)	0.4933(1)	0.4763(4)	223(15)
Na(B)	0.2322(4)	0.9932(2)	0.5200(5)	242(15)
K(1)	0	1.0009(1)	0.0460(3)	510(11)
K(2)	0.0000(3)	0.5011(1)	0.1595(2)	286(7)
C(1A)	0.1544(6)	0.1880(4)	0.2825(11)	187(28)
C(1B)	0.3449(6)	0.6883(4)	0.7184(9)	180(27)
C(2A)	0.1252(6)	0.2741(4)	0.4218(10)	182(27)
C(2B)	0.3755(7)	0.7734(4)	0.5764(9)	191(28)
C(3A)	0.1787(6)	0.2639(4)	0.6416(9)	167(26)
C(3B)	0.3225(6)	0.7638(4)	0.3527(10)	182(28)
C(4A)	0.1538(7)	0.3516(4)	0.7764(8)	204(28)
C(4B)	0.3494(7)	0.8508(4)	0.2212(10)	236(31)
O(1A)	0.1202(5)	0.1087(3)	0.3498(9)	239(24)
O(1B)	0.3805(5)	0.6093(3)	0.6517(8)	213(22)
O(2A)	0.2091(6)	0.2036(3)	0.1173(7)	265(25)
O(2B)	0.2894(6)	0.7028(3)	0.8801(8)	261(25)
O(3A)	0.2353(6)	0.4049(3)	0.8122(9)	338(30)
O(3B)	0.2700(7)	0.9072(4)	0.1892(10)	368(31)
O(4A)	0.0549(6)	0.3628(4)	0.8445(9)	299(28)
O(4B)	0.4489(6)	0.8601(4)	0.1520(8)	301(28)
O(5A)	0.1617(7)	0.3574(3)	0.3217(10)	256(27)
O(5B)	0.3357(6)	0.8570(3)	0.6738(7)	222(23)
O(6A)	0.2957(6)	0.2484(4)	0.6212(9)	250(26)
O(6B)	0.2050(5)	0.7480(3)	0.3684(8)	239(25)
O(7A)	0.3953(6)	0.0825(3)	0.4844(10)	286(28)
O(7B)	0.1052(6)	0.5830(4)	0.5177(11)	313(30)
O(8A)	0.2400(8)	0.0395(4)	0.8828(8)	432(36)
O(8B)	0.2555(8)	0.5418(4)	0.1121(10)	433(38)
O(9A)	0.4376(7)	0.3009(6)	0.0358(14)	519(47)
O(9B)	0.0625(7)	0.8047(6)	0.9628(12)	465(44)
O(10A)	0.4256(7)	0.3993(5)	0.4183(15)	502(43)
O(10B)	0.0777(6)	0.8932(5)	0.5698(12)	425(38)

Table 67A-1-008. $NaKC_4H_4O_6 \cdot 4H_2O$. Relative displacements of atoms corresponding to polarization reversal [96Suz]. T = 273 K. $\delta x = a(x_A + x_B - 0.5)$, $\delta y = b(y_A - y_B + 0.5)$, $\delta z = c(z_A + z_B - 1.0)$ and $\Delta = (\delta x^2 + \delta y^2 + \delta z^2)^{1/2}$. In the paraelectric phase, $\delta x = \delta y = \delta z = \Delta = 0$. As to A and B, see the caption of Table 67A-1-005.

	δx [Å]	δy [Å]	δz [Å]	Δ [Å]
Na	0.009(9)	–0.001(4)	–0.022(5)	0.024(20)
C(1)	–0.007(14)	0.004(11)	0.005(12)	0.009(20)
C(2)	0.010(15)	–0.009(11)	–0.011(11)	0.017(27)
C(3)	0.014(14)	–0.002(11)	–0.034(11)	0.037(34)
C(4)	0.038(16)	–0.011(11)	–0.014(11)	0.042(42)
O(1)	0.008(11)	0.008(8)	0.010(10)	0.015(22)
O(2)	–0.015(14)	–0.012(8)	–0.016(9)	0.025(30)
O(3)	0.063(15)	0.032(9)	0.009(11)	0.071(52)
O(4)	0.046(14)	–0.037(11)	–0.021(10)	0.063(50)
O(5)	–0.029(15)	–0.005(8)	–0.027(10)	0.040(39)
O(6)	0.008(13)	–0.006(9)	–0.064(10)	0.065(40)
O(7)	0.007(14)	0.007(9)	0.013(13)	0.016(26)
O(8)	–0.052(19)	0.032(11)	–0.031(11)	0.068(58)
O(9)	0.001(16)	0.054(17)	–0.007(16)	0.054(46)
O(10)	0.040(15)	–0.086(14)	–0.073(16)	0.120(77)

Table 67A-1-009. $NaKC_4H_4O_6 \cdot 4H_2O$. Interatomic distances between oxygens in phase I (35 °C) and III (–64 °C) [57Maz]. Δ: difference between the distances at –64 °C and 35 °C.

	Distances [Å]		Δ [Å]
	at –64 °C	at +35 °C	
O(1)–O(10)	2.55	2.56	–0.01
O(3)–O(8)	2.71	2.72	–0.01
O(4)–O(9)	2.74	2.75	–0.01
O(6)–O(7)	2.74	2.76	–0.02
O(6)–O(10)	2.79	2.83	–0.04
O(2)–O(8)	2.80	2.82	–0.02
O(9)–O(10)	2.80	2.84	–0.04
O(4)–O(7)	2.94	2.98	–0.04
O(7)–O(8)	2.98	2.97	+0.01
O(5)–O(8)	3.11	3.10	+0.01
O(2)–O(9)	3.10	3.11	–0.01

Table 67A-1-010. $NaKC_4H_4O_6 \cdot 4H_2O$, $NaKC_4D_4O_6 \cdot 4D_2O$. Curie-Weiss constants of several specimens with different histories [86Shi]. C^f and C^p are the Curie-Weiss constants obtained in polar and nonpolar phases, respectively. *d*: thickness of specimen.

Crystal	Θ_f [K]	f [Hz]	C^f [10^3 K]	C^p [10^3 K]	$-C^p/C^f$
RS, cooling after	298.3	1000	–1.5	2.0	1.30
annealing in		1	–8.4		0.23
nonpolar phase.		0	–10.6		0.19
($d = 4.72 \cdot 10^{-3}$ m)	255.4	1000	2.4	–1.45	0.60
		1	4.1		0.36
		0	6.8		0.31
Deuterated RS, cooling	305.4	1000	–0.95	1.6	1.68
after annealing in		1	–2.7		0.59
nonpolar phase.		0	–3.2		0.50
($d = 2.36 \cdot 10^{-3}$ m)	251.6	1000	0.80	–1.5	1.9
		1	0.87		1.7
		0	1.9		0.79
RS, after aging for over	297.8	1000	–1.4	2.4	1.8
a year, and after aging		3	–1.6		1.6
for 7 days in polar phase.		0	–1.9		1.3
($d = 4.1 \cdot 10^{-3}$ m)	298.0	1000	–1.5	2.4	1.6
		3	–1.6		1.5
		0	–1.7		1.4

Table 67A-1-011. $NaKC_4H_4O_6 \cdot 4H_2O$, $NaKC_4D_4O_6 \cdot 4D_2O$. Piezoelectric constants [66Bec].

Crystal	d_{14}	d_{25}	d_{36}	e_{14}	e_{25}	e_{36}	g_{14}	g_{25}	g_{36}	h_{14}	h_{25}	h_{36}	k_{14}	T	Ref.
	[10^{-12} C N^{-1}]			[C m^{-2}]			[10^{-3} m^2 C^{-1}]			[10^8 N C^{-1}]				[°C]	
RS	770	+46	9.4											0	27Val
	333	–55	11.8											RT	28Man
		–56	13.1												39Mas2
	2300	–56	11.8											25	50Mas
	512	–54	12	2.98	–0.16	0.12	180	–660	140	23	–21	14		30, –22	50Van
	187	–54	12	1.65	–0.16	0.12	180	–660	140	23	–21	14		40, –28	
	345	54	12											34	64Ber
				3.7	–0.16	0.11									50Mas
													0.76		62Ber
deuterated		–77	13												40Hol
RS										23.4				RT	40Hol

Table 67A-1-012. $NaKC_4H_4O_6 \cdot 4H_2O$. Elastic constants [66Bec].

s_{11}	s_{22}	s_{33}	s_{12}	s_{13}	s_{23}	s^E_{44}	s^D_{44}	s^E_{55}	s^D_{55}	s^E_{66}	s^D_{66}	T	Ref.
[10^{-12} m^2 N^{-1}]												[°C]	
52.30	34.30	32.40	–21.80	–16.80	–13.3	96.3		337		118			39Hin
52.4	35.0	33.7	–15.4	–9.8	–9.1		74.6	350	312	104	102	20	47Hun
50.2	30.4	31.7	–11.6	–21.4	–8.9	82.0		333		106			49Sun
51.8	34.9	33.4	–15.3	–21.1	–10.3	172		360		102.7		30, –22	50Mas
51.8	34.9	33.4	–15.3	–21.1	–10.3	113.4		346		102		40, –28	50Van
51.8	34.9	33.4	–15.3	–21.1	–10.3		79.6		328		101	30, –22	39Mas2
51.8	34.9	33.4	–15.3	–21.1	–10.3		78.7		310		101	40, –28	39Mas2
52.0	36.8	35.9	–16.3	–11.6	–12.2	150.2		350.3		104.2		34	64Ber

c_{11}	c_{22}	c_{33}	c_{12}	c_{13}	c_{23}	c^E_{44}	c^D_{44}	c^E_{55}	c^D_{55}	c^E_{66}	c^D_{66}	T	Ref.
[10^9 N m^{-2}]												[°C]	
34.7	47.3	80.6	–8.04	31.6	–34.4	(16.4)		(3.24)		(12.4)		20	27Man
26.4	31.8	39.1	18.1	22.3				(3.04)		(9.96)			39Mas2
25.5	38.1	37.1	14.1	11.6	14.6		13.4	2.86	3.21	9.60	9.79	20	47Hun
40.6	52.0	64.0	25.6	34.6	32.0	12.2		3.0		9.5			49Sun
25.8	38.0	37.5	14.0	11.2				3.14		9.97		RT	50Jon
28.0	41.4	39.4	17.4	15.0	19.7	6.66		2.85		9.60		34	64Ber

Table 67A-1-013. $NaKC_4H_4O_6 \cdot 4H_2O$, $NaKC_4D_4O_6 \cdot 4D_2O$, $NaNH_4C_4H_4O_6 \cdot 4H_2O$. Optical indicatrix parameters at T = RT [80Rom].

Crystal	$NaKC_4H_4O_6 \cdot 4\,H_2O$			Deuterated Rochelle salt			$NaNH_4C_4H_4O_6 \cdot 4\,H_2O$		
λ [nm]	680	490	300	680	490	300	680	490	300
n_x	1.4916	1.5018	1.5389	1.4891	1.5002	1.5410	1.4940	1.5052	1.5456
n_y	1.4883	1.4980	1.5346	1.4860	1.4968	1.5337	1.4954	1.5062	1.5440
n_z	1.4864	1.4961	1.5327	1.4840	1.4950	1.5330	1.4917	1.5023	1.5409
$\frac{dn_x}{d\lambda}$ [10^{-5} nm^{-1}]	3	8.5	41	4	8.7	44	4	9.0	48
$\frac{dn_y}{d\lambda}$ [10^{-5} nm^{-1}]	4	8	41	4	9.5	41	4.5	9.5	44
$\frac{dn_z}{d\lambda}$ [10^{-5} nm^{-1}]	4	8	44	4	11	44	4	9	45.5
Optic sign	Positive			Positive			Negative		
Acute bisectrix	*X*			*X*			*Z*		

Table 67A-1-014. $NaKC_4H_4O_6 \cdot 4H_2O$. Electrooptic constants [1894Poc].

r_{41}	r_{52}	r_{63}	λ
[10^{-12} m V^{-1}]			[nm]
–2.0	–1.7	0.32	589

Table 67A-1-015. $NaKC_4H_4O_6 \cdot 4H_2O$. Piezooptic constants [69Nar]. λ = 589 nm. See also [1894Poc].

$p_{\lambda\mu}$ [m m^{-1}]		$\Pi_{\lambda\mu}$ [10^{-12} m^2 N^{-1}]	
p_{11}	0.35	Π_{11}	3.1
p_{12}	0.41	Π_{12}	3.4
p_{13}	0.42	Π_{13}	3.2
p_{21}	0.37	Π_{21}	5.4
p_{22}	0.28	Π_{22}	0.76
p_{23}	0.34	Π_{23}	2.1
p_{31}	0.36	Π_{31}	5.0
p_{32}	0.35	Π_{32}	2.9
p_{33}	0.36	Π_{33}	1.6
p_{44}	–0.030	Π_{44}	–2.5
p_{55}	0.0046	Π_{55}	1.5
p_{66}	–0.025	Π_{66}	–2.5

Table 67A-1-016. $NaKC_4H_4O_6 \cdot 4H_2O$. Frequency [cm^{-1}] of phonon modes determined from Raman spectra [88Bha]. sh: sharp, br: broad, vbr: very broad, sh: shoulder; vs: very strong, s: strong, m: medium, w: weak, vw: very weak.

A			B_1	B_2	B_3
Z(*XX*)*Y*	*Z*(*YY*)*X*	*Y*(*ZZ*)*X*	*Z*(*XY*)*X*	*Z*(*XZ*)*X*	*Z*(*YZ*)*X*
	3522 br, w	3524 vbr, vw			3522 br, vw
	3470 br, m	3470 vbr, w	3472 vbr, w		3468 vbr, vw
3408 br, s	3404 br, m	3406 vbr, m	3408 vbr, w	3406 vbr, m	3408 vbr, w
3262 vbr, s	3220 vbr, w	3264 vbr, w	3264 vbr, w	3294 vbr, m	
2982 sh, vs	2982 sh, s	2980 sh, s	2982 sh, w	2984 sh, s	2984 sh, vw
2938 sh, w	2940 sh, vs	2936 sh, vw	2940 sh, w		2940 sh, vw
	1668 br, vw		1664 vbr, vw	1660 br, vw	
	1622 br, vw	1623 br, w			
1592 br, w		1594 br, vw		1596 br, w	1596 br, vw
1436 sh, w	1434 sh, s	1432 sh, w	1434 so	1436 sh, m	
1412 br, vw	1412 br, vw	1414 br, w	1414 br, w	1410 br, w	1408 br, vw
1384 sh, vw	1386 sh, vs	1384 br, vw	1388 br, w		
1347 br, w	1346 so	1346 br, m	1352 br, w	1348 br, s	1344 br, vw
		1322 sh, w			
1286 sh, vw		1288 sh, w	1292 sh, m	1288 sh, m	1290 sh, vw
		1246 sh, vw			1244 sh, vw
1213 sh, vw		1210 sh, m	1213 sh, w	1212 sh, w	1208 sh, w
	1120 sh, vw	1112 sh, s		1116 sh, w	1120 sh, vw
1072 sh, m	1074 sh, m	1071 sh, vw	1072 sh, w	1070 sh, s	1070 sh, vw
990 sh, vs	990 sh, w	992 sh, vw	992 sh, vw	992 sh, vs	992 sh, vw
	920 sh, s	920 sh, vw	920 sh, vw	922 sh, vw	920 sh, vw
893 sh, s	893 sh, s	888 sh, s	892 sh, w	892 sh, vw	892 sh, vw
	849 sh, m	846 sh, vw		848 sh, vw	850 sh, vw
812 sh, s	810 sh, m	814 sh, m			

Table 67A-1-017. $NaKC_4H_4O_6 \cdot 4H_2O$. Direction cosines of the proton-proton vectors of the water molecules with respect to the crystallographic axes. See also [55Los, 69ElS]. (7), (8), (9) and (10) in the 1st column are numbers of the water molecule as shown in Fig. 67A-1-006.

	Direction cosines of p–p pairs		
	[70Kat]	[67Bjo]	Differences between both directions
(7)	0.52	0.61	~7°
	0.47	0.45	
	0.72	0.65	
(8)	0.21	0.15	~4°
	0.97	0.98	
	0.14	0.15	
(9)	0.88	0.88	~1°
	0.34	0.34	
	0.34	0.33	
(10)	0.39	0.55	~11°
	0.33	0.33	
	0.86	0.77	

Table 67A-1-018. $NaKC_4H_4O_6 \cdot 4H_2O$, $NaKC_4D_4O_6 \cdot 4D_2O$. ^{23}Na quadrupole coupling constant e^2qQ/h and asymmetry parameter η. (A), (B): monoclinic sublattices at 0 °C.

T	RS		Deuterated RS	
[°C]	e^2qQ/h [MHz]	η	e^2qQ/h [MHz]	η
+30	1.313(14)	0.809(21)	1.313(15)	0.800(30)
0(A)	1.2850(185)	0.872(22)	1.323(15)	0.803(30)
0(B)	1.407(20)	0.675(29)	1.419(15)	0.639(30)
–40			1.395(15)	0.636(30)
–25	1.363(4) *)	0.737(4) *)		
Ref.	[66Mil] *) [70Fit]	[66Mil] *) [70Fit]	[64Bli]	[64Bli]

Table 67A-1-019. $NaKC_4H_4O_6 \cdot 4H_2O$. Direction cosines of the principal axes ($X\ Y\ Z$) of an electric-field gradient tensor of Na spectrum relative to the crystallographic axes ($a\ b\ c$) [66Mil]. (A), (B): monoclinic sublattices at 0 °C.

T	Crystal axis	Principal axes		
[°C]		X	Y	Z
30	*a*	0.178	0.574	0.799
	b	–0.021	–0.810	0.586
	c	–0.984	0.122	0.132
0(A)	*a*	0.208	0.559	0.803
	b	–0.068	–0.809	0.583
	c	–0.976	0.182	0.123
0(B)	*a*	0.157	0.592	0.791
	b	–0.008	–0.801	0.599
	c	–0.988	0.090	0.126

Table 67A-1-020. $NaKC_4H_4O_6 \cdot 4H_2O:Cu^{2+}$. ESR data [71Vol].

Paramagnetic center	Cu^{2+} (S = 1/2)
g-factor	g_x = 2.041(5)
	g_y = 2.094(5)
	g_z = 2.326(2)
HFS [10^{-2} m^{-1}]	A_x = –39(4)
	A_y = –21(4)
	A_z = –123(1)
	$Q_z \cong 10$

Table 67A-1-021. $NaKC_4H_4O_6 \cdot 4H_2O$. Spin Hamiltonian parameters g and A [$\cdot 10^{-2}$ m^{-1}] for VO^{2+} ions [80Jai]. T = 300 K. θ: the angle between the b and z axes. φ: the angle between the c axis and the projection of z on the ac plane.

Parameters	Site I	Site II	Site III	Site IV	Powder
g_z	1.958(2)	1.959(2)	1.956(2)	1.947(3)	1.955
g_x	1.979(2)	1.989(2)	1.996(3)	-	1.984
g_y	1.987(2)	1.992(2)	-	-	-
A_z	150.4(5)	148.5(5)	159.0(10)	162.0(20)	151.0
A_x	53.0(10)	37.8(10)	40.0(20)	-	49.0
A_y	42.0(10)	36.8(10)	-	-	-
θ	80(1)°	56(2)°	-	-	-
φ	38(2)°	–40(4)°	-	-	-
Intensity	20	8	3	1	-

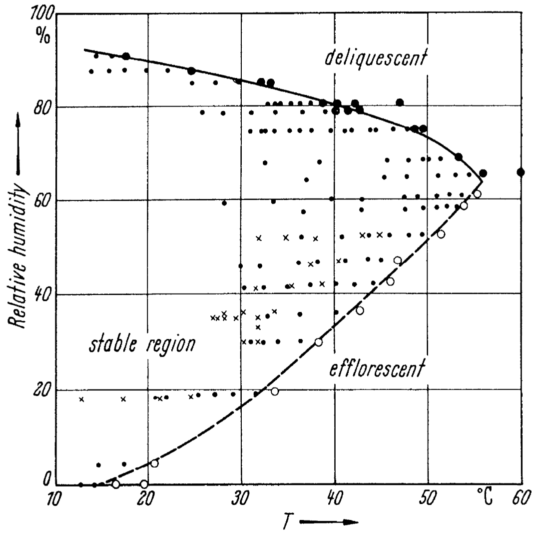

Fig. 67A-1-001. $NaKC_4H_4O_6 \cdot 4H_2O$. Stable region for deliquescence and efflorescence [43Kaw]. Open circle, large full circle: a virgin sample which has undergone efflorescence or deliquescence. Small full circle, cross: a sample which has not undergone any change. Small full circle: a virgin sample. Cross: a sample which has once undergone efflorescence.

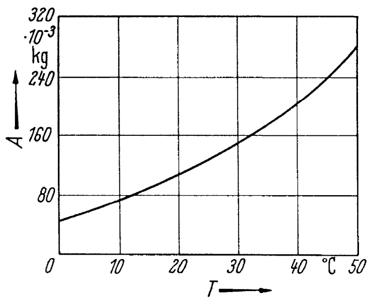

Fig. 67A-1-002. $NaKC_4H_4O_6 \cdot 4H_2O$. A vs. T [49Miy]. A: mass of Rochelle salt soluble in 100 cm^3 (= 10^{-4} m^3) H_2O.

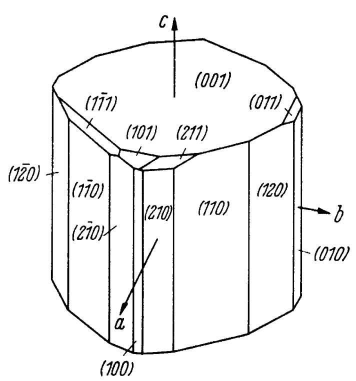

Fig. 67A-1-003. $NaKC_4H_4O_6 \cdot 4H_2O$. Crystal form of d-crystal [68Mar]. $X \parallel a$, $Y \parallel b$, $Z \parallel c$.

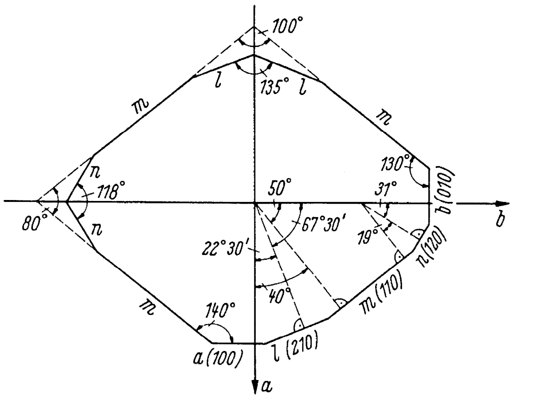

Fig. 67A-1-004. $NaKC_4H_4O_6 \cdot 4H_2O$. Crystal form [62Jon]. The drawing represents the cross-section ⊥ to [001].

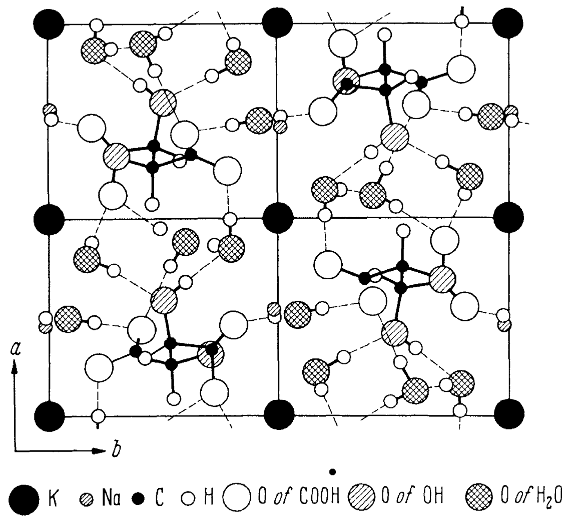

Fig. 67A-1-005. $NaKC_4H_4O_6 \cdot 4H_2O$. Projection of the structure on (001) [55Shi]. The hydrogen bond system.

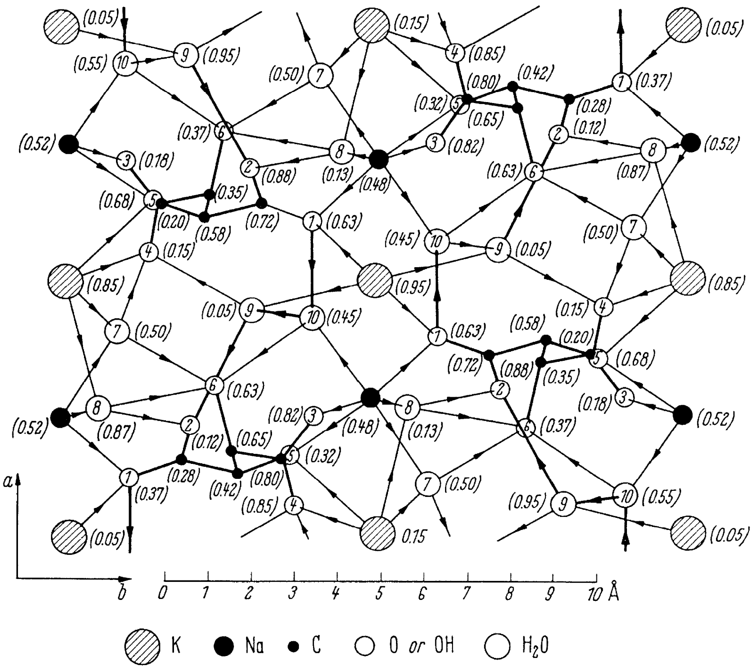

Fig. 67A-1-006. $NaKC_4H_4O_6 \cdot 4H_2O$. Projection of the structure on (001) [41Bee]. The oxygen atoms are numbered from *1* to *10*. Figures in parentheses are *z* coordinates of atoms (see Table 67A-1-002). The arrow heads on the bonds are drawn in a direction from positive atoms to negative atoms. The structure determination was made at RT, but the resolution was not enough to show the effect of the monoclinic symmetry.

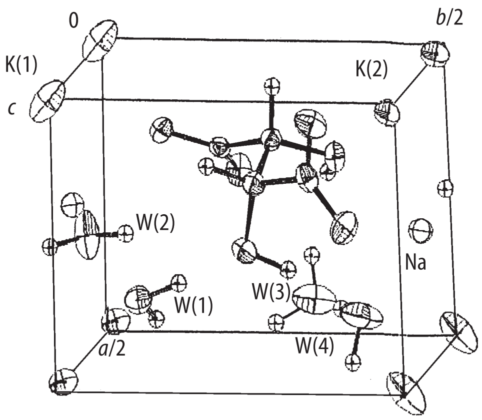

Fig. 67A-1-007. $NaKC_4H_4O_6 \cdot 4H_2O$. Structure of phase I [89Iwa]. View of the crystallographically independent part of a unit cell. Hydrogen atoms (small spheres) are fixed at the positions obtained from the neutron study. Letter "W" means water molecule. Anisotropic temperature parameters are illustrated.

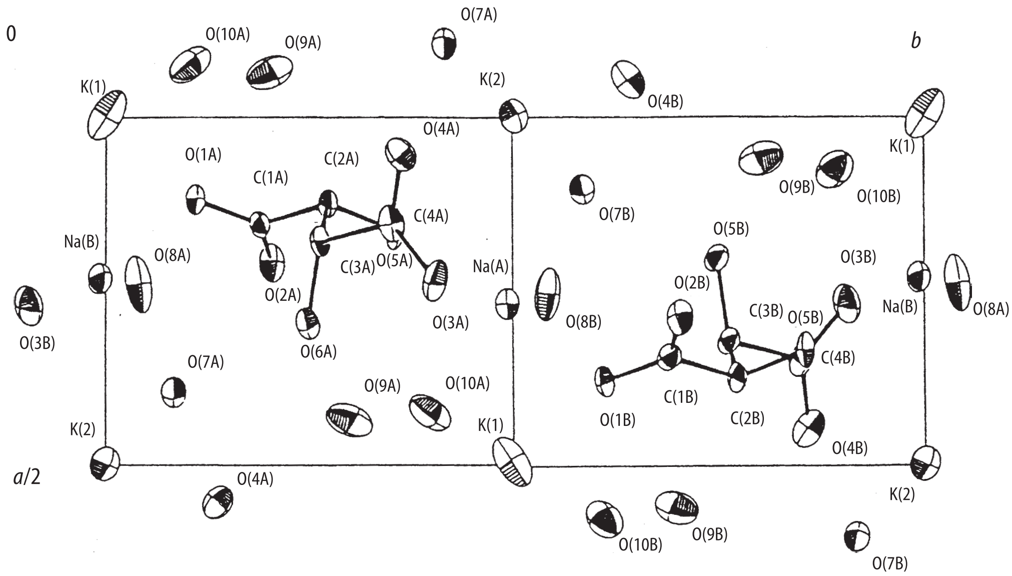

Fig. 67A-1-008. $NaKC_4H_4O_6 \cdot 4H_2O$. Structure of phase II [94Suz]. T = 273 K. Projection along ***c***. Hydrogen atoms are omitted.

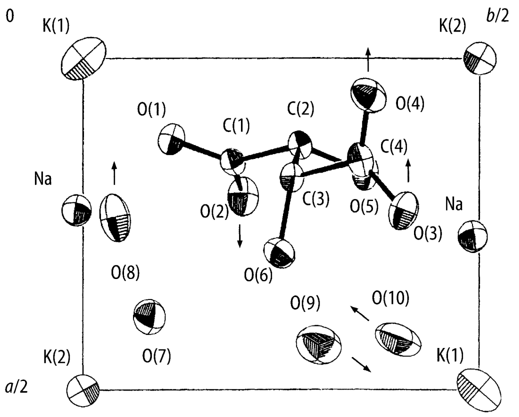

Fig. 67A-1-009. $NaKC_4H_4O_6 \cdot 4H_2O$. Structure of phase III [96Shi]. Projection of the asymmetric unit along *c*. T = 153 K. Arrows show sense of the major atomic displacements from the positions at T = 253 K.

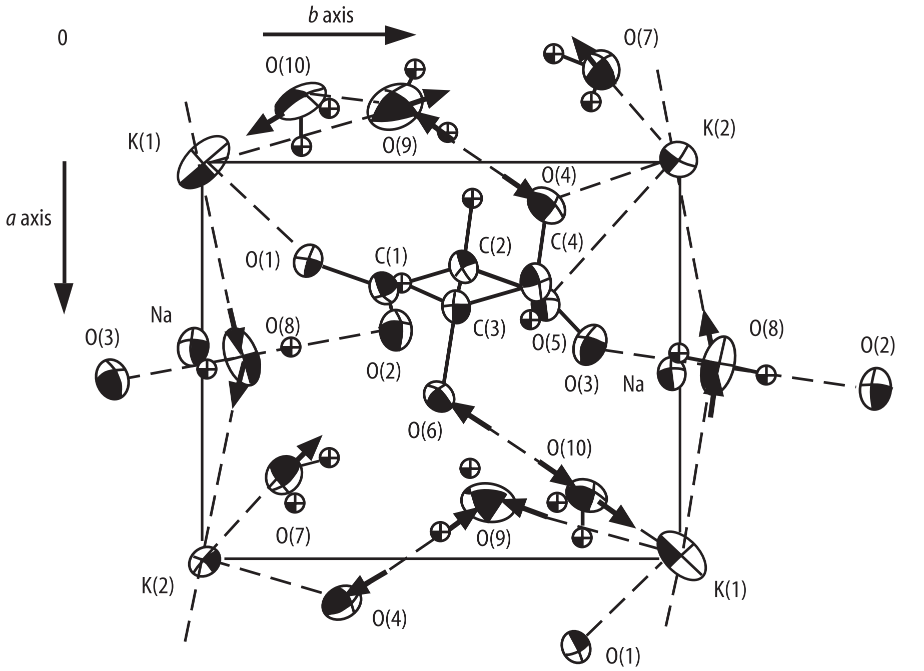

Fig. 67A-1-010. $NaKC_4H_4O_6 \cdot 4H_2O$. Structure of phase III [98Shi]. Projection along *c*. Dashed lines show major interactions. Arrows show sense of the major atomic displacements when temperature is increased to Θ_{III-II}.

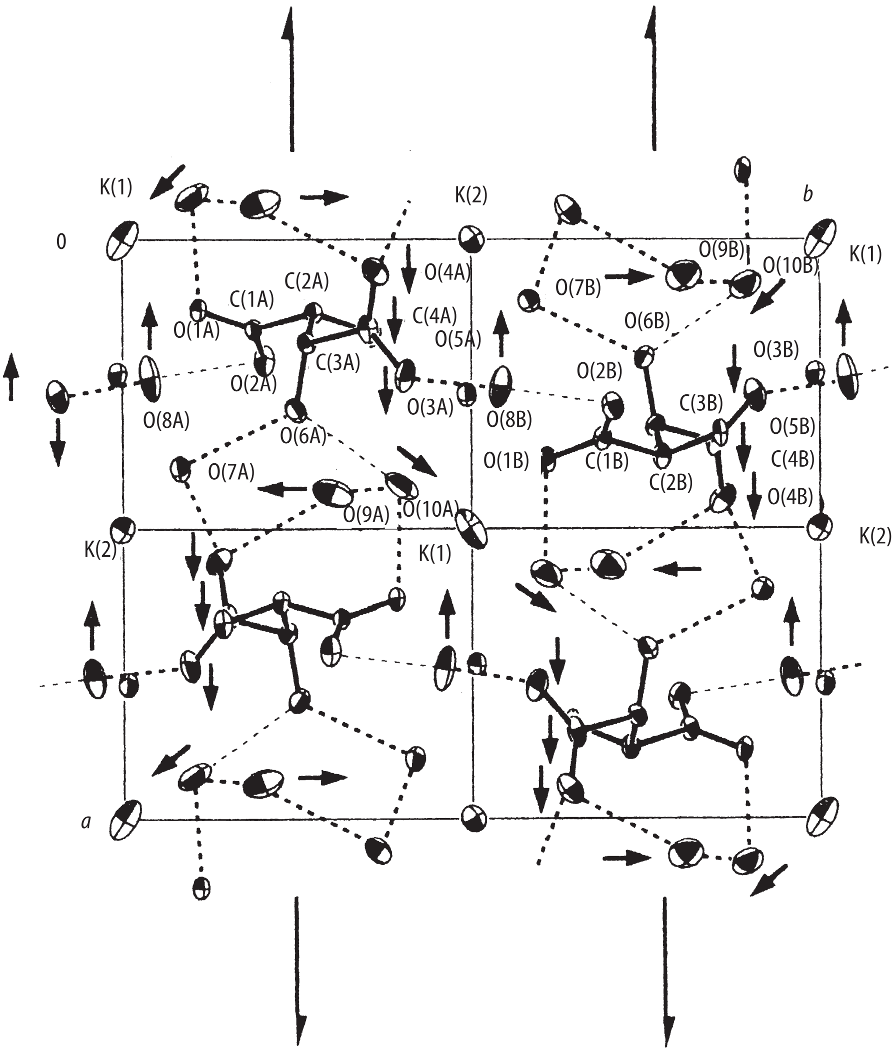

Fig. 67A-1-011. $NaKC_4H_4O_6 \cdot 4H_2O$. Schematic view of the unit cell in phase II viewed along *c* [96Suz]. *T* = 273 K. Arrows indicate the direction of the displacement of atoms from the paraelectric positions.

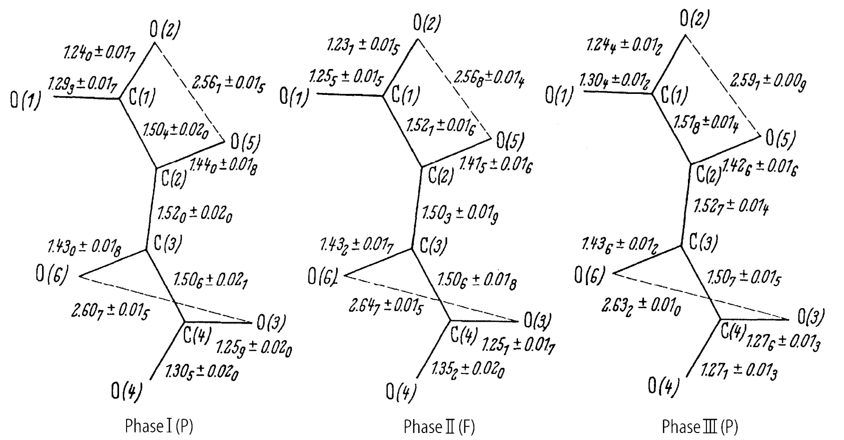

Fig. 67A-1-012. $NaKC_4H_4O_6 \cdot 4H_2O$. Interatomic distances [Å] in the tartrate ion in the phases I, II and III [60Krs].

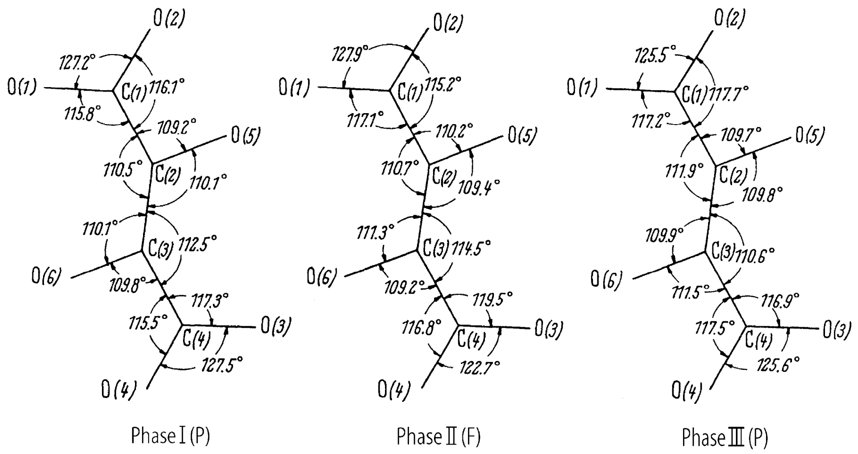

Fig. 67A-1-013. $NaKC_4H_4O_6 \cdot 4H_2O$. Bond angles in the tartrate ion in the phases I, II and III [60Krs].

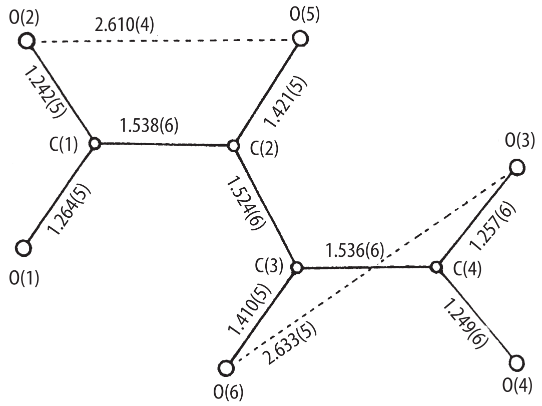

Fig. 67A-1-014. $NaKC_4H_4O_6 \cdot 4H_2O$. Interatomic distances [Å] in the tartrate ion at 24 °C [89Iwa].

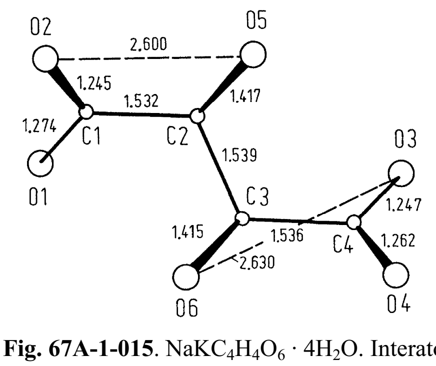

Fig. 67A-1-015. $NaKC_4H_4O_6 \cdot 4H_2O$. Interatomic distances [Å] in the tartrate ion in phase II [72Shi].

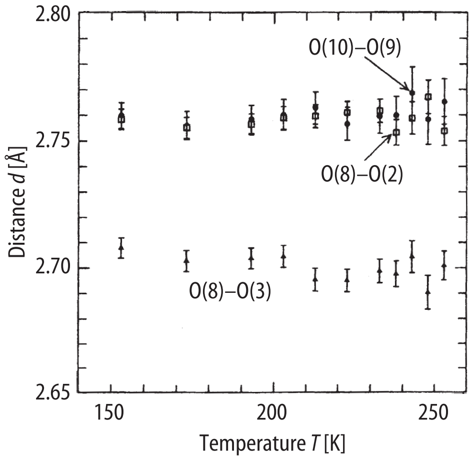

Fig. 67A-1-016. $NaKC_4H_4O_6 \cdot 4H_2O$. d vs. T [98Shi]. d: interatomic distances of O(8)–O(2), O(8)–O(3) and O(10)–O(9).

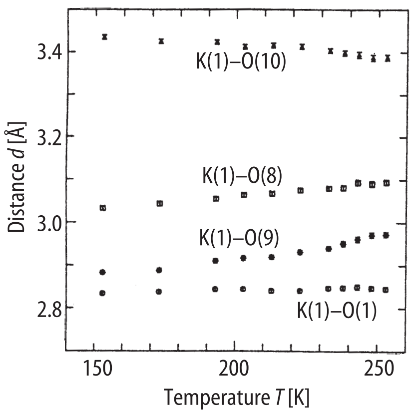

Fig. 67A-1-017. $NaKC_4H_4O_6 \cdot 4H_2O$. d vs. T in phase III [96Shi]. d: interatomic distances between K(1) and the surrounding oxygens.

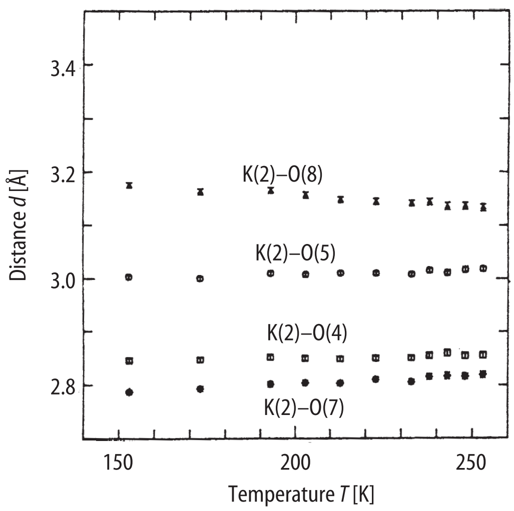

Fig. 67A-1-018. $NaKC_4H_4O_6 \cdot 4H_2O$. d vs. T in phase III [96Shi]. d: interatomic distances between K(2) and the surrounding oxygens.

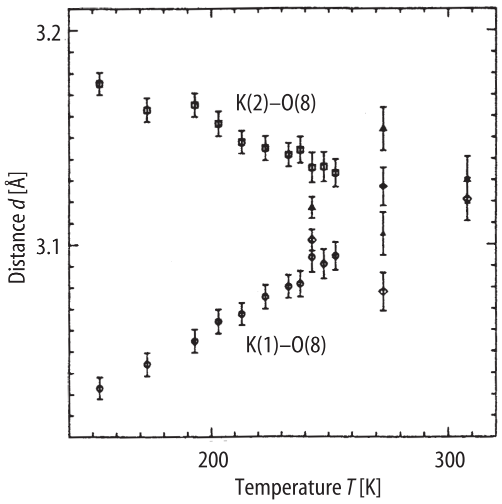

Fig. 67A-1-019. $NaKC_4H_4O_6 \cdot 4H_2O$. d vs. T in phase II [96Shi]. d: interatomic distances between O(8) and K(1), K(2).

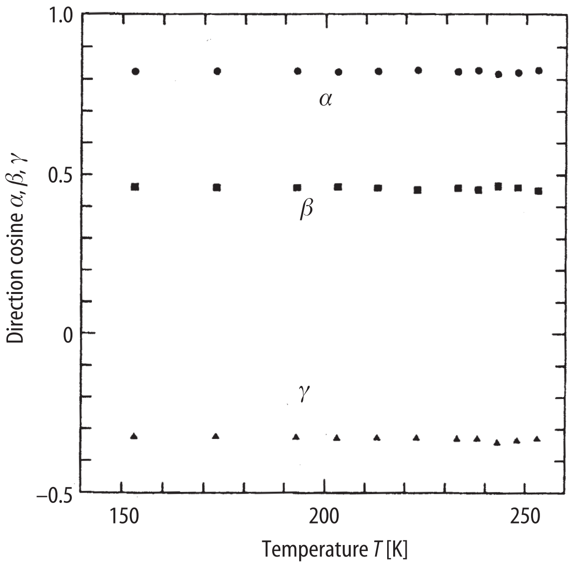

Fig. 67A-1-020. $NaKC_4H_4O_6 \cdot 4H_2O$. α, β, γ vs. T [98Shi]. α, β, γ: direction cosines of C–C–C–C plane of the tartrate molecule in the orthorhombic crystallographic system a, b, c.

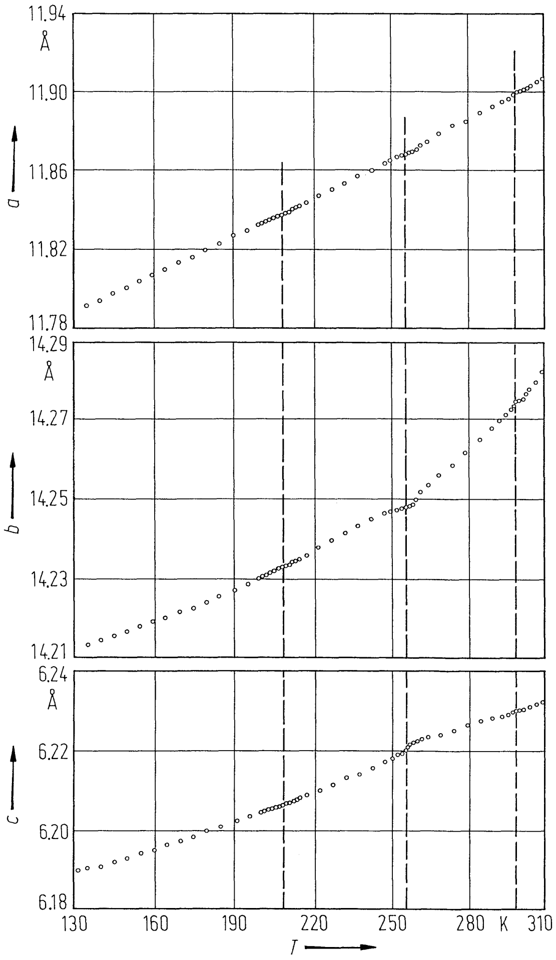

Fig. 67A-1-021. $NaKC_4H_4O_6 \cdot 4H_2O$. *a*, *b*, *c* vs. *T* [81Bro]. *a*, *b*, *c*: unit cell parameters.

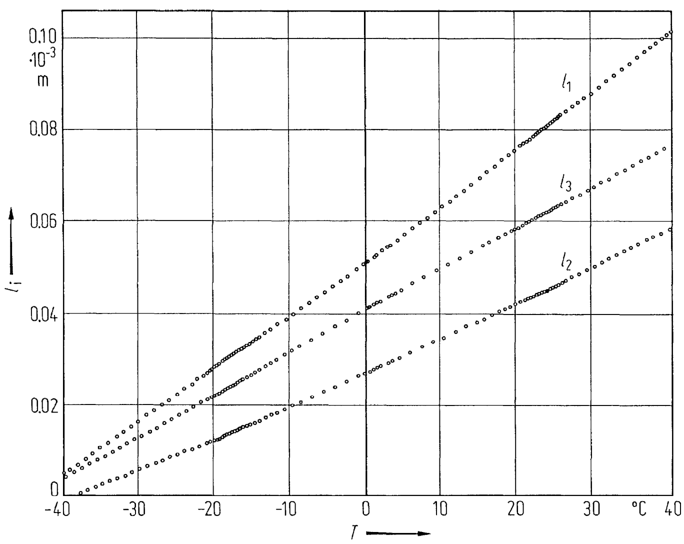

Fig. 67A-1-022. $NaKC_4H_4O_6 \cdot 4H_2O$. l_1, l_2, l_3 vs. *T* [76Ima]. l_1, l_2, l_3: thermal dilatation along the *a*, *b*, *c* axes.

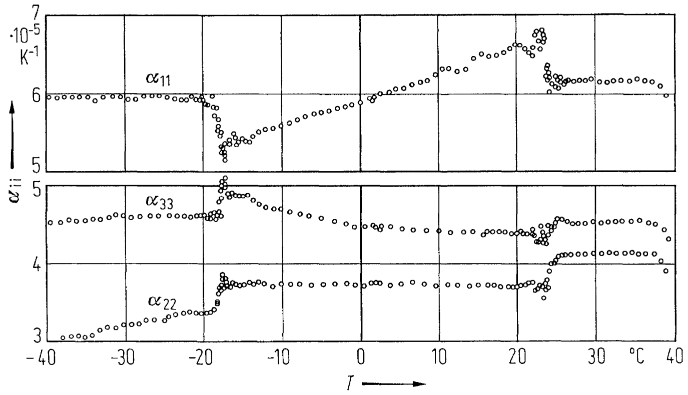

Fig. 67A-1-023. $NaKC_4H_4O_6 \cdot 4H_2O$. α_{11}, α_{22}, α_{33} vs. T [76Ima]. α_{11}, α_{22}, α_{33}: linear thermal expansion coefficients.

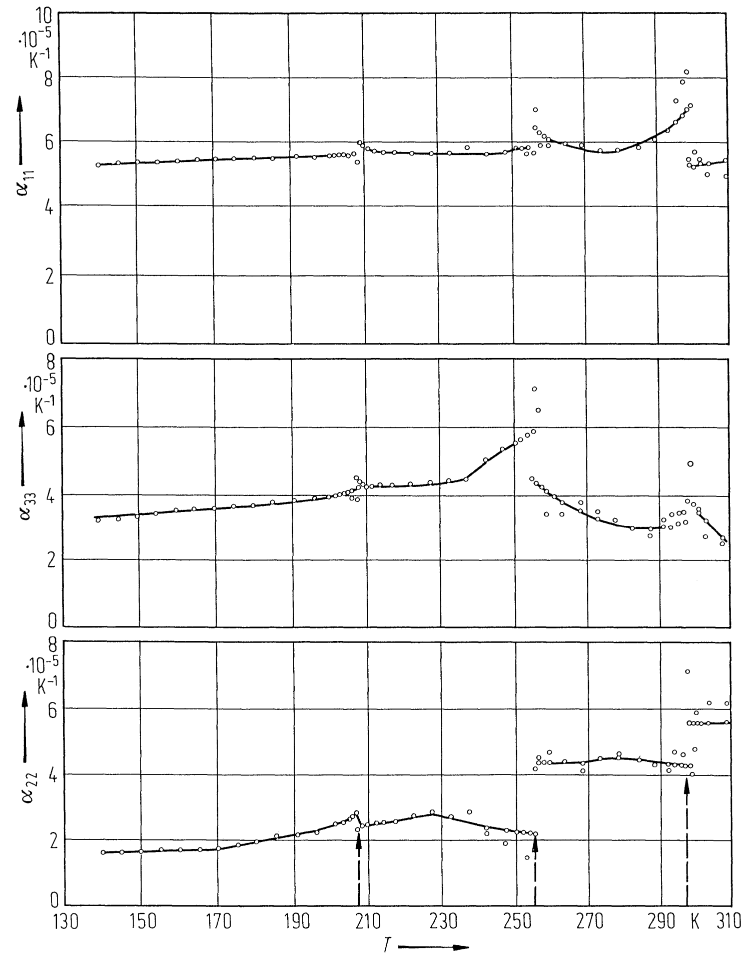

Fig. 67A-1-024. $NaKC_4H_4O_6 \cdot 4H_2O$. α_{11}, α_{22}, α_{33} vs. T [81Bro]. α_{11}, α_{22}, α_{33}: linear thermal expansion coefficients.

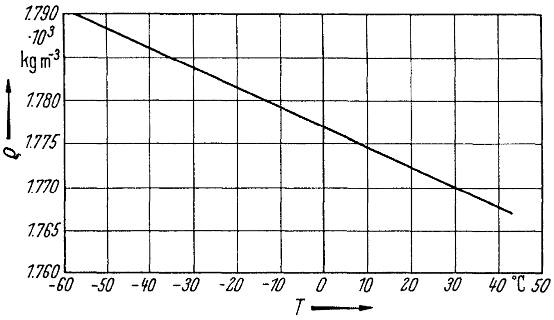

Fig. 67A-1-025. $NaKC_4H_4O_6 \cdot 4H_2O$. ρ vs. T [50Jon]. ρ: density.

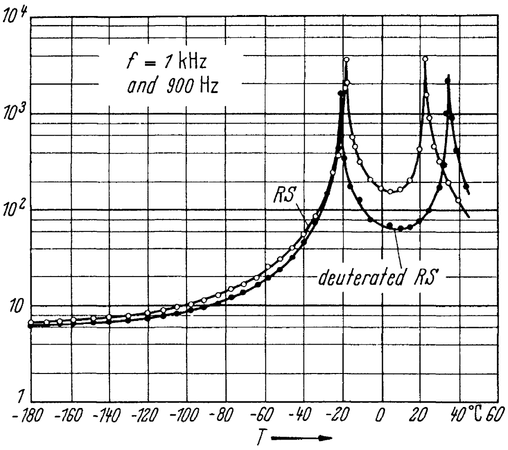

Fig. 67A-1-026. $NaKC_4H_4O_6 \cdot 4H_2O$, $NaKC_4H_2D_2O_6 \cdot 4D_2O$. κ_{11}^{T} vs. T [39Hab].

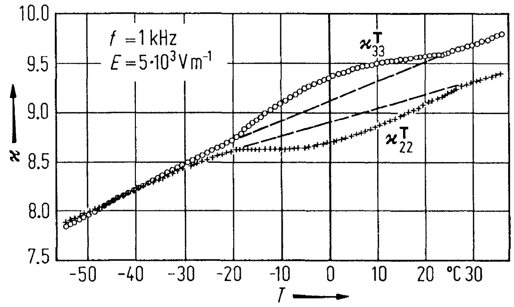

Fig. 67A-1-027. $NaKC_4H_4O_6 \cdot 4H_2O$. κ_{22}^{T}, κ_{33}^{T} vs. T [68For]. Relative humidity: 12 %.

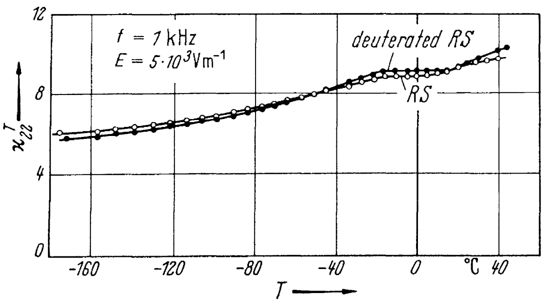

Fig. 67A-1-028. $NaKC_4H_4O_6 \cdot 4H_2O$, $NaKC_4H_2D_2O_6 \cdot 4D_2O$. κ_{22}^{T} vs. T [39Hab].

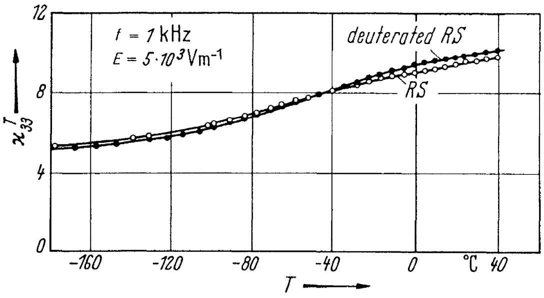

Fig. 67A-1-029. $NaKC_4H_4O_6 \cdot 4H_2O$, $NaKC_4H_2D_2O_6 \cdot 4D_2O$. κ_{33}^{T} vs. T [39Hab].

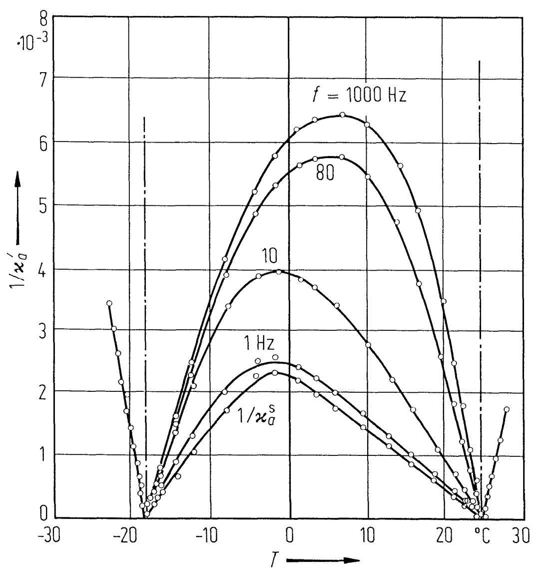

Fig. 67A-1-030. $NaKC_4H_4O_6 \cdot 4H_2O$. $1/\kappa_a'$ vs. T [86Shi]. Parameter: f. κ_a^s : static dielectric constant obtained from the Cole-Cole dispersion equation.

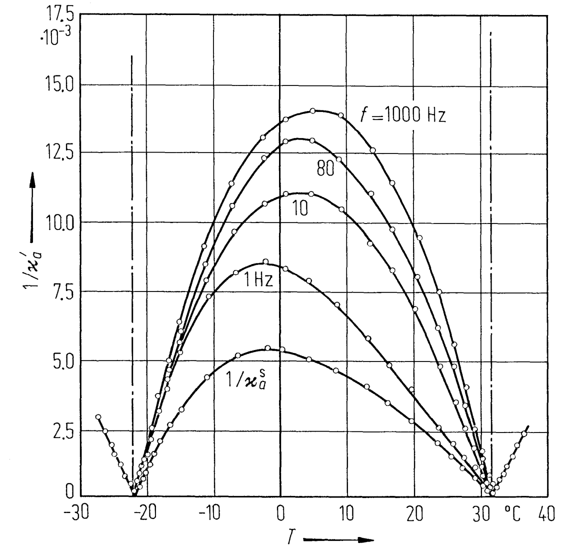

Fig. 67A-1-031. $NaKC_4D_4O_6 \cdot 4D_2O$. $1/\kappa'_a$ vs. T [86Shi]. Parameter: f. κ^s_a : static dielectric constant obtained from the Cole-Cole dispersion equation.

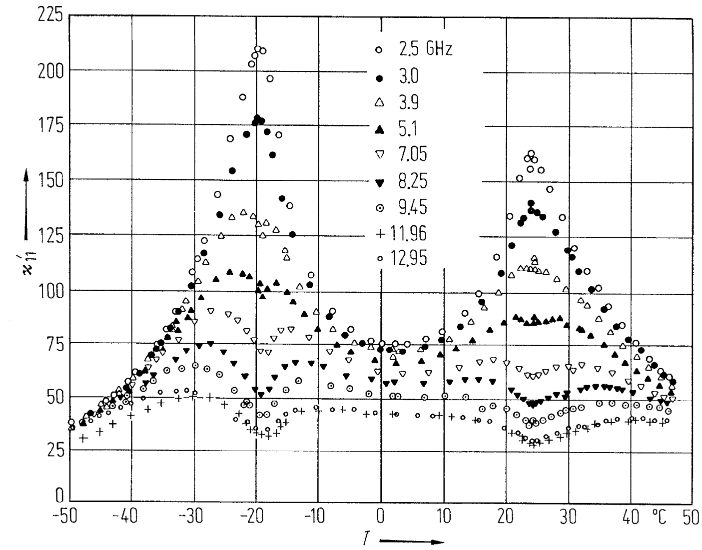

Fig. 67A-1-032. $NaKC_4H_4O_6 \cdot 4H_2O$. κ'_{11} vs. T [68San]. Parameter: f.

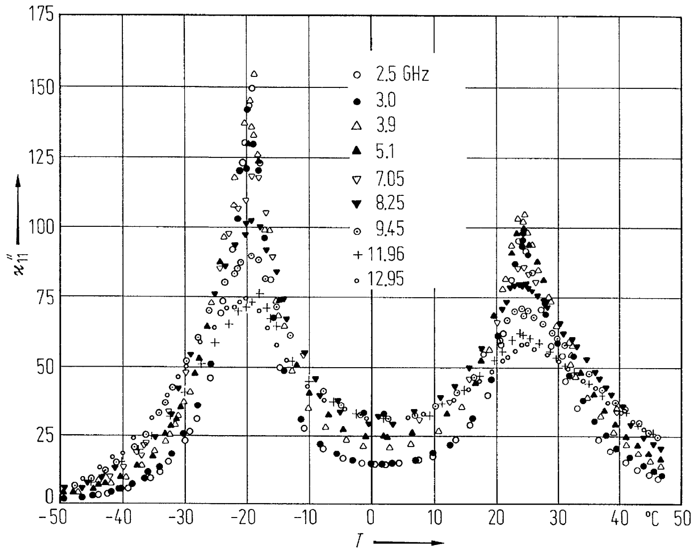

Fig. 67A-1-033. $NaKC_4H_4O_6 \cdot 4H_2O$. κ''_{11} vs. T [68San]. Parameter: *f*.

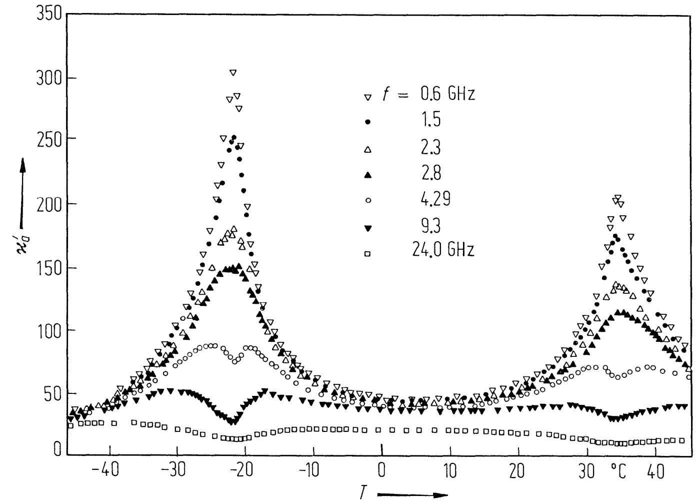

Fig. 67A-1-034. $NaKC_4D_4O_6 \cdot 4D_2O$. κ'_a vs. T [79Hor]. Parameter: *f*.

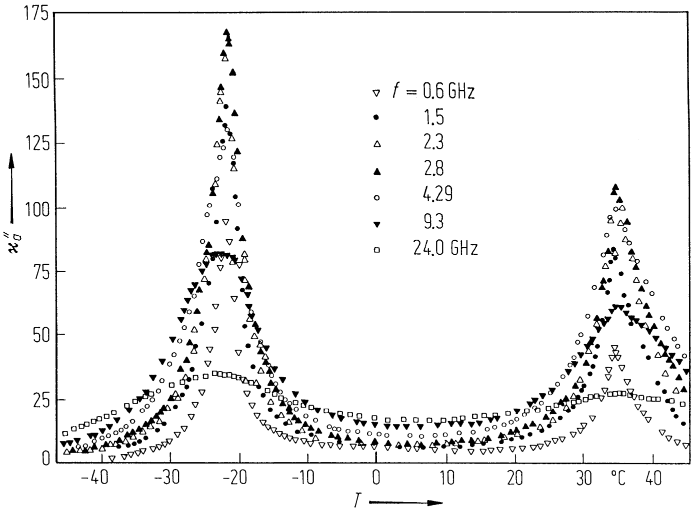

Fig. 67A-1-035. $NaKC_4D_4O_6 \cdot 4D_2O$. κ''_a vs. T [79Hor]. Parameter: f.

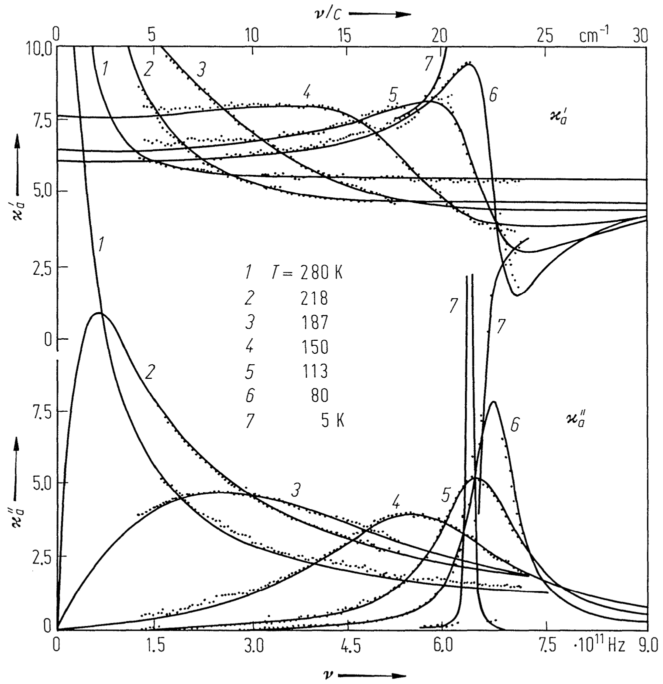

Fig. 67A-1-036. $NaKC_4H_4O_6 \cdot 4H_2O$. κ'_a, κ''_a vs. ν [86Vol]. Parameter: T. Solid line: calculated value of single-oscillator model.

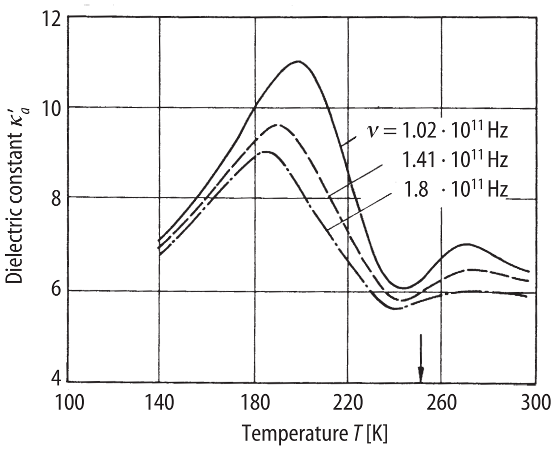

Fig. 67A-1-037. $NaKC_4D_4O_6 \cdot 4D_2O$. κ_a' vs. T [82Vol]. Parameter: ν. The arrow indicates Θ_{III-II}.

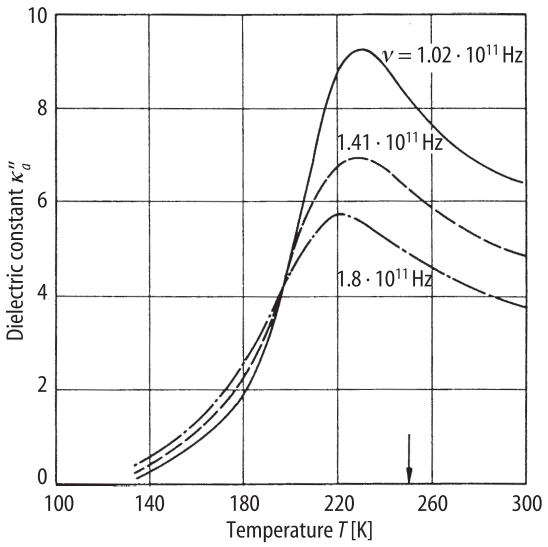

Fig. 67A-1-038. $NaKC_4D_4O_6 \cdot 4D_2O$. κ_a'' vs. T [82Vol]. Parameter: ν. The arrow indicates Θ_{III-II}.

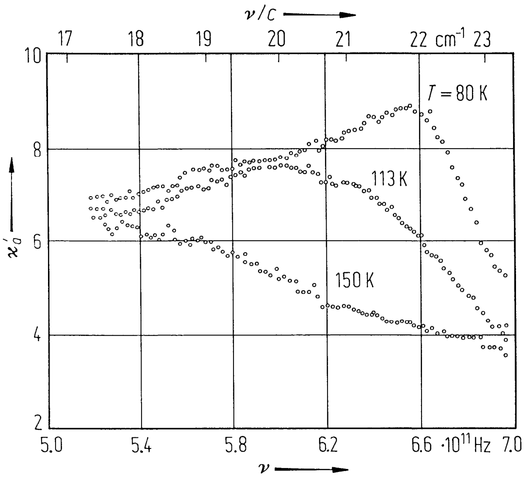

Fig. 67A-1-039. $NaKC_4H_2D_2O_6 \cdot 4D_2O$. κ'_a vs. ν [86Vol]. Parameter: T.

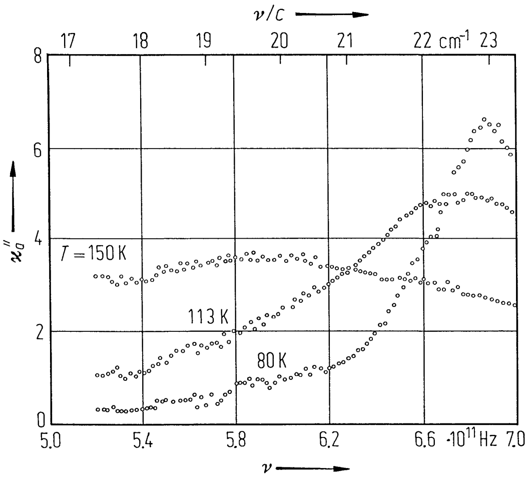

Fig. 67A-1-040. $NaKC_4H_2D_2O_6 \cdot 4D_2O$. κ''_a vs. ν [86Vol]. Parameter: T.

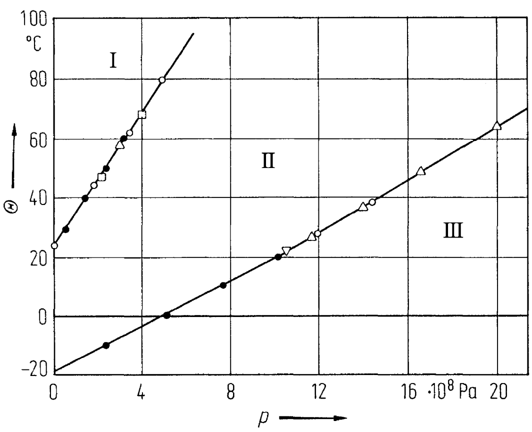

Fig. 67A-1-041. $NaKC_4H_4O_6 \cdot 4H_2O$. Θ vs. p [65Sam]. Full circles are data given by [38Ban]. Different symbols represent results of different runs.

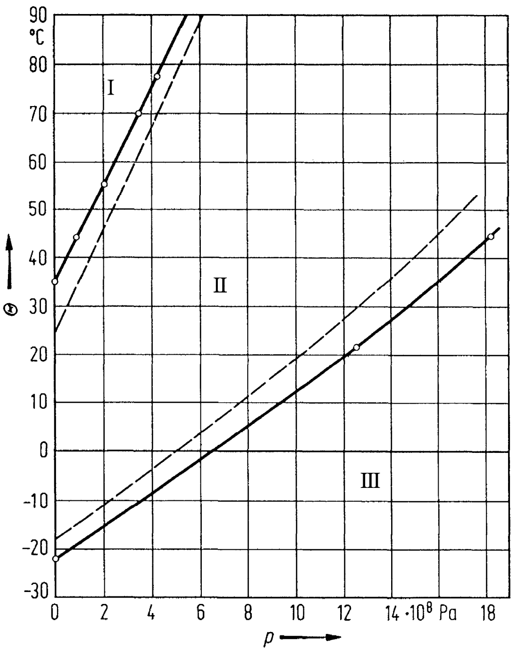

Fig. 67A-1-042. $NaKC_4H_4O_6 \cdot 4H_2O$, $NaKC_4H_2D_2O_6 \cdot 4D_2O$. Θ vs. p [68Sam]. Full line: deuterated salt. Broken line: undeuterated salt.

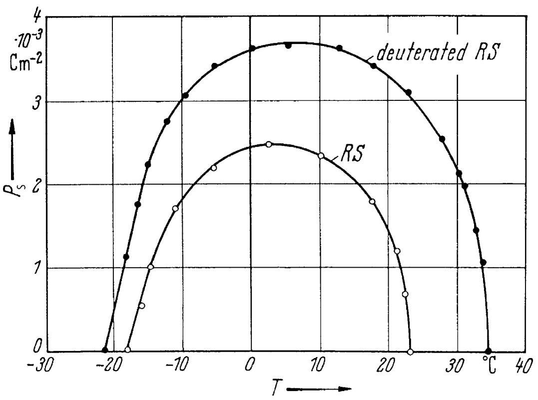

Fig. 67A-1-043. $NaKC_4H_4O_6 \cdot 4H_2O$, $NaKC_4H_2D_2O_6 \cdot 4D_2O$. P_s vs. T [39Hab].

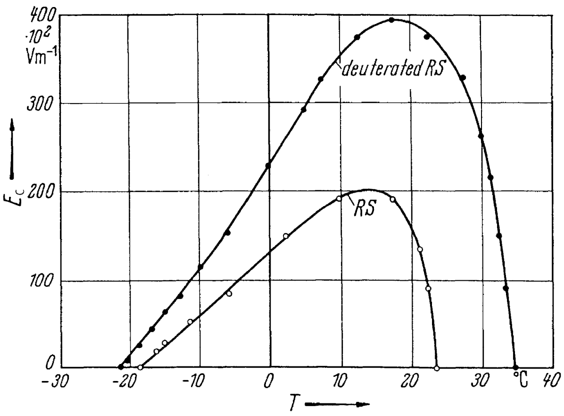

Fig. 67A-1-044. $NaKC_4H_4O_6 \cdot 4H_2O$, $NaKC_4H_2D_2O_6 \cdot 4D_2O$. E_c vs. T [39Hab].

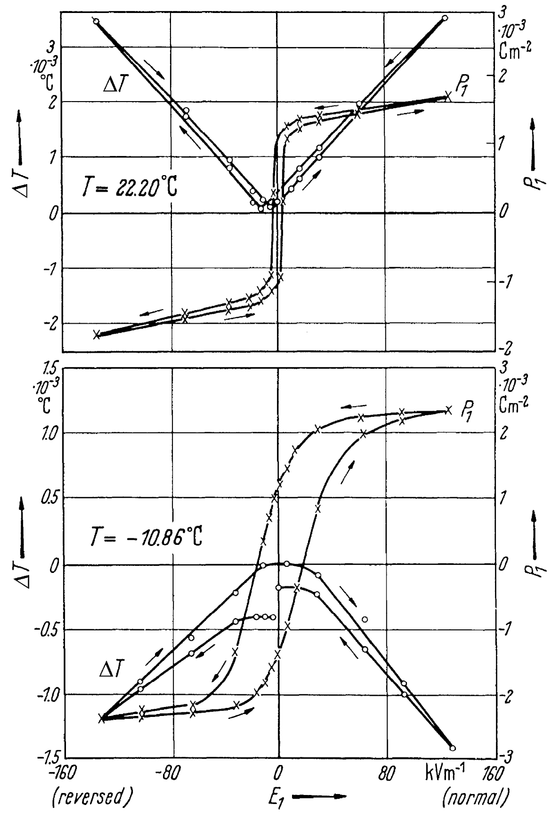

Fig. 67A-1-045. $NaKC_4H_4O_6 \cdot 4H_2O$. ΔT, P_1 vs. E_1 [63Wis]. ΔT: electrocaloric temperature change. P_1, E_1: component of ***P***, ***E***.

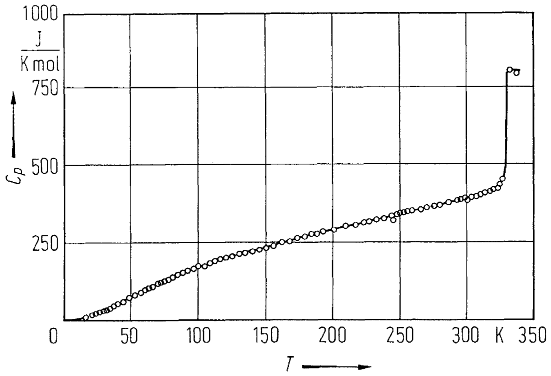

Fig. 67A-1-046. $NaKC_4H_4O_6 \cdot 4H_2O$. C_p vs. T [38Hic].

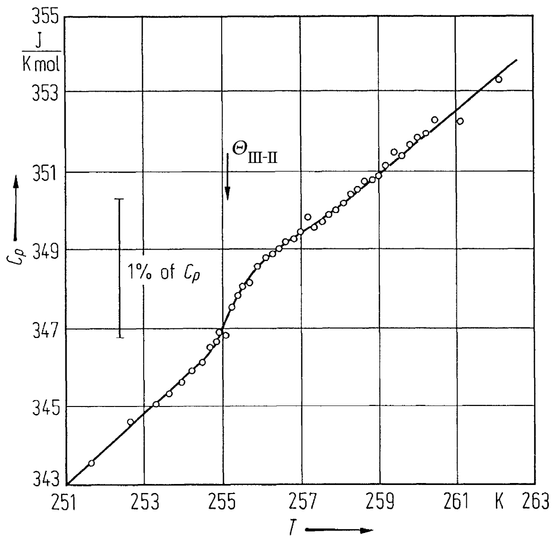

Fig. 67A-1-047. $NaKC_4H_4O_6 \cdot 4H_2O$. C_p vs. T in the vicinity of $\Theta_{III\text{–}II}$ [78Tat].

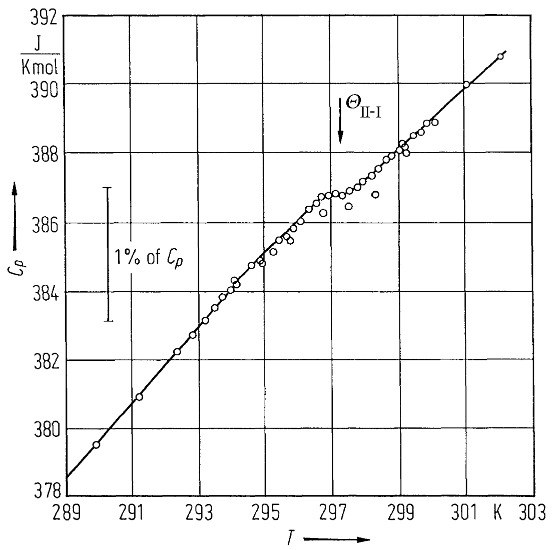

Fig. 67A-1-048. $NaKC_4H_4O_6 \cdot 4H_2O$. C_p vs. T in the vicinity of $\Theta_{II\text{–}I}$ [78Tat].

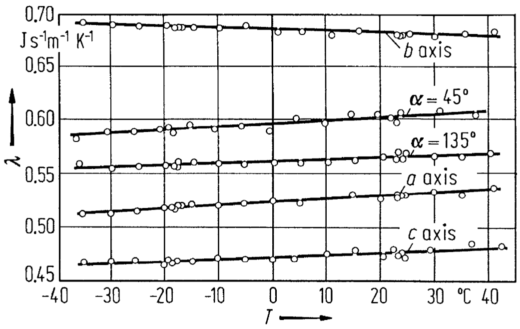

Fig. 67A-1-049. $NaKC_4H_4O_6 \cdot 4H_2O$. λ vs. T [72Sch]. λ: thermal conductivity. $\alpha = 45°$ and $\alpha = 135°$ give two directions perpendicular to the a axis.

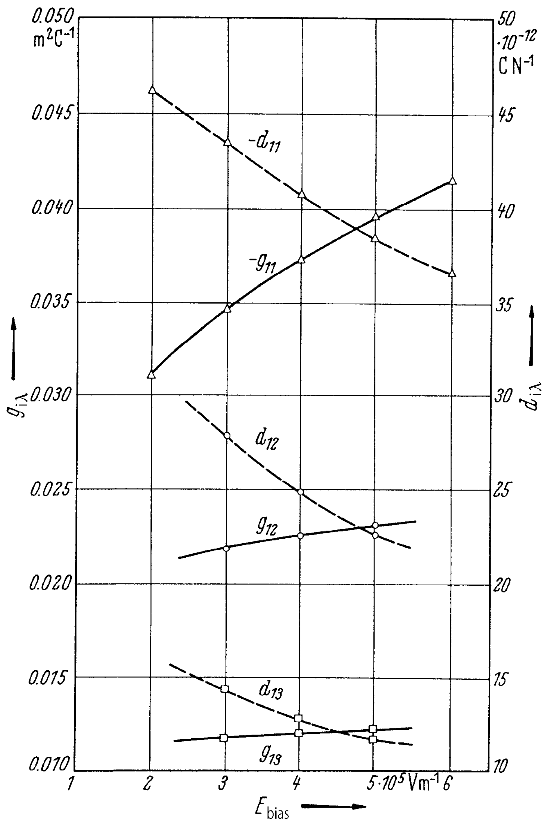

Fig. 67A-1-050. $NaKC_4H_4O_6 \cdot 4H_2O$. $g_{i\lambda}$, $d_{i\lambda}$ vs. E_{bias} at 17 °C [61Sch]. See also [60Fot].

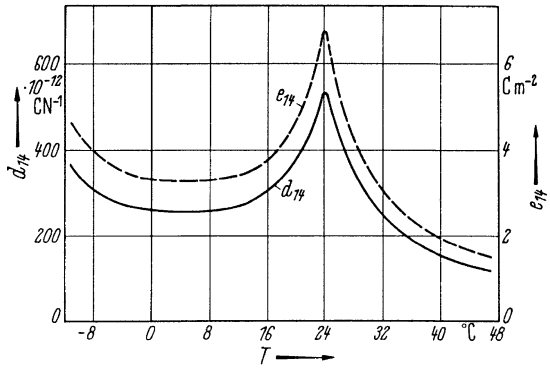

Fig. 67A-1-051. $NaKC_4H_4O_6 \cdot 4H_2O$. d_{14}, e_{14} vs. T [39Mas1].

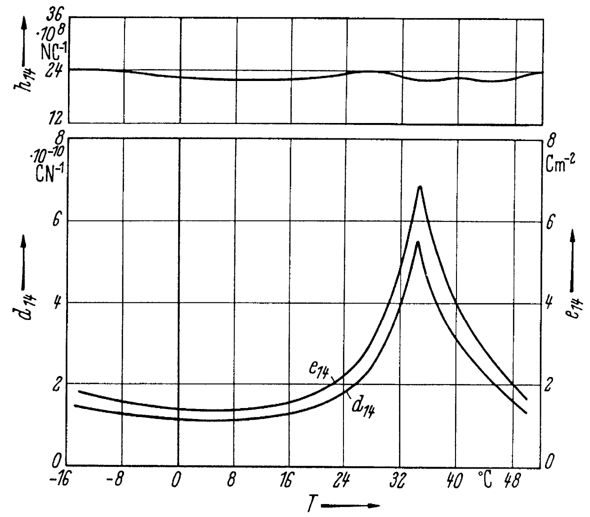

Fig. 67A-1-052. $NaKC_4H_2D_2O_6 \cdot 4D_2O$. d_{14}, e_{14}, h_{14} vs. T [40Hol].

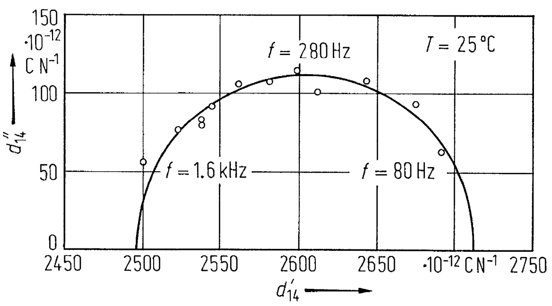

Fig. 67A-1-053. $NaKC_4H_4O_6 \cdot 4H_2O$. Debye circle for d_{14} in the complex plane ($d_{14} = d'_{14} - jd''_{14}$) [72Mus].

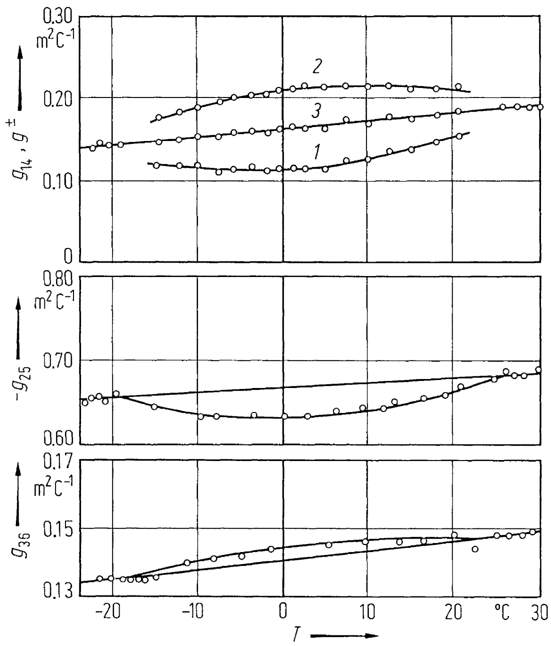

Fig. 67A-1-054. $NaKC_4H_4O_6 \cdot 4H_2O$. $g_{i\lambda}$ vs. T [76Sch]. Strain is measured by capacitive dilatometric method. The curves *1*, *2* show $g^{\pm} = g_{14} \pm (g_{12} + g_{13})$, *3* shows $g_{14} = (g^{+} + g^{-})/2$. See also [67Unr, 56Mus].

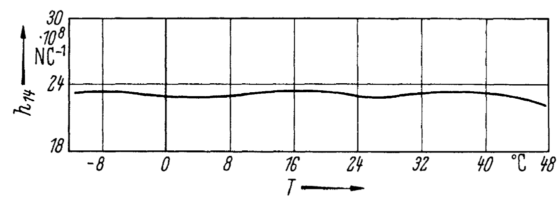

Fig. 67A-1-055. $NaKC_4H_4O_6 \cdot 4H_2O$. h_{14} vs. T [39Mas1].

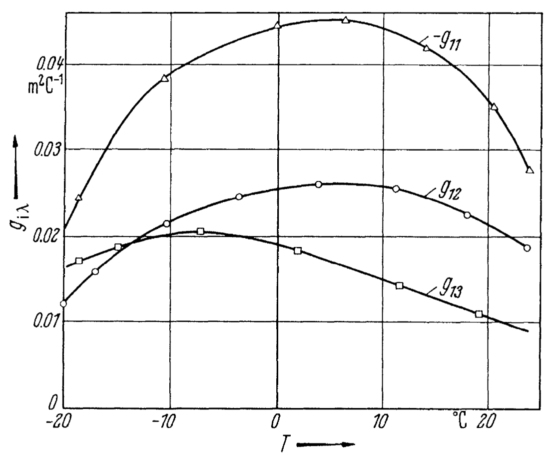

Fig. 67A-1-056. $NaKC_4H_4O_6 \cdot 4H_2O$. $-g_{11}$, g_{12}, g_{13} vs. T [61Sch]. $E_{bias} = 5 \cdot 10^5$ V m^{-1}.

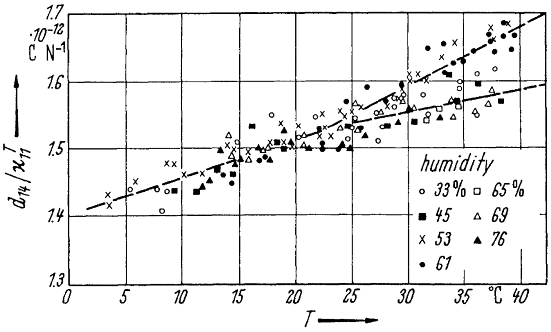

Fig. 67A-1-057. $NaKC_4H_4O_6 \cdot 4H_2O$. d_{14} / κ_{11}^{T} vs. T [47Kaw1]. Parameter: humidity. See also [49Kaw].

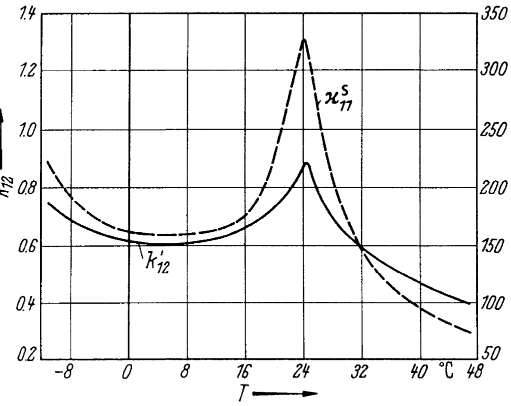

Fig. 67A-1-058. $NaKC_4H_4O_6 \cdot 4H_2O$. κ_{11}^{S}, k'_{12} vs. T [39Mas1]. k'_{12}: electromechanical coupling factor of a 45° X-cut bar (|| [011]), namely $(k'_{12})^2 = (d'_{12})^2 / \varepsilon_{11}^{T}(s'_{22})^{E}$, $d'_{12} = d_{14}/2$, $(s'_{22})^{E} = (s_{22} + s_{33} + 2s_{23} + s_{44}^{E})/4$.

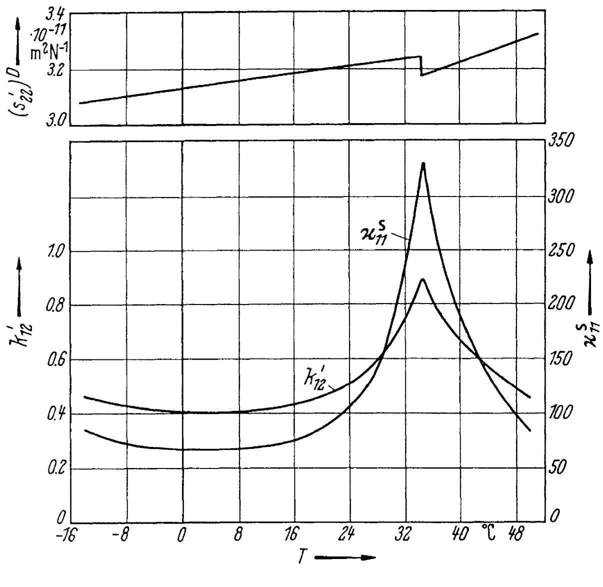

Fig. 67A-1-059. $NaKC_4H_2D_2O_6 \cdot 4D_2O$. $(s'_{22})^{D}$, k'_{12}, κ_{11}^{S} vs. T [40Hol]. See the caption of Fig. 67A-1-058.

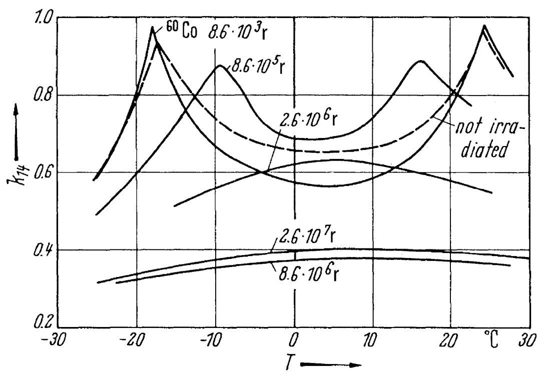

Fig. 67A-1-060. $NaKC_4H_4O_6 \cdot 4H_2O$. k_{14} vs. T [63Kru]. Parameter: ^{60}Co irradiation level. 1r = 2.58 · 10^{-4} C kg^{-1}.

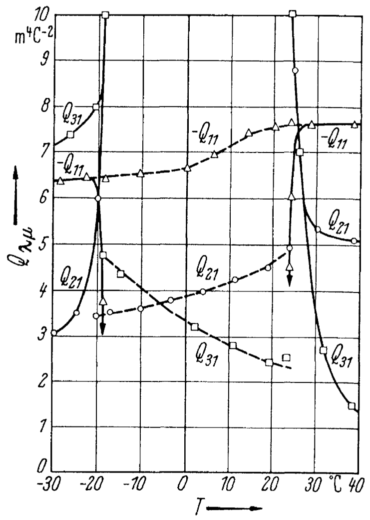

Fig. 67A-1-061. $NaKC_4H_4O_6 \cdot 4H_2O$. $-Q_{11}$, Q_{21}, Q_{31} vs. T [61Sch]. Q_{11}, Q_{21}, Q_{31}: electrostrictive constants. See also [67Unr].

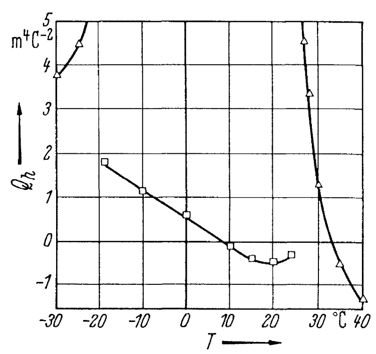

Fig. 67A-1-062. $NaKC_4H_4O_6 \cdot 4H_2O$. Q_h vs. T [61Sch]. Q_h: volume electrostrictive constant.

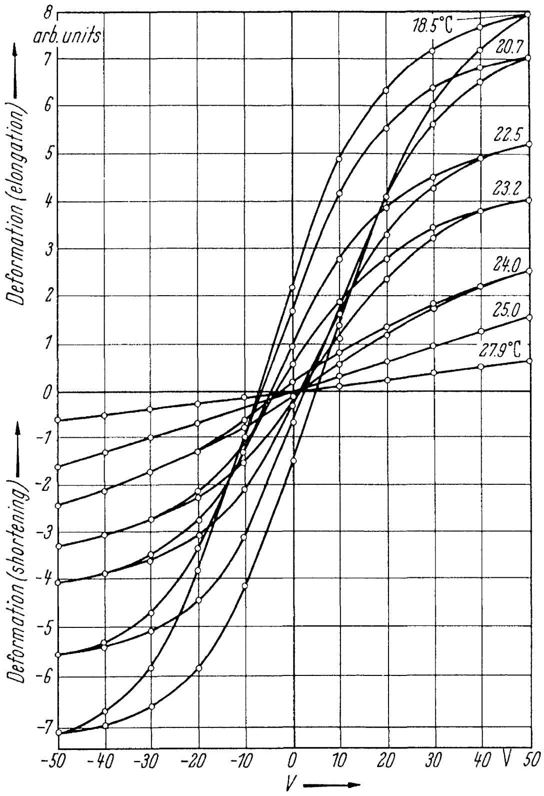

Fig. 67A-1-063. $NaKC_4H_4O_6 \cdot 4H_2O$. Deformation vs. *V* [39Hin]. Parameter: *T*. One division of the deformation corresponds to an elongation of $3.6 \cdot 10^{-5}$ m m^{-1} along [011], and 1 V corresponds to $E = 5.7 \cdot 10^{2}$ V m^{-1} along [100].

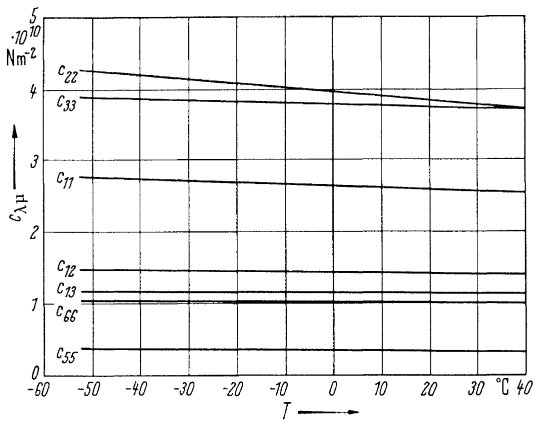

Fig. 67A-1-064. $NaKC_4H_4O_6 \cdot 4H_2O$. $c_{\lambda\mu}$ vs. *T* [50Jon].

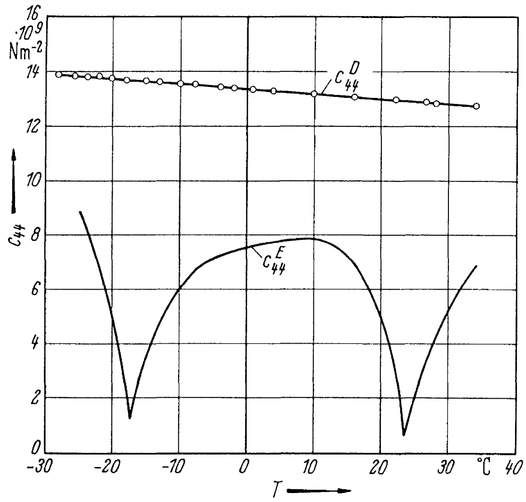

Fig. 67A-1-065. $NaKC_4H_4O_6 \cdot 4H_2O$. c_{44}^D, c_{44}^E vs. T [64Ber].

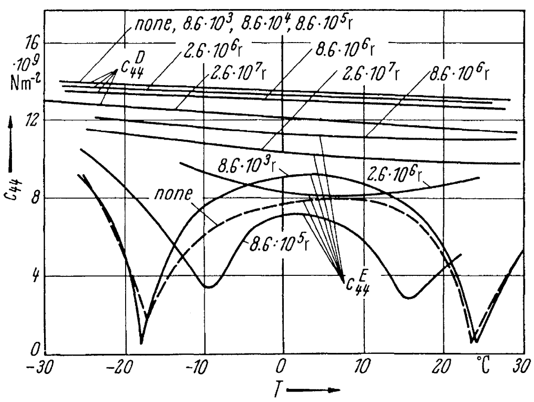

Fig. 67A-1-066. $NaKC_4H_4O_6 \cdot 4H_2O$. c_{44}^D, c_{44}^E vs. T [63Kru]. Parameter: ^{60}Co irradiation level. 1r = 2.58 · 10^{-4} C kg^{-1}.

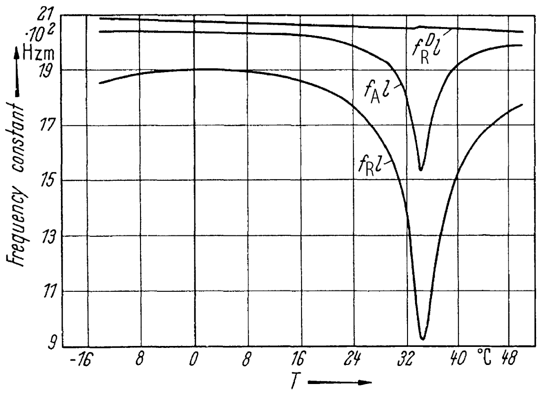

Fig. 67A-1-067. $NaKC_4H_2D_2O_6 \cdot 4D_2O$. $f_R l$, $f_A l$, $f_R^D l$ vs. T [40Hol]. $f_R l$, $f_A l$, $f_R^D l$: frequency constant of a 45° X-cut bar. f_R, f_A: resonant, antiresonant frequency of a plated crystal, $f_R l = [\rho(s_{22} + s_{33} + 2s_{23} + s_{44}^E) / 4]^{-1/2}/2$, f_R^D : resonant frequency of an unplated crystal, $f_R^D l = [\rho(s_{22} + s_{33} + 2s_{23} + s_{44}^D) / 4]^{-1/2}/2$. l: length, ρ: density.

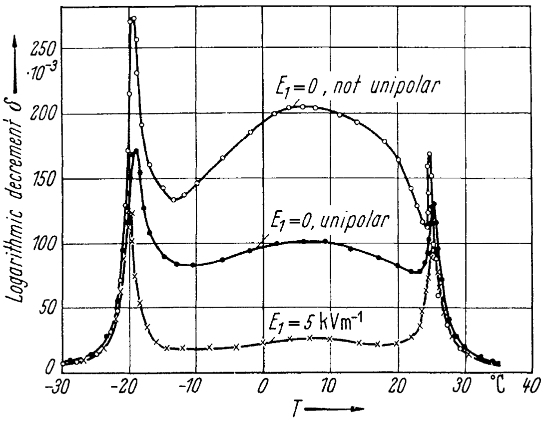

Fig. 67A-1-068. $NaKC_4H_4O_6 \cdot 4H_2O$. δ vs. T [63Shi]. Parameter: applied electric field E_1 along [100]. δ: logarithmic decrement of a 45° X-cut bar.

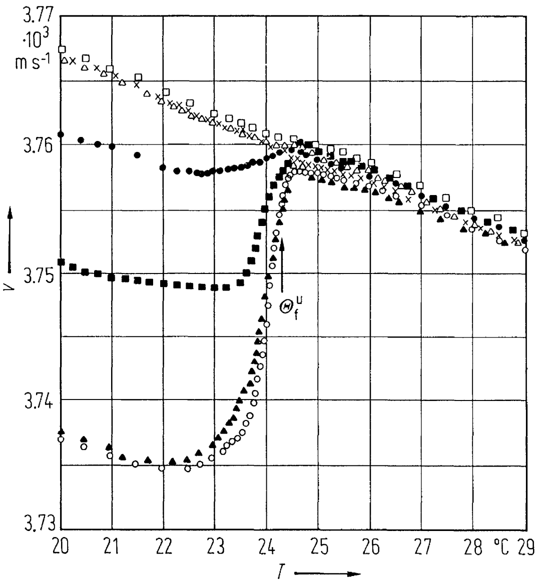

Fig. 67A-1-069. $NaKC_4H_4O_6 \cdot 4H_2O$. v vs. T [76Kaw]. v: ultrasonic velocity of longitudinal wave propagating along the a axis. f = 15 MHz. Open circles: warming run at E_{bias} = 0. Full triangles: cooling run at E_{bias} = 0. Open triangles: warming run at E_{bias} = 18 · 10^3 V m^{-1}. Full circles: cooling run at 18 · 10^3 V m^{-1}. Crosses: warming run at 1 · 10^5 V m^{-1}. Open squares: cooling run at 1 · 10^5 V m^{-1}. Full squares: warming run for the poled crystal.

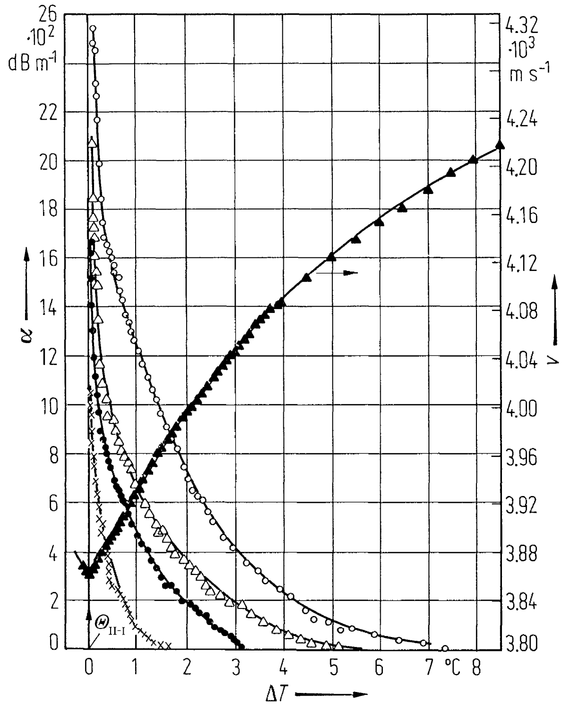

Fig. 67A-1-070. $NaKC_4H_4O_6 \cdot 4H_2O$. α, v vs. ΔT [77Kaw]. α: anomalous part of the attenuation of ultrasonic quasi-longitudinal wave propagated along the 45° direction in a 45° X-cut crystal. Crosses: 7 MHz. Full circles: 21 MHz. Open triangle: 35 MHz. Open circles: 49 MHz. Full triangles: v, velocity for 21 MHz. $\Delta T = T - \Theta_{II-I}$.

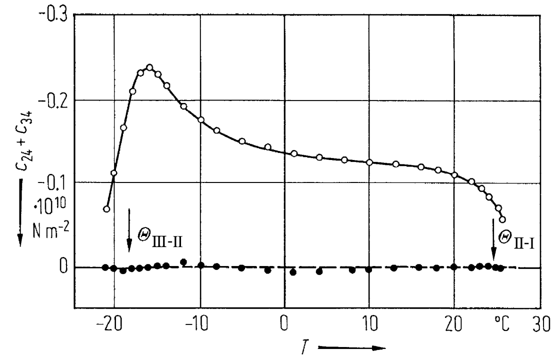

Fig. 67A-1-071. $NaKC_4H_4O_6 \cdot 4H_2O$. $c_{24} + c_{34}$ vs. T [76Sai]. Open circles: $c_{24}^E + c_{34}^E$. Full circles: $c_{24}^D + c_{34}^D$.

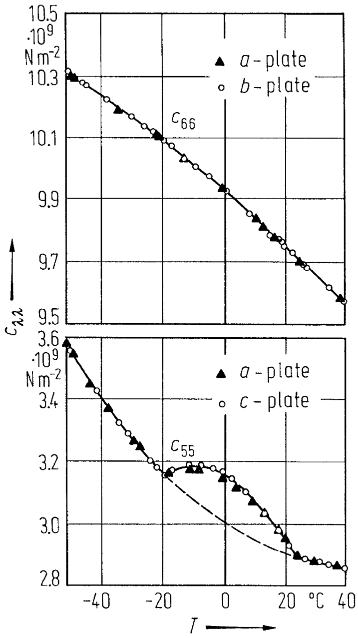

Fig. 67A-1-072. $NaKC_4H_4O_6 \cdot 4H_2O$. $c_{\lambda\lambda}$ vs. T [74Sak]. Values are obtained by measuring frequencies of piezoelectric lines in NQR.

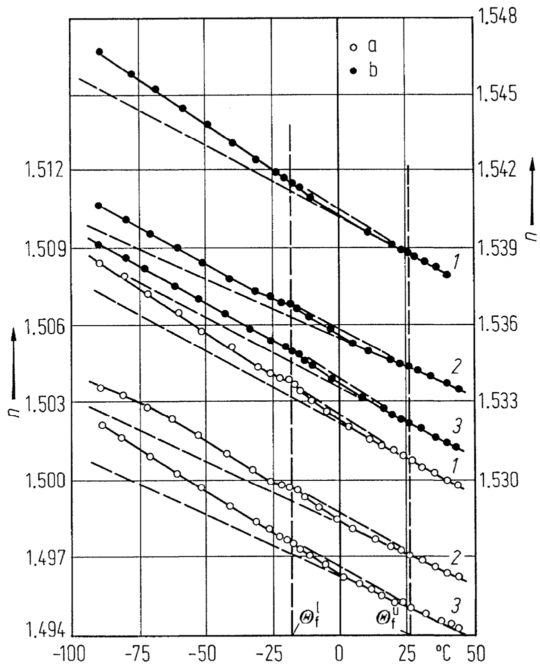

Fig. 67A-1-073. $NaKC_4H_4O_6 \cdot 4H_2O$. n vs. T [76Rom]. a (open circle): λ = 500 nm (left-hand scale). b (full circle): λ = 300 nm (right-hand scale). Curves *1*: n_a, *2*: n_b, *3*: n_c.

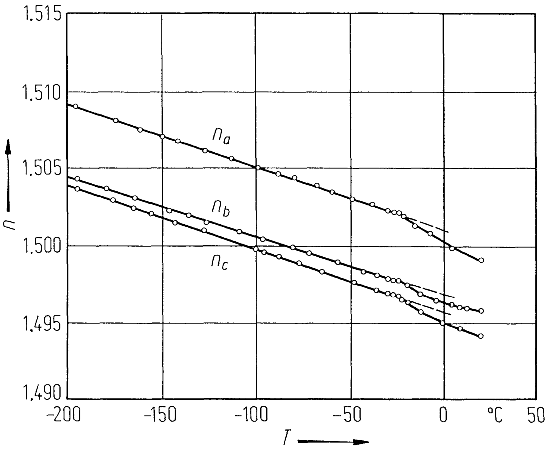

Fig. 67A-1-074. $NaKC_4D_4O_6 \cdot 4D_2O$. n_a, n_b, n_c vs. T [80Rom]. $\lambda = 500$ nm.

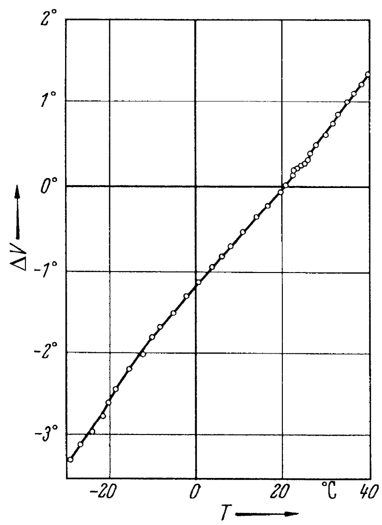

Fig. 67A-1-075. $NaKC_4H_4O_6 \cdot 4H_2O$. ΔV vs. T [66Iva]. ΔV: change in V. $2V$: optical axial angle. $\lambda = 558$ nm.

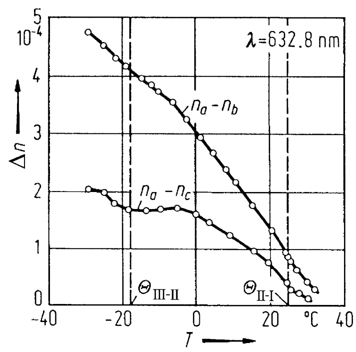

Fig. 67A-1-076. $NaKC_4H_4O_6 \cdot 4H_2O$. Δn vs. T [70Lom].

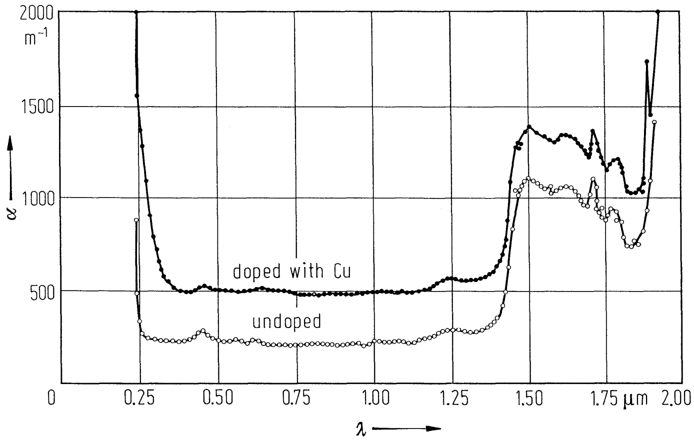

Fig. 67A-1-077. $NaKC_4H_4O_6 \cdot 4H_2O$. α vs. λ [81Leo]. α: optical absorption coefficient.

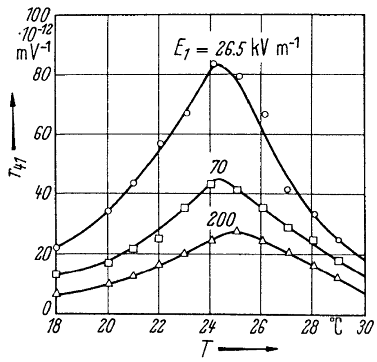

Fig. 67A-1-078. $NaKC_4H_4O_6 \cdot 4H_2O$. r_{41} vs. T [66Ani]. Parameter: applied field E_1 along [100]. λ = 546 nm.

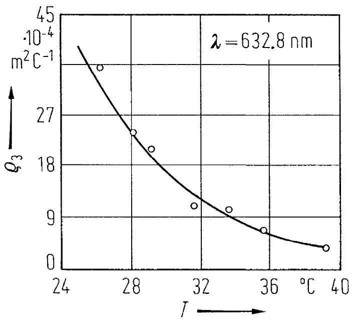

Fig. 67A-1-079. $NaKC_4H_4O_6 \cdot 4H_2O$. ρ_3 vs. T [67Ani]. $\rho_3 = \rho_{11} - (n_c/n_a)^3\rho_{31}$.

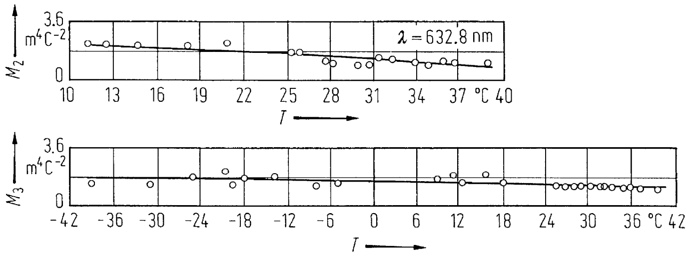

Fig. 67A-1-080. $NaKC_4H_4O_6 \cdot 4H_2O$. M_2, M_3 vs. T [67Ani]. $M_2 = M_{11} - (n_b/n_a)^3M_{21}$, $M_3 = M_{11} - (n_c/n_a)^3M_{31}$.

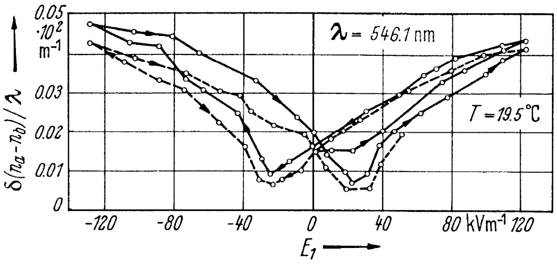

Fig. 67A-1-081. $NaKC_4H_4O_6 \cdot 4H_2O$. $\delta(n_a - n_b)/\lambda$ vs. E_1 [35Mue].

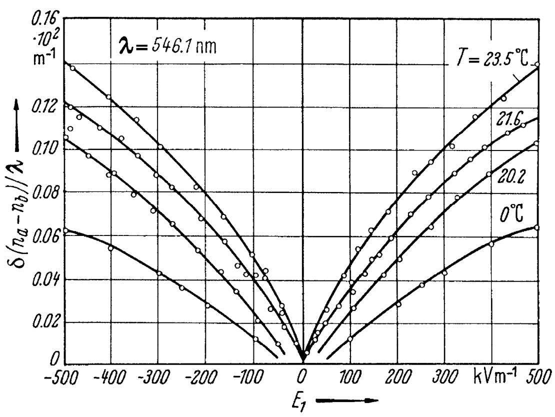

Fig. 67A-1-082. $NaKC_4H_4O_6 \cdot 4H_2O$. $\delta(n_a - n_b)/\lambda$ vs. E_1 [35Mue]. Parameter: T. 0 °C ≤ T ≤ 23.5 °C.

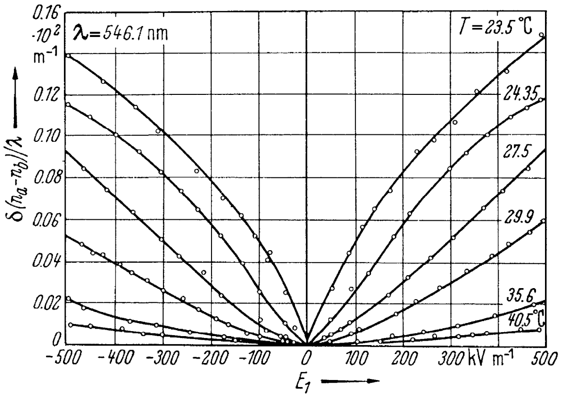

Fig. 67A-1-083. $NaKC_4H_4O_6 \cdot 4H_2O$. $\delta(n_a - n_b)/\lambda$ vs. E_1 [35Mue]. Parameter: T. 23.5 °C ≤ T ≤ 40.5 °C.

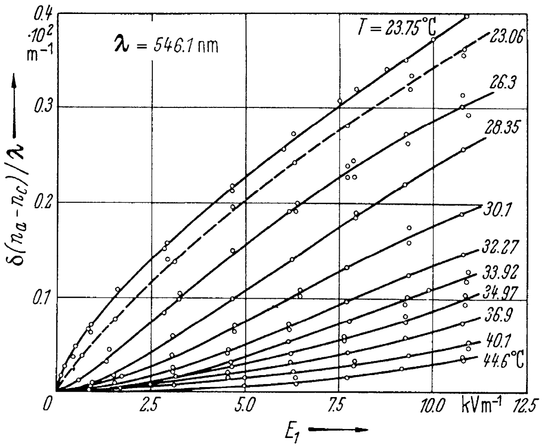

Fig. 67A-1-084. $NaKC_4H_4O_6 \cdot 4H_2O$. $\delta(n_a - n_c)/\lambda$ vs. E_1 [35Mue]. Parameter: *T*.

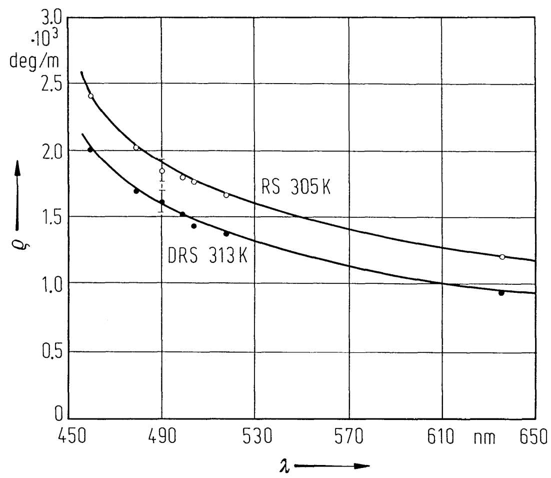

Fig. 67A-1-085. $NaKC_4H_4O_6 \cdot 4H_2O$, $NaKC_4H_2D_2O_6 \cdot 4D_2O$. ρ vs. λ [83Kor]. ρ: optical rotatory power.

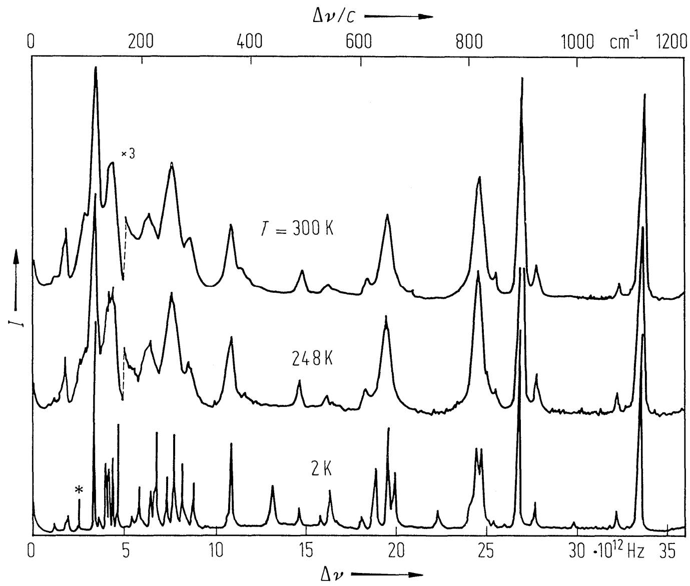

Fig. 67A-1-086. $NaKC_4H_4O_6 \cdot 4H_2O$. I vs. $\Delta\nu$ [80Win]. $\Delta\nu$: Raman shift of A-symmetry mode. Parameter: T. The peak with asterisk * shows a temperature dependence in the ferroelectric phase.

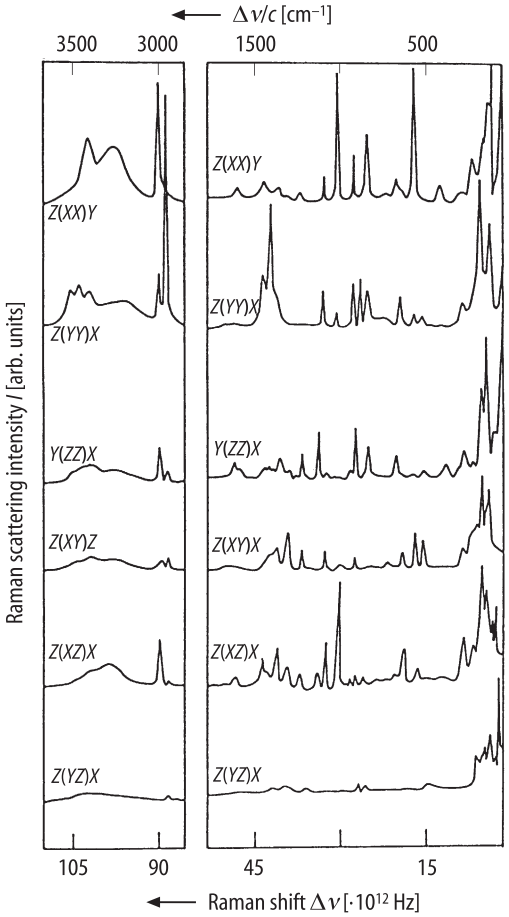

Fig. 67A-1-087. $NaKC_4H_4O_6 \cdot 4H_2O$. I vs. $\Delta\nu$ [88Bha]. I: Raman scattering intensity. $\Delta\nu$: Raman shift. Parameter: scattering geometry.

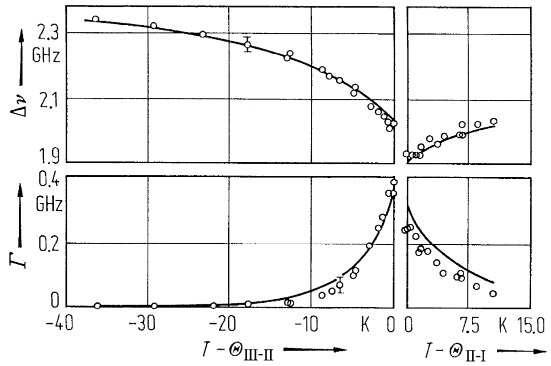

Fig. 67A-1-088. $NaKC_4H_4O_6 \cdot 4H_2O$. $\Delta\nu$, Γ vs. $T - \Theta_{III-II}$ and $T - \Theta_{II-I}$ [75Sai]. $\Delta\nu$: frequency shift of Brillouin scattering. Γ: full width at half maximum of spectral line. Quasi-longitudinal [011] phonon. Scattering angle $\theta = 10.2°$.

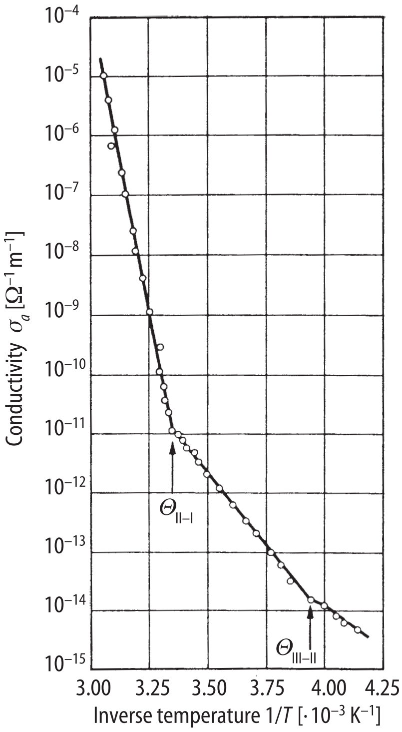

Fig. 67A-1-089. $NaKC_4H_4O_6 \cdot 4H_2O$. σ_a vs. $1/T$ [62Gur]. Three electrode method with shielding electrode. Applied field: 60 kV m^{-1}.

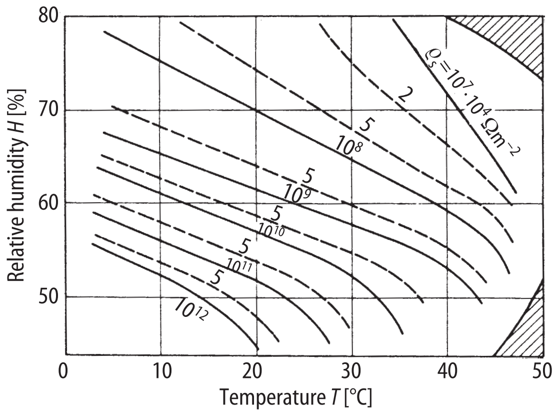

Fig. 67A-1-090. $NaKC_4H_4O_6 \cdot 4H_2O$. Surface resistivity ρ_s of (001) face along [100] as functions of H and T [47Kaw2]. H: relative humidity. Applied electric field: ≈700 V m^{-1}. In the hatched area no stable crystal exists.

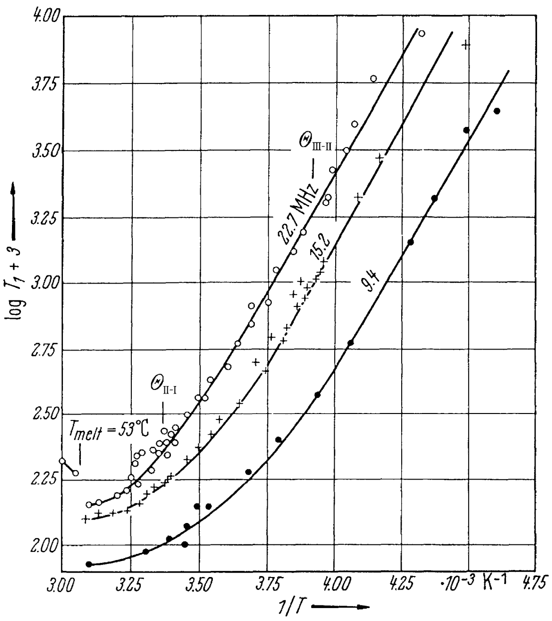

Fig. 67A-1-091. $NaKC_4H_4O_6 \cdot 4H_2O$. (log T_1 + 3) vs. 1/T [66Bli]. Parameter: f. T_1: spin-lattice relaxation time [s] of proton.

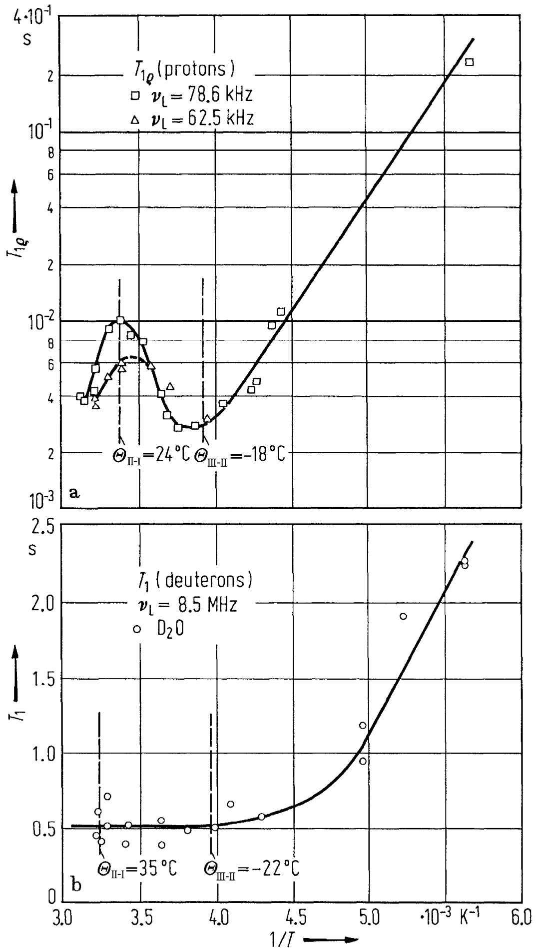

Fig. 67A-1-092. $NaKC_4H_4O_6 \cdot 4H_2O$ (**a**), $NaKC_4H_2D_2O_6 \cdot 4D_2O$ (**b**). $T_{1\rho}$, T_1 vs. $1/T$ [69Bli1]. ν_L: Larmor frequency.

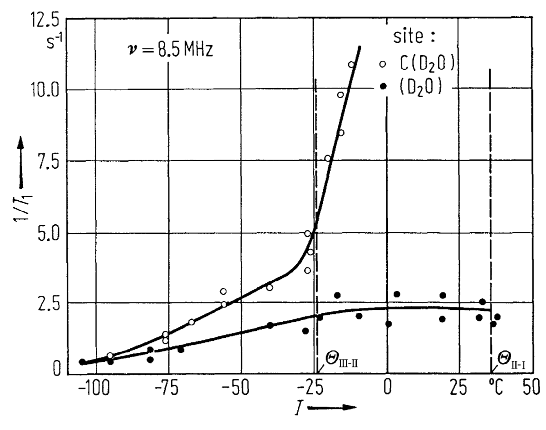

Fig. 67A-1-093. $NaKC_4H_2D_2O_6 \cdot 4D_2O$. $1/T_1$ vs. T [69Bli2]. T_1: deuteron spin-lattice relaxation time. Open circle: D_2O on C site. Full circle: D_2O on A and B sites.

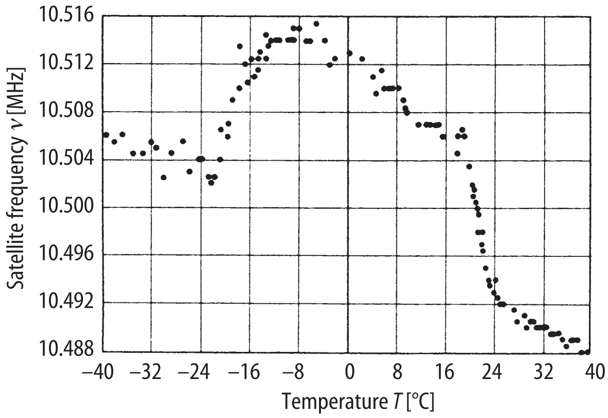

Fig. 67A-1-094. $NaKC_4H_4O_6 \cdot 4H_2O$. ν vs. T [66Mil]. ν: satellite frequency of one ^{23}Na NMR.

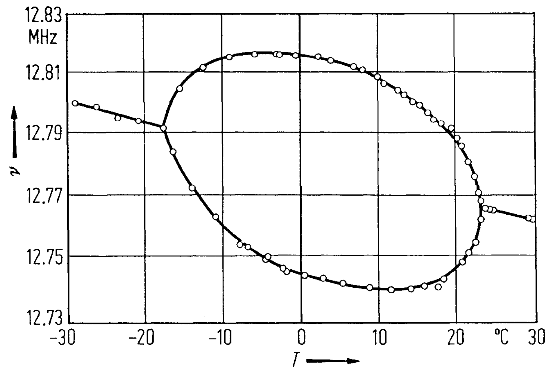

Fig. 67A-1-095. $NaKC_4H_4O_6 \cdot 4H_2O$. ν vs. T [69Oja]. ν: frequency of ^{23}Na NMR satellite line. See also [70Fit].

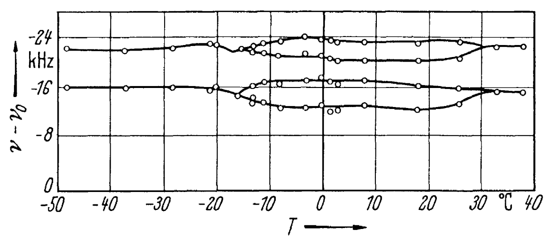

Fig. 67A-1-096. $NaKC_4H_2D_2O_6 \cdot 4D_2O$. $\nu - \nu_0$ vs. T [64Bli]. $\nu - \nu_0$: second order quadrupole shift of ^{23}Na. Direction of magnetic field $\boldsymbol{H}$: $\boldsymbol{c} \perp \boldsymbol{H}$, $\sphericalangle(\boldsymbol{b}, \boldsymbol{H}) = 278°$. ν_0: Larmor frequency.

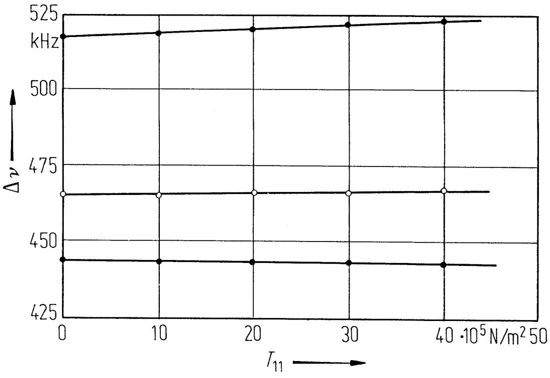

Fig. 67A-1-097. $NaKC_4H_4O_6 \cdot 4H_2O$. $\Delta\nu$ vs. T_{11} [80Kaw]. $\Delta\nu$: ^{23}Na NMR satellite splitting. Open circle: 300 K; full circle: 296 K. ν_L = 9. 573 MHz.

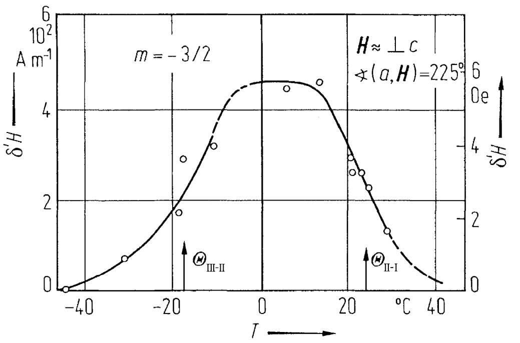

Fig. 67A-1-098. $NaKC_4H_4O_6 \cdot 4H_2O$. $\delta'H$ vs. T [71Vol]. $\delta'H$: shift of Cu^{2+} ESR field under $E = 10^5$ V m^{-1} along [100].

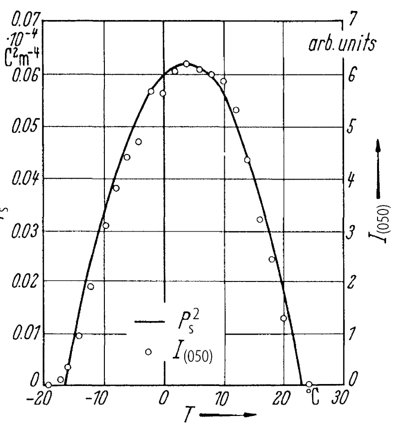

Fig. 67A-1-099. $NaKC_4H_4O_6 \cdot 4H_2O$. $I_{(050)}$, P_s^2 vs. T [67Shi]. $I_{(050)}$: (050) integrated intensity.

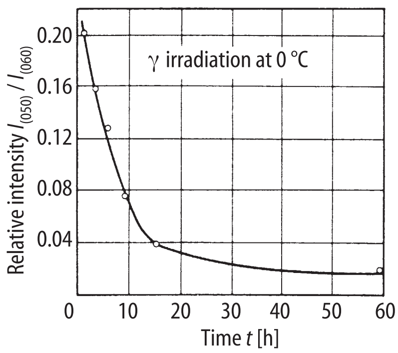

Fig. 67A-1-100. $NaKC_4H_2D_2O_6 \cdot 4D_2O$. $I_{(050)}/I_{(060)}$ vs. t [63Bou]. $I_{(050)}$, $I_{(060)}$: integrated intensities at RT. t: time of γ irradiation at 0 °C.

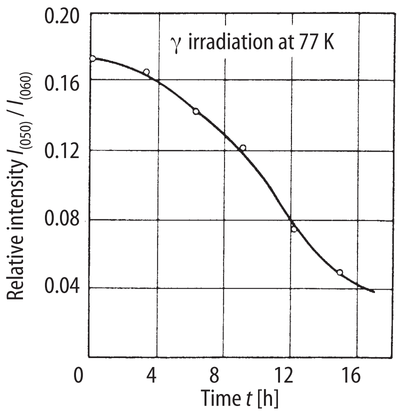

Fig. 67A-1-101. $NaKC_4H_2D_2O_6 \cdot 4D_2O$. $I_{(050)}/I_{(060)}$ vs. t [63Bou]. $I_{(050)}$, $I_{(060)}$: integrated intensities at RT. t: time of γ irradiation at 77 K.

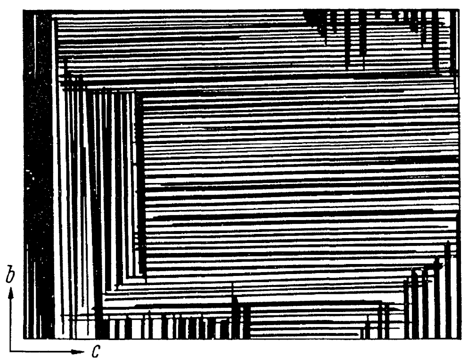

Fig. 67A-1-102. $NaKC_4H_4O_6 \cdot 4H_2O$. Example of complicated domain structure observed with polarization microscope [53Mit].

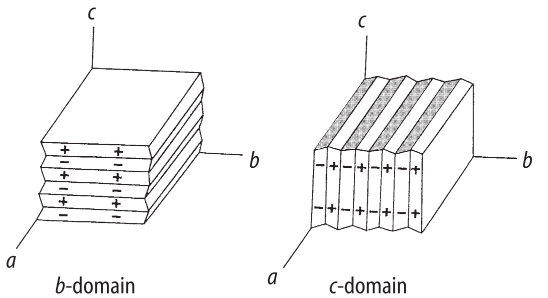

Fig. 67A-1-103. $NaKC_4H_4O_6 \cdot 4H_2O$. Schematic representation of domain structures [85Ume].

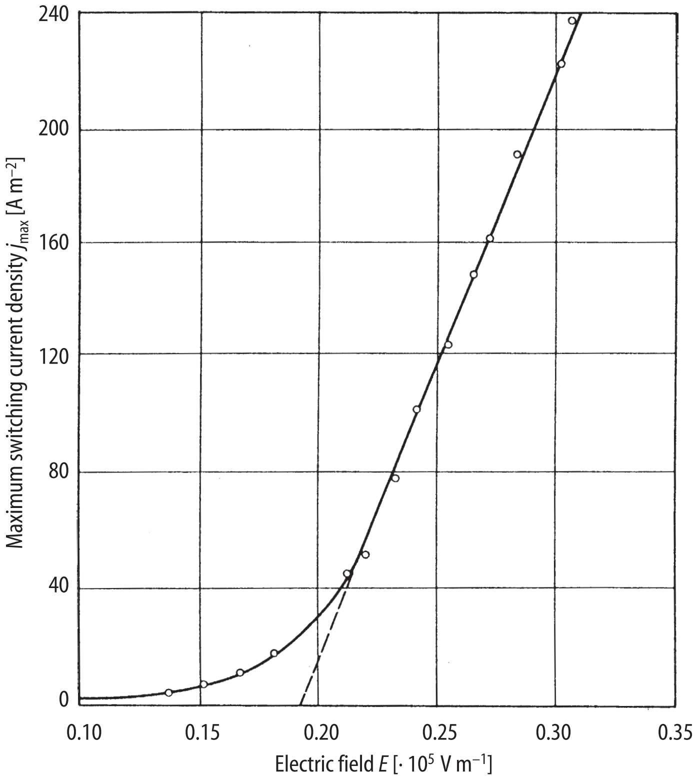

Fig. 67A-1-104. $NaKC_4H_4O_6 \cdot 4H_2O$. j_{max} vs. E [58Wie]. j_{max}: maximum switching current density. Pulse method.

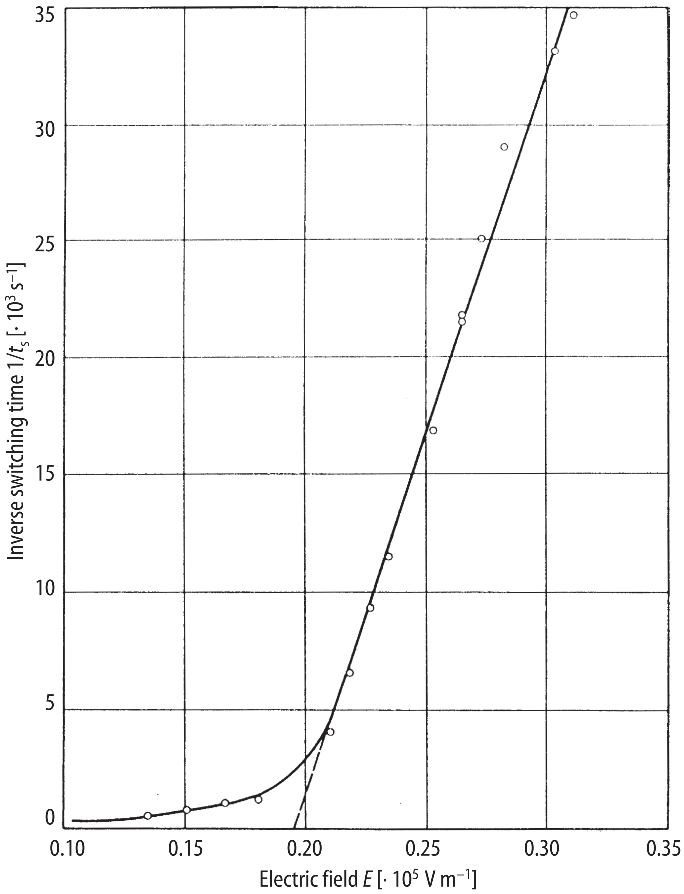

Fig. 67A-1-105. $NaKC_4H_4O_6 \cdot 4H_2O$. $1/t_s$ vs. E [58Wie]. t_s: switching time. Pulse method.

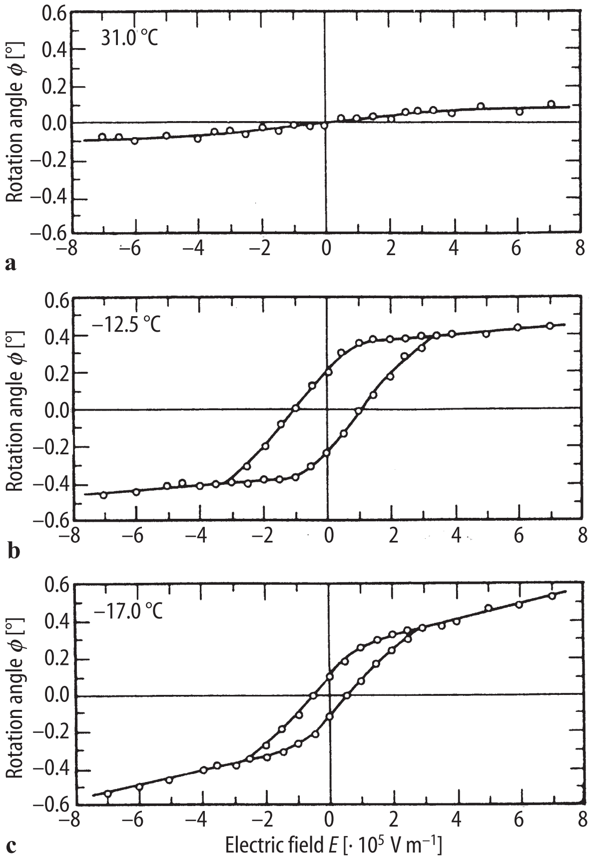

Fig. 67A-1-106. $NaKC_4H_4O_6 \cdot 4H_2O$. ϕ vs. E [58Wie]. Parameter: T. ϕ: rotation angle of optical indicatrix. (**a**) T = 31.0 °C. (**b**) T = –12.5 °C. (**c**) T = –17.0 °C.

References

1894Poc Pockels, F.: Abh. Ges. Wiss. Göttingen **39** (1894) 1.
20Val Valasek, J.: Phys. Rev. **15** (1920) 573.
21Val Valasek, J.: Phys. Rev. **17** (1921) 475.
24Val Valasek, J.: Phys. Rev. **24** (1924) 560.
27Man Mandell, W.: Proc. R. Soc. London, Ser. A **116** (1927) 623.
27Val Valasek, J.: Science **65** (1927) 235.
28Man Mandell, W.: Proc. R. Soc. London, Ser. A **121** (1928) 130.
34Sta Staub, H.: Phys. Z. **35** (1934) 720.
35Hab Hablützel, J.: Helv. Phys. Acta **8** (1935) 498.
35Mue Mueller, H.: Phys. Rev. **47** (1935) 175.
35Vig Vigness, I.: Phys. Rev. **48** (1935) 198.
37Jaf Jaffe, H.V.R.: Phys. Rev. **51** (1937) 43.
38Ban Bancroft, D.: Phys. Rev. **53** (1938) 587.
38Hic Hicks Jr., J.F.G., Hooley, J.G.: J. Am. Chem. Soc. **60** (1938) 2994.
39Hab Hablützel, J.: Helv. Phys. Acta **12** (1939) 489.
39Hin Hinz, H.: Z. Physik **111** (1939) 617.
39Mas1 Mason, W.P.: Phys. Rev. **55** (1939) 1141.
39Mas2 Mason, W.P.: Phys. Rev. **55** (1939) 775.
40Hol Holden, A.N., Mason, W.P.: Phys. Rev. **57** (1940) 54.
40Mue Mueller, H.: Phys. Rev. **58** (1940) 565.
41Bee Beevers, A.C., Hughes, S.: Proc. R. Soc. London, Ser. A **177** (1941) 251.
43Kaw Kawai, H.: J. Phys. Math. Soc. Jpn. **17** (1943) 270.
46Ubb Ubbelohde, A.R., Woodward, I.: Proc. R. Soc. London, Ser. A **185** (1946) 448.
47Hun Huntington, H.B.: Phys. Rev. **72** (1947) 321.
47Kaw1 Kawai, H.: J. Phys. Soc. Jpn. **2** (1947) 113.
47Kaw2 Kawai, H.: Butsuri **2** (1947) 193.
49Kaw Kawai, H., Marutake, M.: J. Phys. Soc. Jpn. **4** (1949) 91.
49Miy Miyake, S.: Rochelle Salt, Tokyo: Koyama-Shoten, 1949.
49Sun Sundara Rao, P.V.G.: Proc. Indian Acad. Sci. A **30** (1949) 173.
50Fur Furuichi, J., Mitsui, T.: Phys. Rev. **80** (1950) 93.
50Jon Jona, F.: Helv. Phys. Acta **23** (1950) 795.
50Mas Mason, W.P.: Piezoelectric Crystals and Their Application to Ultrasonics, Princeton: D. Van Nostrand Co., 1950.
50Van Van Dyke, K.S., Gordon, G.D.: US Signal Corps Contract No. W-28-003-sc-1556, Tenth Report (1950), Wesleyan University, Middleton, Conn.
53Mit Mitsui, T., Furuichi, J.: Phys. Rev. **90** (1953) 193.
55Los Losche, V.A.: Exp. Tech. Phys. **3** (1955) 18.
55Shi Shirane, G., Jona, F., Pepinsky, R.: Proc. I.R.E. **43** (1955) 38.
56Mus Müser, H.E.: Z. Physik **145** (1956) 621.
57Maz Mazzi, F., Jona, F., Pepinsky, R.: Z. Kristallogr. **108** (1957) 359.
58Wie Wieder, H.H.: Phys. Rev. **110** (1958) 29.
59Pea Pearson, G.L., Feldman, W.L.: J. Phys. Chem. Solids **9** (1959) 28.
60Fot Fotchenkov, A.A.: Kristallografiya **5** (1960) 415; Sov. Phys. Crystallogr. (English Transl.) **5** (1960) 390.
60Krs Krstanovic, I., Okaya, Y., Pepinsky, R.: Unpublished work (1960).
60Wie Wieder, H.H., Collins, D.A.: Phys. Rev. **120** (1960) 725.
61Nak Nakamura, T., Ohi, K.: J. Phys. Soc. Jpn. **16** (1961) 209.
61Sch Schmidt, G.: Z. Physik **161** (1961) 579.
62Ber Berlincourt, D.A., Curran, D.R.: Symp. Phys. and Nondestructive Testing, San Antonis, Texas (1962), Clevite Corporation Elec. Res. Div., Cleveland, Ohio.
62Gur Gurevich, V.M.: Thesis of Candidate of Phys. Math. Science, Moskva (1962), cited in [69Gur].
62Jon Jona, F., Shirane, G.: Ferroelectric Crystals, Oxford: Pergamon Press, 1962.

63Bou Boutin, H., Frazer, B.C., Jona, F.: J. Phys. Chem. Solids **24** (1963) 1341.

63Kru Krueger, H.H.A., Cook Jr., W.R., Sartain, C.C., Yockey, H.P.: J. Appl. Phys. **34** (1963) 218.

63Shi Shirokov, A.M., Shuvalov, L.A.: Kristallografiya **8** (1963) 733; Sov. Phys. Crystallogr. (English Transl.) **8** (1964) 586.

63Wis Wiseman, G.G., Kitebler, J.K.: Phys. Rev. **131** (1963) 2023.

64Abe Abe, R.: Jpn. J. Appl. Phys. **3** (1964) 243.

64Ber Berlincourt, D., Curran, D.R., Jaffe, H.: Article on p. 169 in [64Mas].

64Bli Blinc, R., Petkovšek, J., Zupančič, I.: Phys. Rev. **136** (1964) A1684.

64Mas Mason, P.W. (ed.): Physical Acoustics, Vol. I, Part A, New York: Academic Press, 1964.

65Sam Samara, G.A.: J. Phys. Chem. Solids **26** (1965) 121.

66Ani Anistratov, A.T.: Kristallografiya **11** (1966) 823; Sov. Phys. Crystallogr. (English Transl.) **11** (1967) 700.

66Bec Bechmann, R., Hearmon, R.F.S.: Landolt-Börnstein, New Series, Group III, Vol. 1: Elastic, Piezoelectric, Piezooptic and Electrooptic Constants of Crystals, Hellwege, K.-H., Hellwege, A.M. (eds.), Berlin, Heidelberg, New York: Springer, 1966.

66Bli Blinc, R., Uehling, A.: Phys. Lett. **20** (1966) 337.

66Iva Ivanov, N.R., Zotov, V.F.: Kristallografiya **11** (1966) 924; Sov. Phys. Crystallogr. (English Transl.) **11** (1967) 781.

66Mil Miller, N.C., Casabella, P.A.: Phys. Rev. **152** (1966) 228.

67Ani Anistratov, A.T., Aleksandrov, K.S.: Kristallografiya **12** (1967) 459; Sov. Phys. Crystallogr. (English Transl.) **12** (1967) 392.

67Bjo Bjorkstam, J.L., Willmorth, J.H.: Article on p. 728 in [67Bli].

67Bli Blinc, R. (ed.): Magnetic Resonance and Relaxation, Proceedings of the XIX th Coloque Ampere, held at Ljublijana (1966), Amsterdam: North-Holland Publishing Co., 1967.

67Oka Okada, K., Gonzalo, J.A., Rivera, J.M.: J. Phys. Chem. Solids **28** (1967) 689.

67Shi Shiozaki, Y.: J. Phys. Chem. Solids **28** (1967) 2381.

67Suz Suzuki, I., Abe, R.: J. Phys. Soc. Jpn. **23** (1967) 1049.

67Unr Unruh, H.-G., Müser, H.E.: Ann. Phys. (Leipzig) (7) **19** (1967) 28.

68For Forsch, K., Müser, H.E.: Z. Naturforsch. **23a** (1968) 1231.

68Mar Marutake, M.: Unpublished work (1968).

68Sam Samara, G.A.: J. Phys. Chem. Solids **29** (1968) 870.

68San Sandy, F., Jones, R.V.: Phys. Rev. **168** (1968) 481.

69Bli1 Blinc, R., Peterson, E.M., O'Reilly, D.E.: Phys. Lett. A **28** (1969) 624.

69Bli2 Blinc, R., Jamsek, M., Stepisnik, J., Trontelj, Z., Bjorkstam, J.L.: Solid State Commun. **7** (1969) 95.

69ElS El Saffar, Z.M.: J. Chem. Phys. **50** (1969) 4520.

69Gur Gurevich, V.M.: Elektroprovodnost' Segnetoelektrikov, Moskva: Izdatel'stvo Komiteta Standartov, Mer i Izmeritel'nykh Priboroy pri Sovete Ministrov SSSR 1969; Electric Conductivity of Ferroelectrics, Jerusalem: Israel Program for Scientific Translations, 1971.

69Nar Narasimhamurty, T.S.: Phys. Rev. **186** (1969) 945.

69Oja Oja, T., Casabella, P.A.: Phys. Rev. **177** (1969) 830.

70Fit Fitzgerald, M.E., Casabella, P.A.: Phys. Rev. B **2** (1970) 1350.

70Kat Kato, T., Mizuno, O., Abe, R.: J. Phys. Soc. Jpn. **29** (1970) 393.

70Lom Lomova, L.G., Sotiiti, A.S.: Fiz. Tverd. Tela **12** (1970) 3331; Sov. Phys. Solid State (English Transl.) **12** (1971) 2699.

71Vol Volkel, G., Windsch, W.: Phys. Status Solidi (b) **43** (1971) 263.

72Mor Mori, K., Hayashi, M.: J. Phys. Soc. Jpn. **33** (1972) 1396.

72Mus Müser, H.E., Schmitt, H.: J. Phys. (Paris) Colloq. **33** (1972), Suppl. No. C–2, p. 103.

72Myl Mylov, V.P., Leonidva, G.G., Churagulov, B.R.: Fiz. Tverd. Tela **14** (1972) 2184; Sov. Phys. Solid State (English Transl.) **14** (1973) 1893.

72Sch Schafer, H., Albers, J., Helwig, J.: Phys. Lett. A **39** (1972) 159.

72Shi Shiozaki, Y., Mitsui, T.: Acta Crystallogr. Sect. A **28** (1972) S185.

73Hat Hatano, J., Suda, F., Futama, H.: Jpn. J. Appl. Phys. **12** (1973) 1644.

74Mit Mitani, S., Fukui, S., Shibuya, I., Shiozaki, Y., Toyoda, K., Pepinsky, R.: Ferroelectrics **8** (1974) 477.
74Sak Sakami, J.: Phys. Lett. A **50** (1974) 109.
75Sai Sailer, E., Unruh, H.G.: Solid State Commun. **16** (1975) 615.
75Vlo Vlokh, O.G., Laz'ke, L.A., Zheludev, I.S.: Kristallografiya **20** (1975) 1056; Sov. Phys. Crystallogr. (English Transl.) **20** (1976) 646.
76Ima Imai, K.: J. Phys. Soc. Jpn. **41** (1976) 2005.
76Kaw Kawashima, R., Tatsuzaki, I.: Phys. Lett. A **56** (1976) 43.
76Man Mansingh, A., Prasad, E.: J. Phys. D **9** (1976) 1379.
76Rom Romanyuk, N.A., Kostetokii, A.M.: Fiz. Tverd. Tela **18** (1976) 1489; Sov. Phys. Solid State (English Transl.) **18** (1976) 867.
76Sai Sailer, E., Unruh, H.G.: Ferroelectrics **12** (1976) 285.
76Sch Schmitt, H.: Ferroelectrics **14** (1976) 575.
77Kaw Kawashima, R., Tatsuzaki, I.: J. Phys. Soc. Jpn. **42** (1977) 564.
78Tat Tatsumi, M., Matuo, T., Suga, H., Seki, S.: J. Phys. Chem. Solids **39** (1978) 427.
79Hor Horioka, M., Abe, R.: Jpn. J. Appl. Phys. **18** (1979) 2065.
80Jai Jain, V.K., Venkateswarlu, P.: J. Chem. Phys. **73** (1980) 30.
80Kaw Kawamori, A., Akagi, Y., Chihara, H.: J. Phys. Soc. Jpn. **49** Suppl. B (1980) 128.
80Rom Romanyuk, N.A., Gaba, V.M., Kostetskii, A.M.: Kristallografiya **25** (1980) 1076; Sov. Phys. Crystallogr. (English Transl.) **25** (1980) 618.
80Win Winterfeldt, V.: Phys. Status Solidi (b) **100** (1980) 235.
81Bro Bronowska, W.: J. Appl. Crystallogr. **14** (1981) 203.
81Ism Ismailzade, I.H., Ismailov, R.M., Rez, I.S.: Ferroelectrics **34** (1981) 117.
81Leo Leonovici, M., Bunget, I.: Rev. Roum. Phys. **26** (1981) 1013.
82Vol Volkov, A.A., Kozlov, G.V., Lebedev, S.P.: Fiz. Tverd. Tela **24** (1982) 555; Sov. Phys. Solid State (English Transl.) **24** (1982) 312.
83Bei Beige, H., Kühnell, A., Lorenz, B.: Phys. Status Solidi (a) **75** (1983) 129.
83Kla Klapper, H., Roberts, K.J., Gotz, D., Herres, N.: J. Cryst. Growth **65** (1983) 621.
83Kor Koralewski, M., Mróz, M.: Acta Phys. Pol. A **63** (1983) 507.
84Bei1 Beige, H., Kühnell, A.: Phys. Status Solidi (a) **84** (1984) 433.
84Bei2 Beige, H., Schmidt, G.: Ferroelectrics Lett. **1** (1984) 155.
85Aga Agarwal, O.P., Chand, P.: Z. Naturforsch. **40a** (1985) 1164.
85Ume Umezawa, K., Takashima, M., Ogawa, T., Ishida, K., Takagi, S.: Jpn. J. Appl. Phys. **24** (1985) Suppl. 24–2, p. 542.
86Shi Shil'nikov, A.V., Galiyarova, N.M., Nadolinskaya, E.G., Corin, S.V., Shuvaev, M.A.: Kristallografiya **31** (1986) 326; Sov. Phys. Crystallogr. (English Transl.) **31** (1986) 192.
86Vol Volkov, A.A., Kozlov, G.V., Kryukova, E.B., Petzelt, J.: Zh. Eksp. Teor. Fiz. **90** (1986) 192; Sov. Phys. JETP (English Transl.) **63** (1986) 110.
88Bha Bhattacharjee, R., Jain, Y.S., Raghubanshi, G., Bist, H.D.: J. Raman Spectrosc. **19** (1988) 51.
89Iwa Iwata, Y., Koyano, N., Shibuya, I.: Annual Report of the Research Reactor Institute, Kyoto University **22** (1989) 87.
91Kob1 Kobayashi, J., Uchino, K., Matsuyama, H., Saito, K.: J. Appl. Phys. **69** (1991) 409.
91Kob2 Kobayashi, J.: Phase Transitions B **36** (1991) 95.
94Suz Suzuki, E., Amano, A., Nozaki, R., Shiozaki, Y.: Ferroelectrics **152** (1994) 385.
96Shi Shimizu, K., Suzuki, E., Nozaki, R., Shiozaki, Y.: J. Korean Phys. Soc. **29** (1996) S529.
96Suz Suzuki, E., Shiozaki, Y.: Phys. Rev. B **53** (1996) 5217.
98Shi Shiozaki, Y., Shimizu, K., Suzuki, E., Nozaki, R.: J. Korean Phys. Soc. **32** (1998) S192.

No. 67A-2 $NaNH_4C_4H_4O_6 \cdot 4H_2O$, Sodium ammonium tartrate tetrahydrate (Ammonium Rochelle salt, ARS)

(M = 261.16; [D: 277.26])

1a Dielectric anomaly was observed by Jona et al. in 1953, and polarization reversal by mechnical stress was observed by Takagi et al. in 1958. 53Jon 58Tak

b 58Tak

phase	II	I
state	(F)	P
crystal system	monoclinic	orthorhombic
space group	$P2_1 - C_2^2$	$P2_12_12 - D_2^3$
Θ [K]	109	

P_s ∥ [010]; P_s can be reversed only by mechanical stress. 58Tak
$\rho = 1.587 \cdot 10^3$ kg m^{-3}. 33Blo
Transparent, colorless. Deliquescent. 58Mak

2a Crystal growth: cooling or evaporation method from aqueous solution.

3a Unit cell parameters: a = 12.206(7) Å, b = 14.451(6) Å, c = 6.250(4) Å at 294 K. 96Suz

b Z = 4. 96Suz
Crystal structure: Fig. 67A-2-001.
See also Table 67B-1-001, Table 67B-1-004, Table 67B-1-006, Table 67B-1-007 in No. 67B-1.
Superlattice structure: X-ray superlattice reflections due to $2a$ appear in phase II. 71Saw

4 Spontaneous strain: Fig. 67A-2-002.

5a Dielectric constant: Fig. 67A-2-003, Fig. 67A-2-004, Fig. 67A-2-005.

c Spontaneous polarization: $P_s = 2.1 \cdot 10^{-3}$ C m^{-2} at 92 K. 58Tak
Coercive stress for polarization reversal: $T_5 \cong 5 \cdot 10^6$ N m^{-2} at 92 K. 58Tak
See Fig. 67A-2-009 in subsection 7c.

d Pyroelectricity: Fig. 67A-2-006.

7a Piezoelectricity: Table 67A-2-001; Fig. 67A-2-007, Fig. 67A-2-008.

c Nonlinear electromechanical properties: Fig. 67A-2-009.

8a Elastic compliance and stiffness: Table 67A-2-002; Fig. 67A-2-010; see also Fig. 67B-1-035 in No. 67B-1.

9a Refractive indices: $n_\alpha = n_c = 1.4953$, $n_\beta = n_a = 1.4985$, $n_\gamma = n_b = 1.4496$, $2V = 119° 20'$ at 20 °C for NaD line; 1894Lav
see also Table 67A-1-013 in No. 67A-1.
Temperature dependence of refractive indices: Fig. 67A-2-011, Fig. 67A-2-012.
Birefringence: Fig. 67A-2-013, Fig. 67A-2-014.

c Piezooptic constant (λ = 589.0 nm, T = RT). 82Sha
Strain-optical, $p_{11} = -0.48$, $p_{12} = -0.61$, $p_{13} = -0.68$, $p_{21} = -0.55$, $p_{22} = -0.76$, $p_{23} = -0.83$, $p_{31} = -0.44$, $p_{32} = -0.57$, $p_{33} = -0.71$, $p_{44} = 0.0077$, $p_{55} = 0.013$, $p_{66} = -0.0026$.
Stress-optical [$\cdot 10^{-12}$ m^2 N^{-1}], $\Pi_{11} = -0.320$, $\Pi_{12} = -5.32$, $\Pi_{13} = -7.14$, $\Pi_{21} = -1.39$, $\Pi_{22} = -7.83$, $\Pi_{23} = -9.30$, $\Pi_{31} = -0.90$, $\Pi_{32} = -4.05$, $\Pi_{33} = -9.73$, $\Pi_{44} = 0.73$, $\Pi_{55} = 4.42$, $\Pi_{66} = -0.30$.

d	Rotatory power: $\rho = 1.55(15) \cdot 10^3\ ^\circ\ m^{-1}$ for $\lambda = 589.3$ nm.	30Ast
13a	NMR: Table 67A-2-003, Table 67A-2-004; Fig. 67A-2-015, Fig. 67A-2-016.	
b	ESR: Table 67A-2-005.	
14a	Bragg reflections due to structural modulation: Fig. 67A-2-017, Fig. 67A-2-018.	
15a	Domain structure: Fig. 67A-2-019, Fig. 67A-2-020.	

Table 67A-2-001. $NaNH_4C_4H_4O_6 \cdot 4H_2O$. Piezoelectric strain constants and piezoelectric stress constants [66Bec].

d_{14}	d_{25}	d_{36}	e_{14}	e_{25}	e_{36}	T	Ref.
[10^{-12} C N^{-1}]			[C m^{-2}]			[°C]	
18.7	–49.8	9.4					28Man
±19.0	±31.7	±10.3				25	50Mas
			0.212	0.137	–0.080	20	28Man

Table 67A-2-002. $NaNH_4C_4H_4O_6 \cdot 4H_2O$. Elastic constants [66Bec].

s_{11}	s_{22}	s_{33}	s_{12}	s_{13}	s_{23}	s_{44}	s_{55}	s_{66}	T	Ref.
[10^{-12} m^2 N^{-1}]									[°C]	
53.7	38.4	37.3	–8.7	–34.3	–5.0	87.4	360	118		28Man
57.0	38.5	40	–15.5	–22	–15.5	94.5	330	115	25	50Mas

c_{11}	c_{22}	c_{33}	c_{12}	c_{13}	c_{23}	c_{44}	c_{55}	c_{66}	T	Ref.
[10^9 N m^{-2}]									[°C]	
53.1	34.1	77.8	18.7	51.3	21.6	11.8	2.9	8.8		28Man

Table 67A-2-003. $NaND_4C_4H_2D_2O_6 \cdot 4D_2O$. Eigenvalues [kHz] and transformation matrices of ND_4^+ deuteron electric field gradient tensors [76ElS].

		ϕ_{xx} (1)	ϕ_{yy} (2)	ϕ_{zz} (3)
297 K		–2.5	–2.8	5.3
(Volkoff's method)	1	90	90	0
	2	108	18	90
	3	18	72	90
297 K		–2.5	–2.9	5.4
(El Saffar's method)	1	90	90	0
	2	107	17	90
	3	17	73	90
224 K		–2.7	–3.2	5.9
173 K		–2.8	–3.3	6.1
122 K		Ferroelectric transition		
113 K	1	–1.2	–3.4	4.7
	2	109	36	119
	3	119	72	34
		35	60	74
93 K		–1.3	–3.6	4.9
77 K		–0.7	–3.6	4.3
	1	101	11	89
	2	110	94	21
	3	23	81	70

Table 67A-2-004. $NaND_4C_4H_2D_2O_6 \cdot 4D_2O$. Eigenvalues [kHz] and transformation matrices of D_2O deuteron electric field gradient tensors [76ElS].

Site		$\phi_{xx}(1)$	$\phi_{yy}(2)$	$\phi_{zz}(3)$
α		–7	–104	111
	1	–0.279	0.958	–0.065
	2	0.900	0.286	0.329
	3	–0.337	–0.035	0.941
β		–35	–100	135
	1	0.074	0.956	–0.284
	2	0.689	0.153	0.700
	3	0.712	–0.250	–0.656
γ		–2	–108	110
	1	0.761	–0.558	0.330
	2	0.312	0.764	0.564
	3	–0.567	–0.328	0.755
δ		–9	–105	114
	1	–0.219	0.168	0.961
	2	–0.155	0.984	–0.092
	3	0.945	0.184	0.271

Table 67A-2-005. $NaNH_4C_4H_4O_6 \cdot 4H_2O$. Spin Hamiltonian parameters of Cu^{2+} at RT [72Suz]. A_1, A_2, A_3 in [$\cdot 10^{-2}\,m^{-1}$].

	g_1	g_2	g_3	A_1	A_2	A_3
ARS	2.064	2.095	2.316	58.7	28.3	128

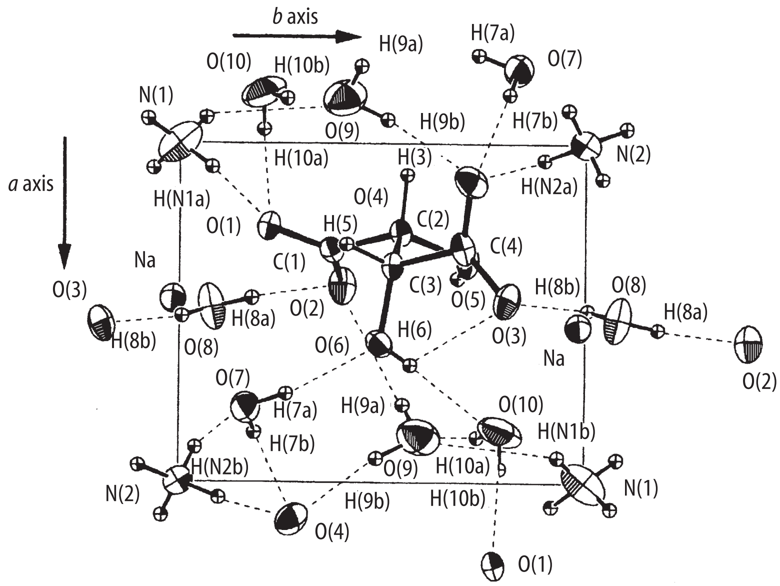

Fig. 67A-2-001. $NaNH_4C_4H_4O_6 \cdot 4H_2O$. Structure of phase I viewed along *c* [96Suz].

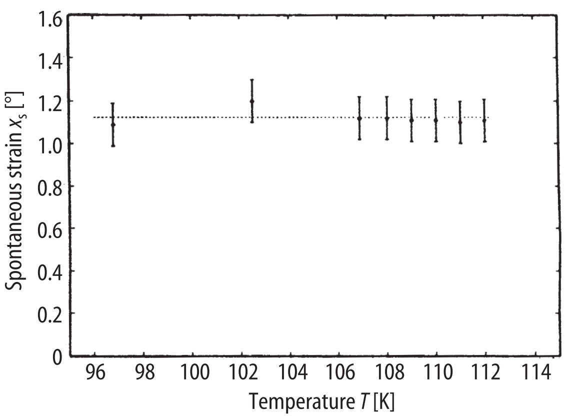

Fig. 67A-2-002. $NaNH_4C_4H_4O_6 \cdot 4H_2O$. x_s vs. *T* derived from angle of splitting of (001) Bragg reflection [96Kik]. x_s: spontaneous strain.

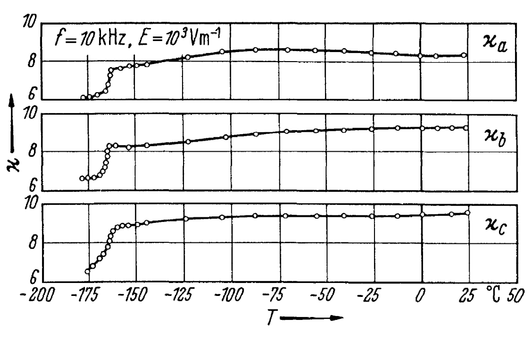

Fig. 67A-2-003. $NaNH_4C_4H_4O_6 \cdot 4H_2O$. κ_a, κ_b, κ_c vs. *T* [53Jon].

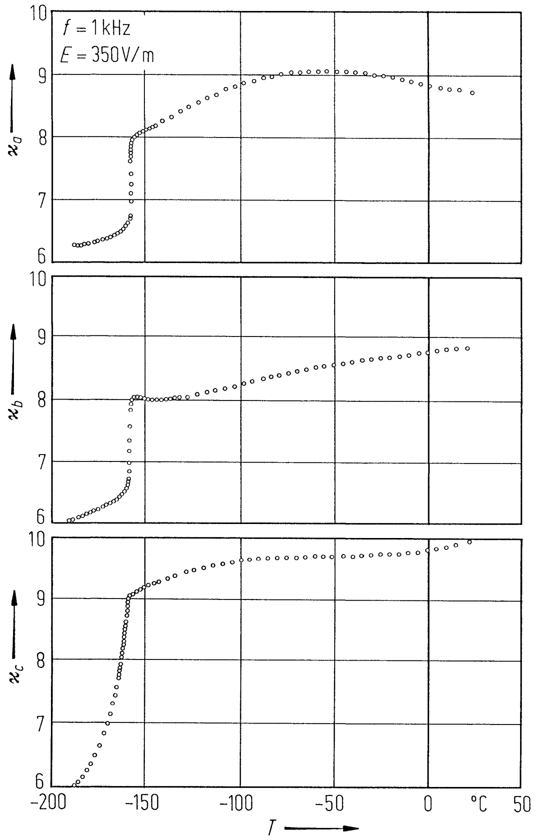

Fig. 67A-2-004. $NaND_4C_4H_2D_2O_6 \cdot 4D_2O$. κ_a, κ_b, κ_c vs. T [84Fil].

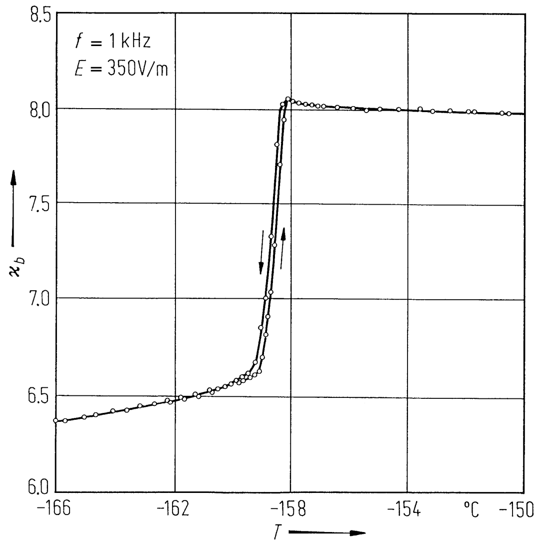

Fig. 67A-2-005. $NaND_4C_4H_2D_2O_6 \cdot 4D_2O$. κ_b vs. T in the vicinity of $\Theta_{II\text{–}I}$ [84Fil].

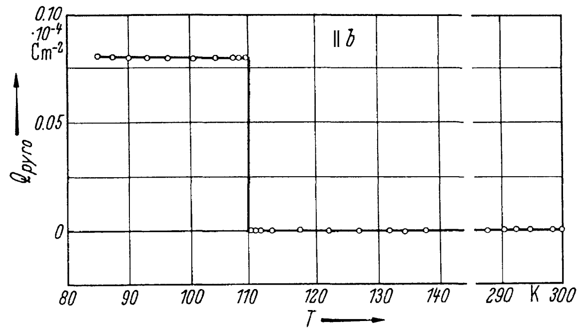

Fig. 67A-2-006. $NaNH_4C_4H_4O_6 \cdot 4H_2O$. Q_{pyro} vs. T [58Tak]. Q_{pyro}: pyroelectric charge along b axis.

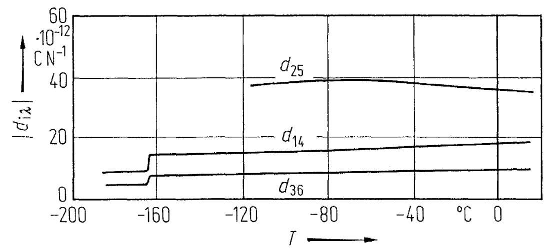

Fig. 67A-2-007. $NaNH_4C_4H_4O_6 \cdot 4H_2O$. $| d_{i\lambda}|$ vs. T [59Mak].

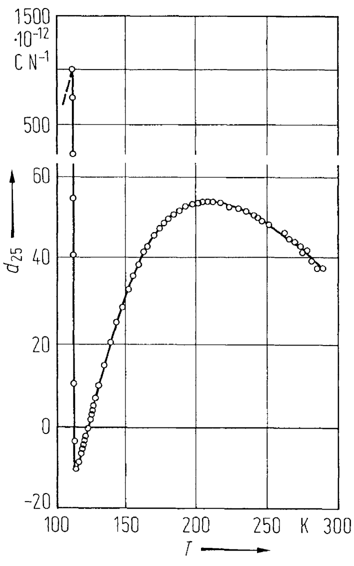

Fig. 67A-2-008. $NaNH_4C_4H_4O_6 \cdot 4H_2O$. d_{25} vs. T [77Gla].

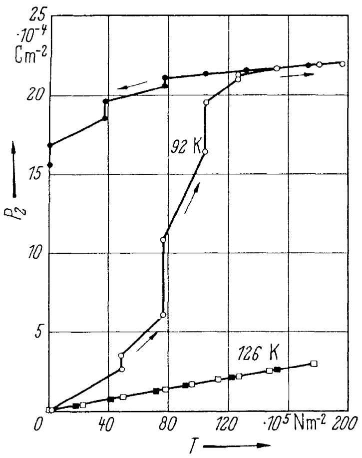

Fig. 67A-2-009. $NaNH_4C_4H_4O_6 \cdot 4H_2O$. P_2 vs. T [58Tak]. P_2: polarization along [010]. T: uniaxial pressure along [101].

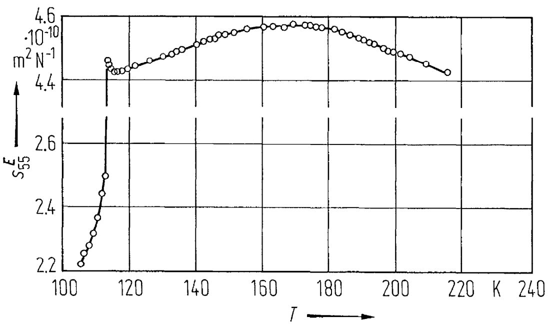

Fig. 67A-2-010. $NaNH_4C_4H_4O_6 \cdot 4H_2O$. s^E_{55} vs. T [77Gla].

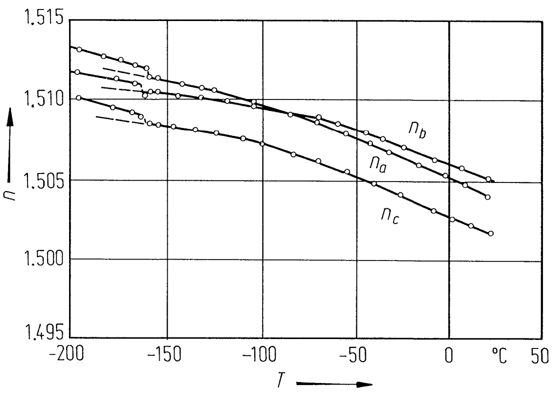

Fig. 67A-2-011. $NaNH_4C_4H_4O_6 \cdot 4H_2O$. n_a, n_b, n_c vs. T [80Rom]. $\lambda = 500$ nm.

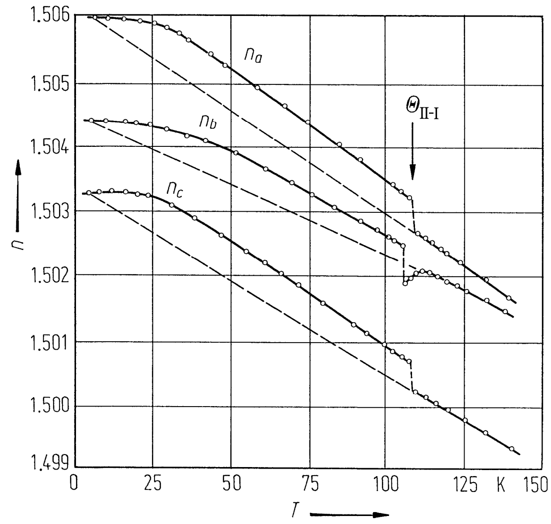

Fig. 67A-2-012. $NaNH_4C_4H_4O_6 \cdot 4H_2O$. n_a, n_b, n_c vs. T [83Gab]. $\lambda = 500$ nm.

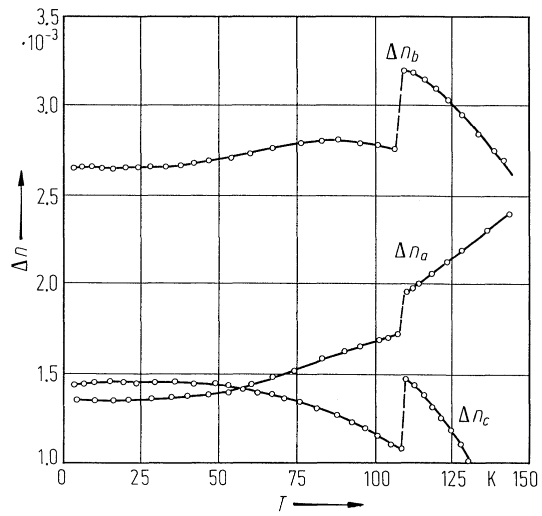

Fig. 67A-2-013. $NaNH_4C_4H_4O_6 \cdot 4H_2O$. Δn_a, Δn_b, Δn_c vs. T [83Gab]. $\lambda = 700$ nm.

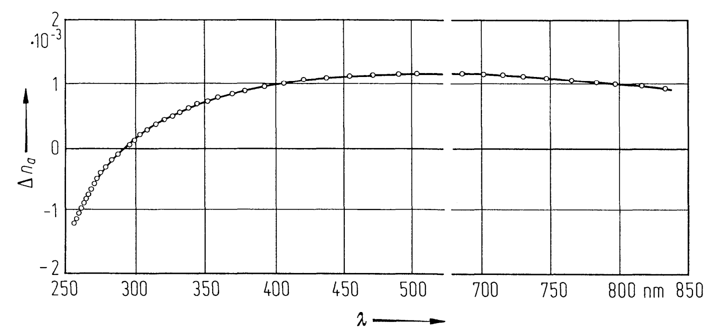

Fig. 67A-2-014. $NaNH_4C_4H_4O_6 \cdot 4H_2O$. Δn_a vs. λ at 4.2 K [83Gab]. $\Delta n_a = n_b - n_c$.

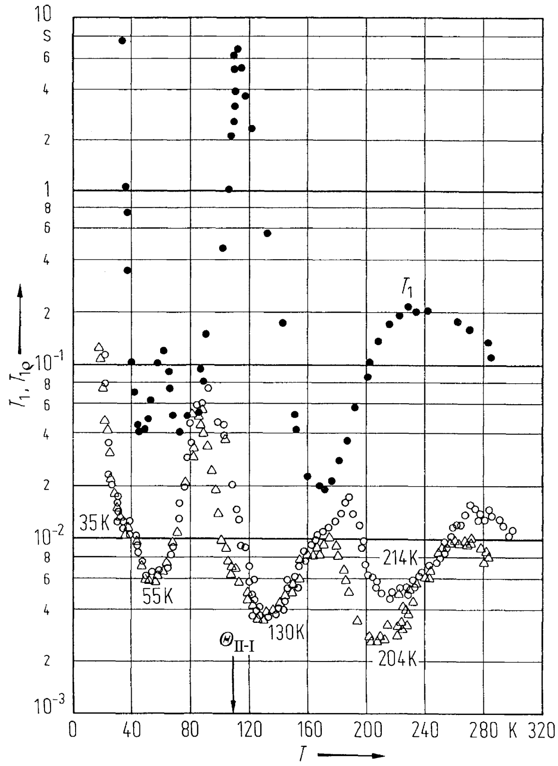

Fig. 67A-2-015. $NaNH_4C_4H_4O_6 \cdot 4H_2O$. T_1, $T_{1\rho}$ vs. T [76Mor]. T_1: proton spin-lattice relaxation time. $T_{1\rho}$: proton spin-lattice relaxation time in rotating frame. Full circle: T_1 at 10 MHz. Open circle: $T_{1\rho}$ at $H_1 = 1.4 \cdot 10^3$ A m^{-1}. Open triangle: $T_{1\rho}$ at $H_1 = 0.72 \cdot 10^3$ A m^{-1}. H_1: amplitude of the radio frequency magnetic field.

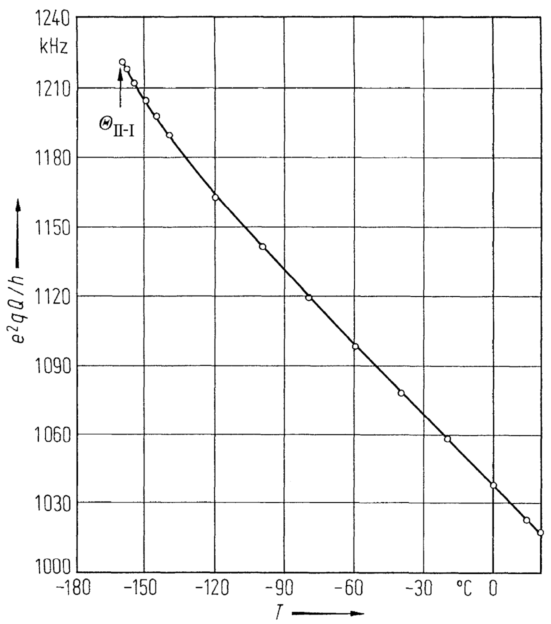

Fig. 67A-2-016. $NaNH_4C_4H_4O_6 \cdot 4H_2O$. e^2qQ/h vs. T [75Tak]. e^2qQ/h for ^{23}Na.

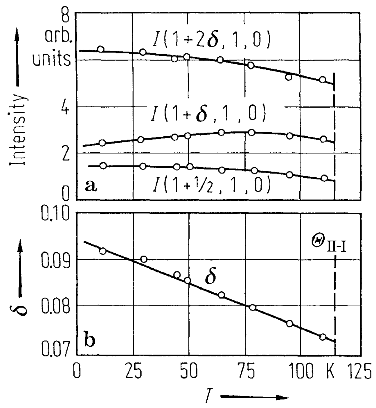

Fig. 67A-2-017. $NaND_4C_4H_2D_2O_6 \cdot 4D_2O$. *I*, δ vs. *T* in phase II [78Iiz]. *I*: neutron diffraction intensities at (1 + nδ, 1, 0), n = 1, 2 and (1 + 1/2, 1, 0). (**a**) *I*(1 + 2δ, 1, 0), *I* (1 + δ, 1, 0), *I*(1 + 1/2, 1, 0). (**b**) δ in units of $2\pi/a$.

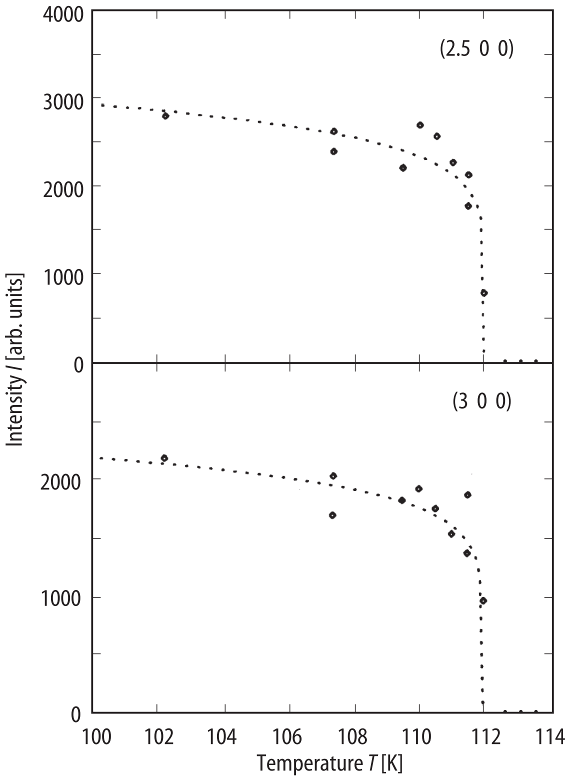

Fig. 67A-2-018. $NaNH_4C_4H_4O_6 \cdot 4H_2O$. *I*(2.5, 0, 0), *I*(3, 0, 0) vs. *T* [96Kik]. Broken lines are guide to eyes.

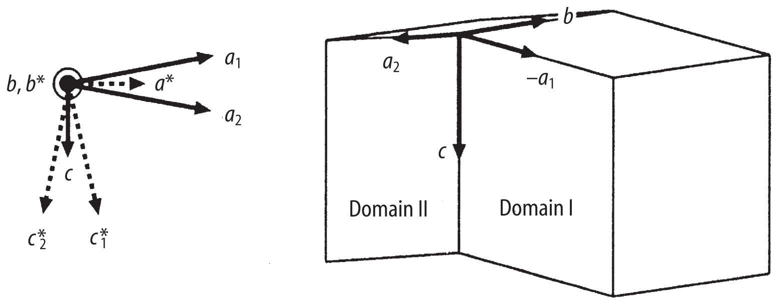

Fig. 67A-2-019. $NaNH_4C_4H_4O_6 \cdot 4H_2O$. Two types of domains and the relations of the crystallographic systems observed in phase II [97Kik].

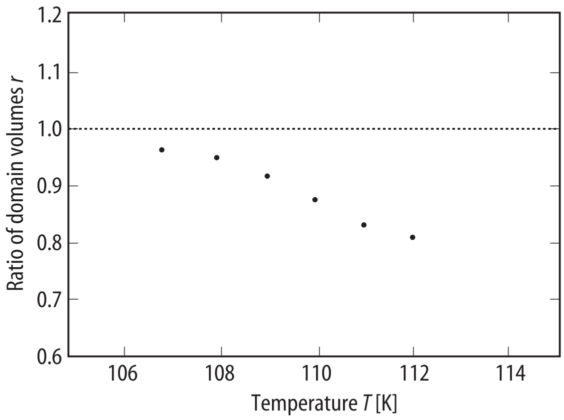

Fig. 67A-2-020. $NaNH_4C_4H_4O_6 \cdot 4H_2O$. *r* vs. *T* [96Kik]. *r*: ratio of the two kind of domain volumes measured by splitted (001) Bragg reflection intensities.

References

1894Lav Lavinir, A.: Bull. Soc. Fr. Mineral. Cristallogr. **17** (1894) 153.
28Man Mandell, W.: Proc. R. Soc. London, Ser. A **121** (1928) 130.
30Ast Astbury, W.T.: p. 353 in [30Was].
30Was Washburn, E.W. (ed.): International Critical Tables, Vol. 7, New York: McGraw-Hill Book Co. Inc., 1930.
33Blo Bloomenthal, S.: Physics **4** (1933) 172.
50Mas Mason, W.P.: Piezoelectric Crystals and Their Applications to Ultrasonics, Princeton: D. Van Nostrand Co., 1950.
53Jon Jona, F., Pepinsky, R.: Phys. Rev. **92** (1953) 1577.
58Mak Makita, Y., Takagi, Y.: J. Phys. Soc. Jpn. **13** (1958) 367.
58Tak Takagi, Y. Makita, Y.: J. Phys. Soc. Jpn. **13** (1958) 272.
59Mak Makita, Y.: Unpublished work (1959).
66Bec Bechmann, R., Hearmon, R.F.S.: Landolt-Börnstein, New Series, Group III, Vol. 1: Elastic, Piezoelectric, Piezooptic and Electrooptic Constants of Crystals, Hellwege, K.-H., Hellwege, A.M. (eds.), Berlin, Heidelberg, New York: Springer, 1966.
71Saw Sawada, A., Takagi, Y.: J. Phys. Soc. Jpn. **31** (1971) 952.
72Suz Suzuki, I., Maeda, M., Abe, R.: J. Phys. Soc. Jpn. **33** (1972) 860.
75Tak Takoshima, T., Tatsuzaki, I.: Solid State Commun. **16** (1975) 537.
76ElS El Saffar, Z.M.: J. Chem. Phys. **64** (1976) 3283.
76Mor Morimoto, K.: J. Phys. Soc. Jpn. **40** (1976) 804.
77Gla Gladkii, V.V., Magamaev, V.K., Kirikov, V.A.: Fiz. Tverd. Tela **19** (1977) 1102; Sov. Phys. Solid State (English Transl.) **19** (1977) 641.
78Iiz Iizumi, M., Gesi, K.: J. Phys. Soc. Jpn. **45** (1978) 711.
80Rom Romanyuk, N.A., Gaba, V.M., Kostetskii, A.M.: Kristallografiya **25** (1980) 1076; Sov. Phys. Crystallogr. (English Transl.) **25** (1980) 618.
82Sha Shahabuddin Khan, Md., Narasimhamurthy, T.S.: Solid State Commun. **43** (1982) 941.
83Gab Gaba, V.M., Zheludev, I.S., Kostetskii, A.M., Romanyuk, N.A.: Izv. Akad. Nauk. SSSR, Ser. Fiz. **47** (1983) 633; Bull. Acad. Sci. USSR, Phys. Ser. (English Transl.) **47** (1983) 8.
84Fil Filipic, C., Blinc, R., Levstik, A.: Solid State Commun. **51** (1984) 809.
96Kik Kikuta, T., Nozaki, R., Shiozaki, Y.: J. Korean Phys. Soc. **29** (1996) S525.
96Suz Suzuki, E., Muta, T., Nozaki, R., Shiozaki, Y.: Acta Crystallogr. Sect. B **52** (1996) 296.
97Kik Kikuta, T., Shimizu, K., Nozaki, R., Shiozaki, Y.: Ferroelectrics **190** (1997) 51.

No. 67A-3 $NaRbC_4H_4O_6 \cdot 4H_2O$, Sodium rubidium tartrate tetrahydrate
(M = 328.59)

1a	Dielectric properties were studied by Jona et al. in 1953 and no anomalies were found.	53Jon
b	Crystal system: orthorhombic. Space group: $P2_12_12 - D_2^3$.	57Meg
3a	Unit cell parameters: a = 12.05 Å, b = 14.40 Å, c = 6.21 Å at RT.	41Bee
5a	Dielectric constant at f = 10 kHz:	53Jon

T [K]	4.2	88	298	333
κ_a	6.8	7.3	9.7	11.2
κ_b	5.8	6.0	7.6	8.4
κ_c	5.3	5.6	8.3	13.7

References

41Bee Beevers, A.C., Hughes, S.: Proc. R. Soc. London, Ser. A **177** (1941) 251.
53Jon Jona, F., Pepinsky, R.: Phys. Rev. **92** (1953) 1577.
57Meg Megaw, H.D.: Ferroelctricity in Crystals, London: Methuen, 1957.